UC San Diego
UC San Diego Previously Published Works

Title

Search for physics beyond the standard model in events with jets and two same-sign or at least three charged leptons in proton-proton collisions at s=13TeV

Permalink

Journal

ISSN

Authors

Sirunyan, AM
Tumasyan, A
Adam, W
et al.

Publication Date

DOI

Copyright Information

Peer reviewed

Regular Article - Experimental Physics

Search for physics beyond the standard model in events with jets and two same-sign or at least three charged leptons in proton-proton collisions at $\sqrt{s} = 13$ TeV

CMS Collaboration[*]

CERN, 1211 Geneva 23, Switzerland

© CERN for the benefit of the CMS collaboration 2020

Abstract A data sample of events from proton-proton collisions with at least two jets, and two isolated same-sign or three or more charged leptons, is studied in a search for signatures of new physics phenomena. The data correspond to an integrated luminosity of 137 fb^{-1} at a center-of-mass energy of 13 TeV, collected in 2016–2018 by the CMS experiment at the LHC. The search is performed using a total of 168 signal regions defined using several kinematic variables. The properties of the events are found to be consistent with the expectations from standard model processes. Exclusion limits at 95% confidence level are set on cross sections for the pair production of gluinos or squarks for various decay scenarios in the context of supersymmetric models conserving or violating R parity. The observed lower mass limits are as large as 2.1 TeV for gluinos and 0.9 TeV for top and bottom squarks. To facilitate reinterpretations, model-independent limits are provided in a set of simplified signal regions.

1 Introduction

In the standard model (SM), the production of multiple jets in conjunction with two same-sign (SS) or three or more charged leptons is a very rare process in proton-proton (pp) collisions. These final states provide a promising starting point in the search for physics beyond the SM (BSM). Many models attempting to address the shortcomings of the SM lead to such signatures. Examples include the production of supersymmetric (SUSY) particles [1,2], SS top quark pairs [3,4], scalar gluons (sgluons) [5,6], heavy scalar bosons of extended Higgs sectors [7,8], Majorana neutrinos [9], and vector-like quarks [10].

In SUSY models [11–19], the decay chain of pair-produced gluinos or squarks can contain multiple W or Z bosons, with the potential to have at least one pair of SS W bosons. Such a decay chain is realized, for example in

gluino pair production, when a gluino decays into a top quark-antiquark pair and a neutralino, or into a pair of quarks and a chargino that subsequently decays into a W boson and a neutralino. In R parity [20] conserving (RPC) scenarios, the lightest SUSY particle is neutral and stable and escapes detection, leading to an imbalance in the measured transverse momentum. The magnitude of the missing transverse momentum strongly depends on the details of the model, and in particular on the mass spectrum of the particles involved. Scenarios with R parity violation (RPV) [21,22] additionally allow decays of SUSY particles into SM particles only, leading in many cases to signatures with little or no missing transverse momentum. For many SUSY models, the SS and multilepton signatures provide complementarity with searches in the zero- or one-lepton final states, and they are particularly suitable for probing compressed mass spectra and other scenarios involving low-momentum leptons or low missing transverse momentum. Both the ATLAS [23] and CMS [24,25] Collaborations have carried out searches in these channels using LHC data collected up to and including 2016. The ATLAS Collaboration has also recently released a search with the full data set recorded between 2015 and 2018 [26].

In this paper, we extend and refine the searches described in Refs. [24,25] using a larger data set of pp collisions at $\sqrt{s} = 13$ TeV recorded by the CMS detector at the CERN LHC in 2016–2018, corresponding to an integrated luminosity of 137 fb^{-1}. We base our search on an initial selection of events with at least two hadronic jets and two SS or three or more light leptons (electrons and muons), including those from leptonic decays of τ leptons. Several signal regions (SRs) are then constructed with requirements on variables such as the number of leptons, the number of jets (possibly identified as originating from b quarks), and the magnitude of missing transverse momentum. A simultaneous comparison of the observed and SM plus BSM expected event yields in all SRs is performed to constrain the BSM models described in Sect. 2. After a brief description of the CMS experiment

---

[*] e-mail: cms-publication-committee-chair@cern.ch

in Sect. 3, we present the details of the search strategy and event selection in Sect. 4 and discuss the various relevant backgrounds from SM processes in Sect. 5. The systematic uncertainties considered in the analysis are presented in Sect. 6. In Sect. 7, the observed yields are compared to the background expectation and the results are interpreted to constrain the various BSM models introduced earlier. Model independent limits are also derived. Finally, the main results are summarized in Sect. 8.

2 Background and signal simulation

Monte Carlo (MC) simulations are used to study the SM backgrounds and to estimate the event selection efficiency of the BSM signals under consideration. Three sets of simulated events for each process are used in order to match the different data taking conditions in 2016, 2017, and 2018.

The hard scattering process of the dominant backgrounds estimated from simulation (including the $t\bar{t}W$, $t\bar{t}Z$ and WZ contributions) is simulated with the MADGRAPH5_aMC@NLO 2.2.2 (2.4.2) [27–29] generator for 2016 (2017 and 2018) conditions. An exception is the WZ process for the 2016 conditions that, as with a few subdominant backgrounds, is simulated using the POWHEG v2 [30–34] next-to-leading order (NLO) generator. Samples of signal events, as well as of SS W boson pairs and other very rare SM processes, are generated at leading order (LO) accuracy with MADGRAPH5_aMC@NLO, with up to two additional partons in the matrix element calculations. The set of parton distribution functions (PDFs) used was NNPDF3.0 [35] for the 2016 simulation and NNPDF3.1 [36] for the 2017 and 2018 simulations.

Parton showering and hadronization, as well as the double parton scattering production of $W^{\pm}W^{\pm}$, are described using the PYTHIA 8.230 generator [37] with the CUETP8M1 (CP5) underlying event tune for 2016 (2017 and 2018) simulation [38–40]. The response of the CMS detector is modeled using the GEANT4 program [41] for SM background samples, while the CMS fast simulation package [42,43] is used for signal samples.

To improve the MADGRAPH5_aMC@NLO modeling of the multiplicity of additional jets from initial-state radiation (ISR), 2016 MC events are reweighted according to the number of ISR jets (N_J^{ISR}). The reweighting factors are extracted from a study of the light-flavor jet multiplicity in dilepton $t\bar{t}$ events. They vary between 0.92 and 0.77 for N_J^{ISR} between 1 and 4, with one half of the deviation from unity taken as the systematic uncertainty. This reweighting is not necessary for the 2017 and 2018 MC samples that are generated using an updated PYTHIA tune.

The phenomenology of a given SUSY model strongly depends on its underlying details such as the masses of the SUSY particles and their couplings with the SM particles and each other, many of which can be free parameters. The signal models used by this search are simplified SUSY models [44,45] of either gluino or squark pair production, followed by a variety of RPC (Figs. 1, 2) or RPV (Fig. 3) decays
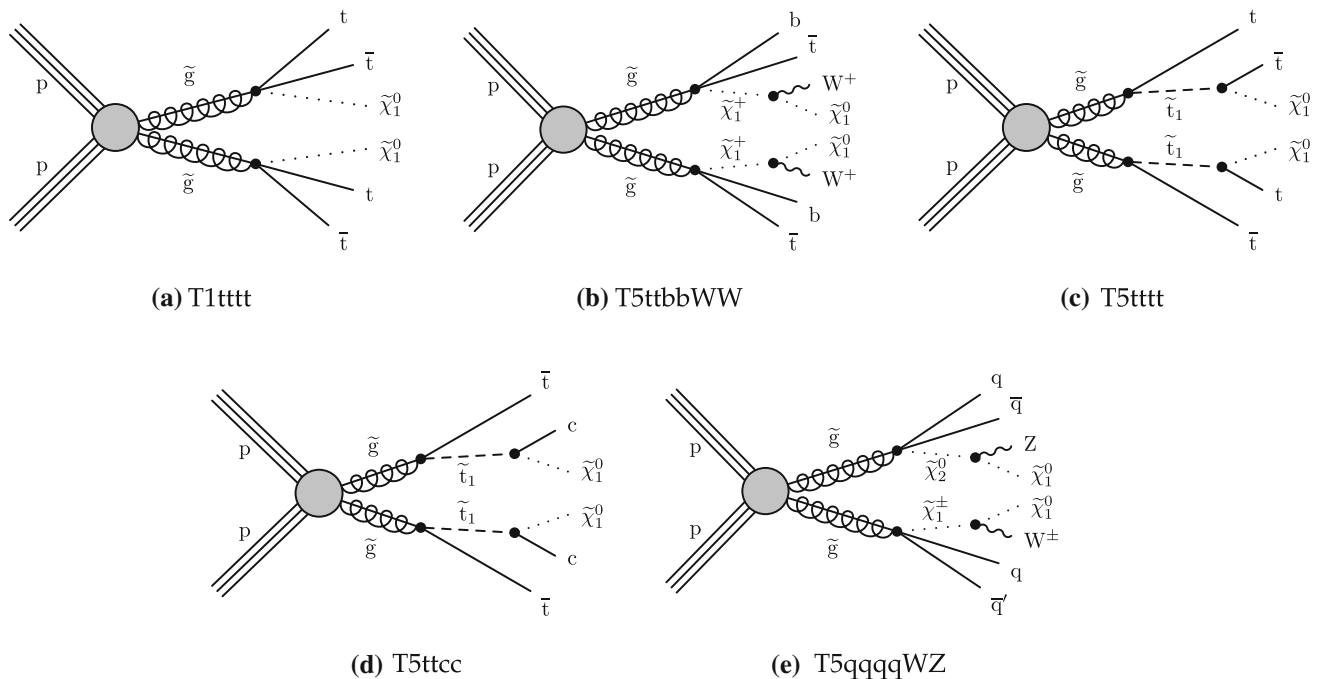

(a) T1tttt   **(b)** T5ttbbWW   **(c)** T5tttt

(d) T5ttcc   **(e)** T5qqqqWZ

Fig. 1 Diagrams illustrating the simplified RPC SUSY models with gluino production considered in this analysis

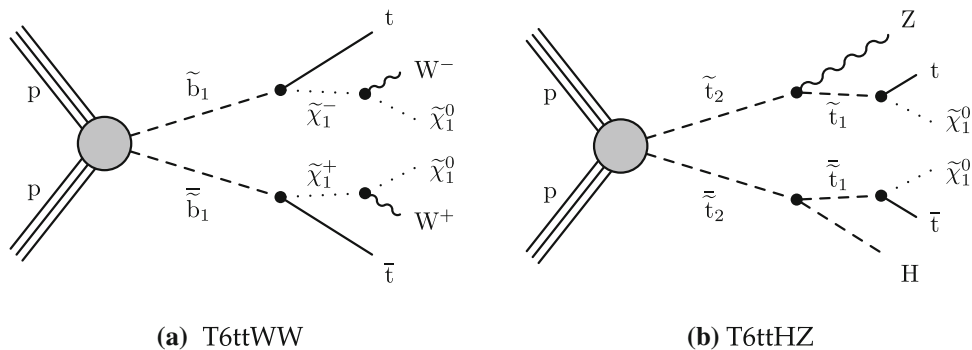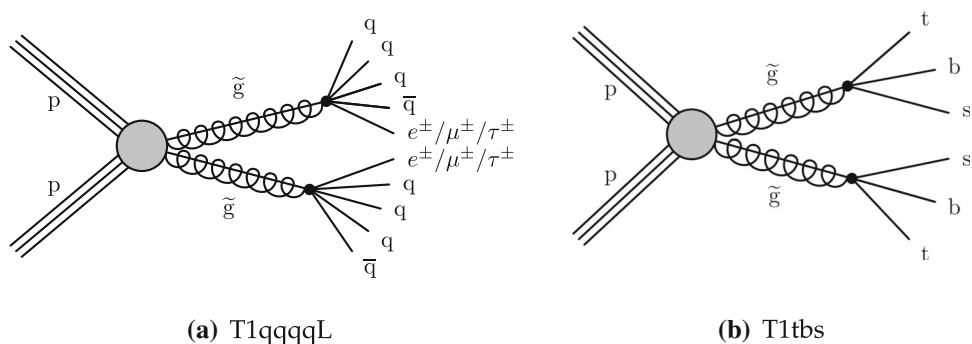**Fig. 2** Diagrams illustrating the simplified RPC SUSY models with squark production considered in this analysis

(a) T6ttWW

(b) T6ttHZ

Fig. 3 Diagrams illustrating the two simplified RPV SUSY models considered in this analysis

(a) T1qqqqL

(b) T1tbs

and where several leptons can arise in the final state. Production cross sections are calculated at approximate next-to-next-to-leading order plus next-to-next-to-leading logarithmic (NNLO+NNLL) accuracy [46–58]. The branching fractions for the decays shown are assumed to be 100%, unless otherwise specified, and all decays are assumed to be prompt.

Gluino pair production models giving rise to signatures with up to four b quarks and up to four W bosons are shown in Fig. 1. In these models, the gluino decays to the lightest squark ($\tilde{g} \to \tilde{q}q$), which in turn decays to same-flavor ($\tilde{q} \to q\tilde{\chi}_1^0$) or different-flavor ($\tilde{q} \to q'\tilde{\chi}_1^\pm$) quarks. The chargino ($\tilde{\chi}_1^\pm$) decays to a W boson and a neutralino ($\tilde{\chi}_1^0$) via $\tilde{\chi}_1^\pm \to W^\pm\tilde{\chi}_1^0$, where the $\tilde{\chi}_1^0$ is taken to be the lightest stable SUSY particle and escapes detection.

The first scenario, denoted by T1tttt and displayed in Fig. 1a, includes an off-shell top squark ($\tilde{t}$) leading to the three-body decay of the gluino, $\tilde{g} \to t\bar{t}\tilde{\chi}_1^0$, resulting in events with four W bosons and four b quarks. Figure 1b presents a similar model (T5ttbbWW) where the gluino decay results in a chargino that further decays into a neutralino and a W boson. The model shown in Fig. 1c (T5tttt) is the same as T1tttt except that the intermediate top squark is on-shell. The mass splitting between the $\tilde{t}$ and the $\tilde{\chi}_1^0$ is taken to be $m_{\tilde{t}} - m_{\tilde{\chi}_1^0} = m_t$, where m_t is the top quark mass. This choice maximizes the kinematic differences between this model and T1tttt, and also corresponds to one of the most challenging regions of parameter space for the observation of the $\tilde{t} \to t\tilde{\chi}_1^0$ decay since the neutralino is produced at rest in the top squark rest frame. The decay chain of Fig. 1d (T5ttcc) is

identical to that of T5tttt except that the $\tilde{t}$ decay involves a cquark. In Fig. 1e, the decay process includes a virtual light-flavor squark, leading to three-body decays of $\tilde{g} \to qq'\tilde{\chi}_1^\pm$ or $\tilde{g} \to qq'\tilde{\chi}_2^0$, with a resulting signature of two W bosons, two Z bosons, or one of each (the case shown in Fig. 2e), and four light-flavor jets. This model, T5qqqqWZ, with a resulting signature of one W boson and one Z boson, is studied with two different assumptions for the chargino mass: $m_{\tilde{\chi}_1^\pm} = 0.5(m_{\tilde{g}} + m_{\tilde{\chi}_1^0})$, and $m_{\tilde{\chi}_1^\pm} = m_{\tilde{\chi}_1^0} + 20\,\text{GeV}$, producing on- and off-shell bosons, respectively. The model is also considered with the assumption of decays to two W bosons exclusively (T5qqqqWW).

Figure 2a shows a model of bottom squark production with subsequent decay of $\tilde{b}_1 \to t\tilde{\chi}_1^\pm$, yielding two b quarks and four W bosons. This model, T6ttWW, is considered as a function of the the lightest bottom squark, $\tilde{b}_1$, and $\tilde{\chi}_1^\pm$ masses. The $\tilde{\chi}_1^0$ mass is fixed to be 50 GeV, causing two of the W bosons to be produced off-shell when the $\tilde{\chi}_1^\pm$ mass is less than approximately 130 GeV. Figure 2b displays a model similar to T6ttWW, but with top squark pair production and a subsequent decay of $\tilde{t}_2 \to \tilde{t}_1H/Z$, with $\tilde{t}_1 \to t\tilde{\chi}_1^0$, producing signatures with two H bosons, two Z bosons, or one of each. In this model, T6ttHZ, the $\tilde{\chi}_1^0$ mass is fixed such that $m(\tilde{t}_1) - m(\tilde{\chi}_1^0) = m_t$.

The R parity violating decays considered in this analysis are T1qqqqL (Fig. 3a) and T1tbs (Fig. 3b). In T1qqqqL, the gluino decays to the lightest squark ($\tilde{g} \to \tilde{q}q$), which in turn decays to a quark ($\tilde{q} \to q\tilde{\chi}_1^0$), but decays with the $\tilde{\chi}_1^0$ off shell (violating R parity) into two quarks and a charged

lepton, giving rise to a prompt 5-body decay of the gluino. In T1tbs, each gluino decays into three different SM quarks (a top, a bottom, and a strange quark).

3 The CMS detector and event reconstruction

The central feature of the CMS detector is a superconducting solenoid of 6 m internal diameter, providing a magnetic field of 3.8 T. Within the solenoid volume are a silicon pixel and strip tracker, a lead tungstate crystal electromagnetic calorimeter (ECAL), and a brass and scintillator hadron calorimeter (HCAL), each composed of a barrel and two endcap sections. Forward calorimeters extend the pseudorapidity (η) coverage provided by the barrel and endcap detectors. Muons are detected in gas-ionization chambers embedded in the steel flux-return yoke outside the solenoid. A more detailed description of the CMS detector, together with a definition of the coordinate system used and the relevant kinematic variables, can be found in Ref. [59].

Events of interest are selected using a two-tiered trigger system [60]. The first level, composed of custom hardware processors, uses information from the calorimeters and muon detectors to select events at a rate of around 100 kHz within a fixed time interval of less than 4 μs. The second level, known as the high-level trigger, consists of a farm of processors running a version of the full event reconstruction software optimized for fast processing, and reduces the event rate to around 1 kHz before data storage.

The reconstructed vertex with the largest value of summed physics-object squared-transverse-momentum is taken to be the primary pp interaction vertex. The physics objects are the jets, clustered using the jet finding algorithm of Refs. [61,62] with the tracks assigned to the vertex as inputs, and the associated missing transverse momentum, taken as the negative vector sum of the transverse momentum (p_T) of those jets.

The particle-flow (PF) algorithm [63] aims to reconstruct and identify each individual particle in an event, with an optimized combination of information from the various elements of the CMS detector. The energy of photons is directly obtained from the ECAL measurement. The energy of electrons is determined from a combination of the electron momentum at the primary interaction vertex as determined by the tracker, the energy of the corresponding ECAL cluster, and the energy sum of all bremsstrahlung photons spatially compatible with the electron track [64]. The momentum of muons is obtained from the curvature of the corresponding track, combining information from the silicon tracker and the muon system [65]. The energy of charged hadrons is determined from a combination of their momentum measured in the tracker and the matching ECAL and HCAL energy deposits, corrected for the response function of the calorimeters to hadronic showers. The energy of neutral hadrons is obtained from the corresponding corrected ECAL and HCAL energies.

Hadronic jets are clustered from charged PF candidates associated with the primary vertex and from all neutral PF candidates using the anti-k_T algorithm [61,62] with a distance parameter of 0.4. The jet momentum is determined as the vectorial sum of all PF candidate momenta in the jet. An offset correction is applied to jet energies to take into account the contribution from pileup [66]. Additional jet energy corrections are derived from simulation to bring the detector response to unity, and are improved with in situ measurements of the energy balance in dijet, multijet, photon+jets, and leptonically decaying Z+jets events [67,68]. Additional selection criteria are applied to each jet to remove jets potentially dominated by instrumental effects or reconstruction failures. Jets originating from b quarks are identified as b-tagged jets using a deep neural network algorithm, DeepCSV [69], with a working point chosen such that the efficiency to identify a b jet is 55–70% for a jet p_T between 20 and 400 GeV. The misidentification rate for a light-flavor jet is 1–2% in the same jet p_T range.

The vector $\vec{p}_T^{\text{miss}}$ is defined as the projection onto the plane perpendicular to the beams of the negative vector sum of the momenta of all reconstructed PF candidates in an event [70]. Its magnitude, called missing transverse momentum, is referred to as p_T^{miss}. The scalar p_T sum of all jets in an event is referred to as H_T.

4 Search strategy and event selection

The search strategy is similar to the one adopted in Refs. [24,25]. The event selection requires the presence of at least two hadronic jets and at least two leptons, among which is an SS pair, as described below. Each selected event is assigned to an SR, based on its content. Maximum likelihood fits of the background (or signal plus background) predictions to the data in all SRs are then performed. Such a strategy ensures sensitivity to a broad range of possible signatures of new physics, even beyond the signal benchmarks considered in this analysis.

The kinematic requirements applied to leptons and jets are presented in Table 1. The analysis requires at least two jets with $p_T > 40$ GeV and two light SS leptons with $p_T > 15$ GeV (10 GeV) for electrons (muons). Electrons are identified based on a discriminant using shower shape and track quality variables, while the muon identification relies on the quality of the geometrical matching between the tracker and muon system measurements. In order to reject leptons from the decay of heavy flavor hadrons, the tracks are required to have an impact parameter compatible with the position of the primary vertex. Several isolation criteria are

Table 1 Transverse momentum and pseudorapidity requirements for leptons and jets. Note that the p_T thresholds to count jets and b-tagged jets are different; the jet multiplicity N_{jets} includes b-tagged jets if their p_T exceeds 40 GeV

Object	p_T (GeV)	$|\eta|$
Electrons	> 15	< 2.5
Muons	> 10	< 2.4
Jets	> 40	< 2.4
b-tagged jets	> 25	< 2.4

also applied, based on the scalar sum of hadron and photon p_T within a cone centered on the lepton direction and whose radius decreases with its p_T, the ratio of the p_T of the lepton to that of the closest jet, and the relative p_T of the lepton to that of the closest jet after lepton momentum subtraction. These criteria are designed to mitigate the loss of lepton efficiency caused by lepton-jet overlaps that occurs frequently in events with significant hadronic activity. A more detailed description of the set of identification and isolation variables used in the lepton selection can be found in Ref. [71].

The lepton reconstruction and identification efficiency is in the range of 45–70% (70–90%) for electrons (muons), with $p_T > 25$ GeV, increasing as a function of p_T and reaching the maximum value for $p_T > 60$ GeV. In the low-momentum regime, $15 < p_T < 25$ GeV for electrons and $10 < p_T < 25$ GeV for muons, the efficiencies are approximately 40% for electrons and 55% for muons. The lepton trigger efficiency for electrons is in the range of 90–98%, converging to the maximum value for $p_T > 30$ GeV, and it is around 92% for muons.

In order to reduce backgrounds from the decays of c- and b-hadrons or from the Drell–Yan process, we reject events with same-flavor lepton pairs with invariant mass ($m_{\ell\ell}$) less than 12 GeV, where leptons are reconstructed with a looser set of requirements compared to the nominal selection. Furthermore, events containing a lepton pair with $m_{\ell\ell} < 8$ GeV, regardless of charge or flavor, are rejected in order to emulate a similar condition applied at the trigger level. Events are then separated according to the p_T of the leptons forming the SS pair: high-high if both have $p_T > 25$ GeV, low-low if both have $p_T < 25$ GeV, and high-low otherwise.

Two sets of trigger algorithms are used to select the events: pure dilepton triggers, which require the presence of two isolated leptons with p_T thresholds on the leading (subleading) lepton in the 17–23 (8–12) GeV range, and dilepton triggers with no isolation requirements, a lower p_T threshold of 8 GeV, an invariant mass condition $m_{\ell\ell} > 8$ GeV to reject low mass resonances, and with a minimum H_T in the range of $300-350$ GeV. The ranges listed here reflect the varying trigger conditions during the data taking periods. The pure dilepton triggers are used to select high-high and high-low

pairs, while low-low pairs are selected using the triggers with H_T requirements.

Six exclusive categories are then defined as follows:

– High-High SS pair, significant p_T^{miss} (HH): exactly 2 leptons, both with $p_T > 25$ GeV, and $p_T^{miss} > 50$ GeV;
– High-Low SS pair, significant p_T^{miss} (HL): exactly 2 leptons, one with $p_T > 25$ GeV, one with $p_T < 25$ GeV, and $p_T^{miss} > 50$ GeV;
– Low-Low SS pair, significant p_T^{miss} (LL): exactly 2 leptons, both with $p_T < 25$ GeV and $p_T^{miss} > 50$ GeV;
– Low p_T^{miss} (LM): exactly 2 leptons, both with $p_T > 25$ GeV, and $p_T^{miss} < 50$ GeV; and
– Multilepton with an on-shell Z boson (on-Z ML): ≥ 3 leptons, at least one with $p_T > 25$ GeV, $p_T^{miss} > 50$ GeV, $\geq$ Z boson candidate formed by a pair of opposite-sign (OS), same-flavor leptons with $76 < m_{\ell\ell} < 106$ GeV.
– Multilepton without an on-shell Z boson (off-Z ML): same as on-Z ML but without a Z boson candidate.

The categories are typically sensitive to different new physics scenarios and enriched in different SM backgrounds. For example the HH category drives the sensitivity for most of the RPC scenarios (T1tttt, T5ttbbWW, T5tttt, T1tttt, T5qqqqWW) with a large mass splitting between the gluino and the lightest neutralino. The HL and LL categories become relevant for lower mass splitting when one or both leptons tend to be soft. Scenarios resulting in the presence of one or multiple Z bosons in the final state such as T5qqqqWZ and T6ttHZ will typically be primarily constrained by the on-Z or off-Z category, also depending on the considered SUSY mass spectrum. Finally the LM category enhances the analysis sensitivity for RPV scenarios, in particular for T1qqqqL where no genuine p_T^{miss} is expected.

Various SRs are constructed based on the jet multiplicity N_{jets}, the b-tagged jet multiplicity N_b, H_T, p_T^{miss}, the charge of the SS pair, and m_T^{min}, which is defined below. The m_T^{min} variable, introduced in Ref. [71], is defined as the minimum of the transverse masses calculated from each of the leptons forming the SS pair and $\vec{p}_T^{miss}$, except for the on-Z ML category where we only consider the transverse mass computed using the leptons not forming the Z candidate. It is characterized by a kinematic cutoff for events where p_T^{miss} only arises from the leptonic decay of a single W boson and is effective at discriminating signal and background signatures.

A subset of SRs is split by the charge of the leptons in an SS pair which is used to take advantage of the charge asymmetry in most of the background processes, such as WZ, $t\bar{t}W$ or SS WW. The SRs corresponding to each category, HH, HL, LL, LM, on-Z ML, and off-Z ML, are summarized in Tables 2, 3, 4, 5, 6 and 7, respectively. The binning ranges are chosen to maximize the sensitivity to a variety of SUSY benchmark points and are such that the expected SM yield in

Table 2 The SR definitions for the HH category. Charge-split regions are indicated with (++) and (- -). The three highest H_T regions are split only by N_{jets}, resulting in 62 regions in total. Quantities are specified in units of GeV where applicable.

N_b	m_T^{min}	p_T^{miss}	N_{jets}	$H_T < 300$	$H_T \in [300, 1125]$	$H_T \in [1125, 1300]$	$H_T \in [1300, 1600]$	$H_T > 1600$
0	<120	50–200	2–4	SR1	SR2	SR54 $N_{jets} < 5$	SR55 $N_{jets} < 5$	SR56 $N_{jets} < 5$
			≥5		SR4			
		200–300	2–4	SR3	SR5 (++) / SR6 (- -)			
			≥5		SR7			
	>120	50–200	2–4		SR8 (++) / SR9 (- -)			
			≥5					
		200–300	2–4		SR10			
			≥5					
1	<120	50–200	2–4	SR11	SR12	SR57 $N_{jets} = 5$ or 6	SR58 $N_{jets} = 5$ or 6	SR59 $N_{jets} = 5$ or 6
			≥5		SR15 (++) / SR16 (- -)			
		200–300	2–4		SR17 (++) / SR18 (- -)			
			≥5	SR13 (++) / SR14 (- -)	SR19			
	>120	50–200	2–4		SR20 (++) / SR21 (- -)			
			≥5					
		200–300	2–4		SR22			
			≥5					
2	<120	50–200	2–4	SR23	SR24	SR60 $N_{jets} > 6$	SR61 $N_{jets} > 6$	SR62 $N_{jets} > 6$
			≥5		SR27 (++) / SR28 (- -)			
		200–300	2–4		SR29 (++) / SR30 (- -)			
			≥5	SR25 (++) / SR26 (- -)	SR31			
	>120	50–200	2–4		SR32 (++) / SR33 (- -)			
			≥5					
		200–300	2–4		SR34			
			≥5					
≥3	<120	50–200	2–4	SR35 (++) / SR36 (- -)	SR37 (++) / SR38 (- -)			
			≥5		SR39 (++) / SR40 (- -)			
		200–300	2–4		SR37 (++) / SR38 (- -)			
			≥5		SR39 (++) / SR40 (- -)			
	>120	50–300	2–4	SR41	SR42 (++) / SR43 (- -)			
			≥5		SR44 (++) / SR45 (- -)			
Inclusive	Inclusive	300–500	2–4	–	SR46 (++) / SR47 (- -)			
		>500			SR48 (++) / SR49 (- -)			
		300–500	≥5		SR50 (++) / SR51 (- -)			
		>500			SR52 (++) / SR53 (- -)			

Table 3 The SR definitions for the HL category. Charge-split regions are indicated with (++) and (- -). There are 43 regions in total. Quantities are specified in units of GeV where applicable.

N_b	m_T^{min}	p_T^{miss}	N_{jets}	$H_T < 300$	$H_T \in [300, 1125]$	$H_T \in [1125, 1300]$	$H_T > 1300$
0	<120	50–200	2–4	SR1	SR2	SR40 (++) / SR41 (- -)	SR42 (++) / SR43 (- -)
			≥5		SR4		
		200–300	2–4	SR3	SR5 (++) / SR6 (- -)		
			≥5		SR7		
1	<120	50–200	2–4	SR8	SR9		
			≥5	SR10 (++) / SR11 (- -)	SR12 (++) / SR13 (- -)		
		200–300	2–4		SR14		
			≥5		SR15 (++) / SR16 (- -)		
2	<120	50–200	2–4	SR17	SR18		
			≥5	SR19 (++) / SR20 (- -)	SR21 (++) / SR22 (- -)		
		200–300	2–4		SR23 (++) / SR24 (- -)		
			≥5		SR25		
≥3	<120	50–200	≥2	SR26 (++) / SR27 (- -)	SR28 (++) / SR29 (- -)		
		200–300			SR30		
Inclusive	>120	50–300	≥2	SR31	SR32		
Inclusive	Inclusive	300–500	2–4	–	SR33 (++) / SR34 (- -)		
		>500			SR35 (++) / SR36 (- -)		
		300–500	≥5		SR37 (++) / SR38 (- -)		
		>500			SR39		

Table 4 The SR definitions for the LL category. All SRs in this category require $N_{jets} \geq 2$. There are 8 regions in total. Quantities are specified in units of GeV where applicable.

N_b	m_T^{min}	H_T	$p_T^{miss} \in [50, 200]$	$p_T^{miss} > 200$
0			SR1	SR2
1	<120		SR3	SR4
2		>400	SR5	SR6
≥3			SR7	
Inclusive	>120		SR8	

Table 5 The SR definitions for the LM category. All SRs in this category require $p_T^{miss} < 50$ GeV and $H_T > 300$ GeV. The two high-H_T regions are split only by N_{jets}, resulting in 11 regions in total. Quantities are specified in units of GeV where applicable.

N_b	N_{jets}	$H_T \in [300, 1125]$	$H_T \in [1125, 1300]$	$H_T > 1300$
0	2–4	SR1		
	≥5	SR2	SR8 ($N_{jets} < 5$)	SR10 ($N_{jets} < 5$)
1	2–4	SR3		
	≥5	SR4		
2	2–4	SR5	SR9 ($N_{jets} \geq 5$)	SR11 ($N_{jets} \geq 5$)
	≥5	SR6		
≥3	≥2	SR7		

Table 6 The SR definitions for the on-ZML category. All SRs in these categories require $N_{jets} \geq 2$. Regions marked with † are split by $m_T^{min} = 120$ GeV, with the high-m_T^{min} region specified by the second SR label. There are 23 regions in total. Quantities are specified in units of GeV where applicable.

N_b	H_T	$p_T^{miss} \in [50, 150]$	$p_T^{miss} \in [150, 300]$	$p_T^{miss} \geq 300$
0	<400	SR1/SR2†	SR3/SR4†	
	400–600	SR5/SR6†	SR7/SR8†	
1	<400	SR9	SR10	
	400–600	SR11	SR12	
2	<400	SR13	SR14	SR22/SR23†
	400–600	SR15	SR16	
≥3	<600	SR17		
Inclusive	≥600	SR18/SR19†	SR20/SR21†	

Table 7 The SR definitions for the off-Z category. All SRs in these categories require $N_{jets} \geq 2$. Regions marked with † are split by $m_T^{min} = 120$ GeV, with the high-m_T^{min} region specified by the second SR label. There are 21 regions in total. Quantities are specified in units of GeV where applicable.

N_b	H_T	$p_T^{miss} \in [50, 150]$	$p_T^{miss} \in [150, 300]$	$p_T^{miss} \geq 300$
0	<400	SR1/SR2†	SR3/SR4†	
	400–600	SR5	SR6	
1	<400	SR7	SR8	
	400–600	SR9	SR10	
2	<400	SR11	SR12	SR20/SR21†
	400–600	SR13	SR14	
≥3	<600	SR15		
Inclusive	≥600	SR16/SR17†	SR18/SR19†	

any SR has relative statistical uncertainties typically smaller than unity.

5 Backgrounds

Several SM processes can lead to the signatures studied in this analysis. There are three background categories, depending on the lepton content of the event:

– Events with two or more prompt leptons, including an SS pair;

– Events with at least one nonprompt lepton (defined below); and

– Events with a pair of OS leptons, one of which is reconstructed with the wrong charge.

The first category includes a variety of low cross section processes where multiple electroweak bosons are produced, possibly in the decay of top quarks, which then decay leptonically leading to an SS lepton pair. This category usually dominates the background yields in SRs with large p_T^{miss} or H_T and in most of the ML SRs with a Z candidate. The main contributions arise from the production of a WZ or an SS W pair,

Table 8 Summary of the sources of systematic uncertainty and their effect on the yields of different processes in the SRs. The first two groups list experimental and theoretical uncertainties assigned to processes estimated using simulation, while the last group lists uncertainties assigned to processes whose yield is estimated from the data. The uncertainties in the first group also apply to signal samples. Reported values are representative for the most relevant signal regions

Source	Typical uncertainty (%)	Correlation across years
Integrated luminosity	2.3–2.5	Uncorrelated
Lepton selection	2–10	Uncorrelated
Trigger efficiency	2–7	Uncorrelated
Pileup	0–6	Uncorrelated
Jet energy scale	1–15	Uncorrelated
b tagging	1–10	Uncorrelated
Simulated sample size	1–20	Uncorrelated
Scale and PDF variations	10–20	Correlated
Theoretical background cross sections	30–50	Correlated
Nonprompt leptons	30	Correlated
Charge misidentification	20	Uncorrelated
N_J^{ISR}	1–30	Uncorrelated

or of a $t\bar{t}$ pair in association with a W, Z or H boson. The event yields for these processes are estimated individually. In contrast, the expected event yields from other rare processes (including ZZ, triple boson production, tWZ, tZq, $t\bar{t}t\bar{t}$, and double parton scattering) are summed up into a single contribution denoted as "Rare". Processes including a genuine photon, such as Wγ, Zγ, $t\bar{t}\gamma$, and tγ, are also considered and grouped together. They are referred to as "Xγ". All contributions from this category are estimated using simulated samples. Correction factors are applied to take into account small differences between data and simulation, including trigger, lepton selection, and b tagging efficiencies, with associated systematic uncertainties listed in Sect. 6.

The second category consists of events where one of the selected leptons, generically denoted as "nonprompt lepton", is either a decay product of a heavy flavor hadron or, more rarely, a misidentified hadron. This category is typically the dominant one in SRs with moderate or low p_T^{miss} or low m_T^{min} (except for the on-Z ML SRs). This background is estimated directly from data using the "tight-to-loose" method [24,25]. This method is based on the probability for a nonprompt lepton passing loose selection criteria to also satisfy the tighter lepton selection used in the analysis. The number of events in an SR with N leptons, including at least one nonprompt lepton, can be estimated by applying this probability to a corresponding control region (CR) of events with N loose leptons where at least one of them fails the tight selection.

The measurement of the tight-to-loose ratio is performed in a sample enriched in dijet events with exactly one loose lepton, low p_T^{miss}, and low m_T^{min}. This sample is contaminated by prompt leptons from W boson decays. The contamination is estimated from the m_T^{min} distribution, and it is subtracted before calculating the ratio. The tight-to-loose ratio is computed separately for electrons and muons, and is parameterized as a function of the lepton η and p_T^{corr}. The p_T^{corr} variable is defined as the sum of the lepton p_T and the energy in the isolation cone exceeding the isolation threshold value applied to tight leptons. This parametrization improves the stability of the tight-to-loose ratio with respect to variations in the p_T of the partons from which the leptons originate.

The performance of the tight-to-loose ratio was assessed in a MC closure test. A tight-to-loose ratio was extracted from a MC sample of QCD events. This ratio was then used to predict the number of events with one prompt and one nonprompt SS dileptons in MC $t\bar{t}$ and W+jets events. The predicted and observed rates of SS dileptons were compared as a function of kinematic properties and found to agree within 30%. The data driven estimate was also compared to a direct prediction from simulation and a similar level of agreement was reached.
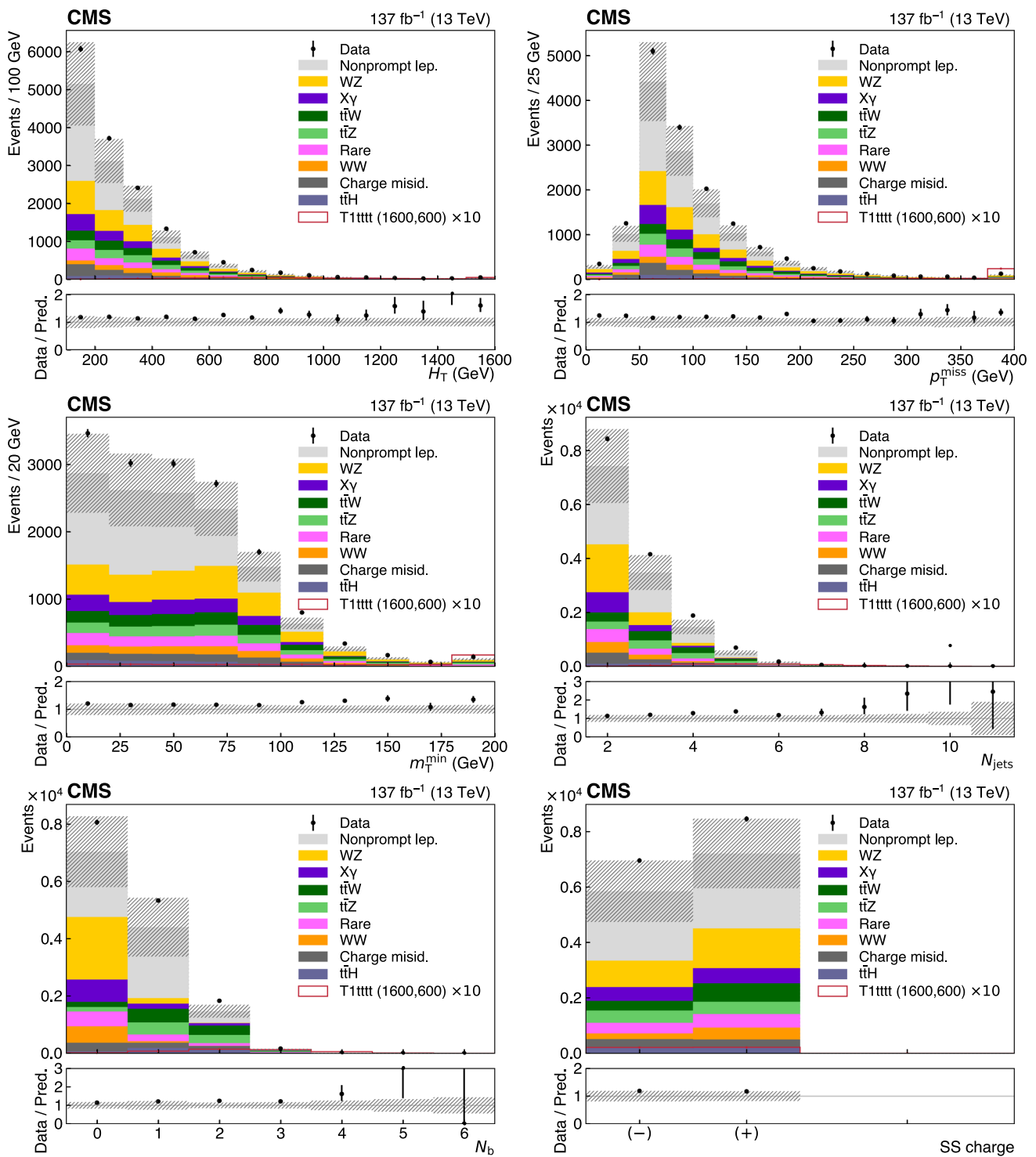
Fig. 4 Distributions of the main analysis variables after the event selection: H_T, p_T^{miss}, m_T^{min}, N_{jets}, N_b, and the charge of the SS pair, where the last bin includes the overflow (where applicable). The hatched area represents the total statistical and systematic uncertainty in the background prediction. The lower panels show the ratio of the observed event yield to the background prediction. The prediction for the SUSY model T1tttt with $m_{\tilde{g}} = 1600\,\text{GeV}$ and $m_{\tilde{\chi}_1^0} = 600\,\text{GeV}$ is overlaid
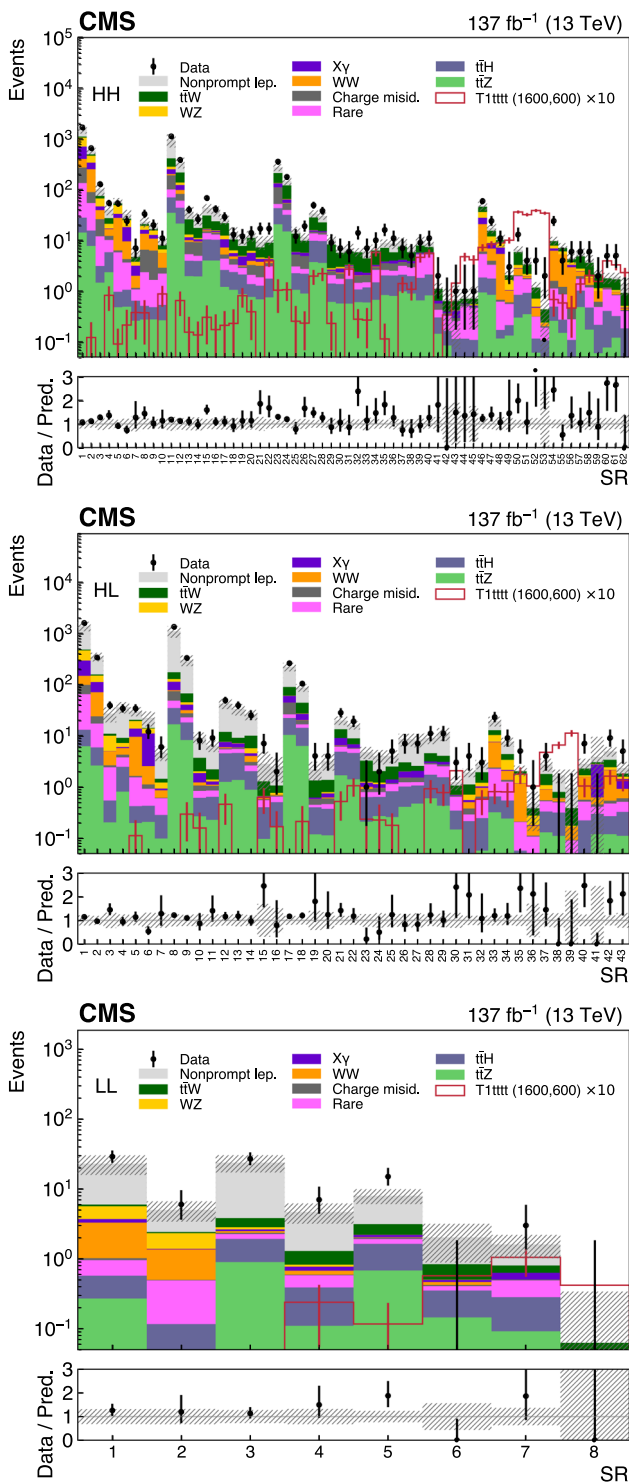
Fig. 5 Expected and observed SR yields for the HH, HL, LL signal categories. The hatched area represents the total statistical and systematic uncertainty in the background prediction
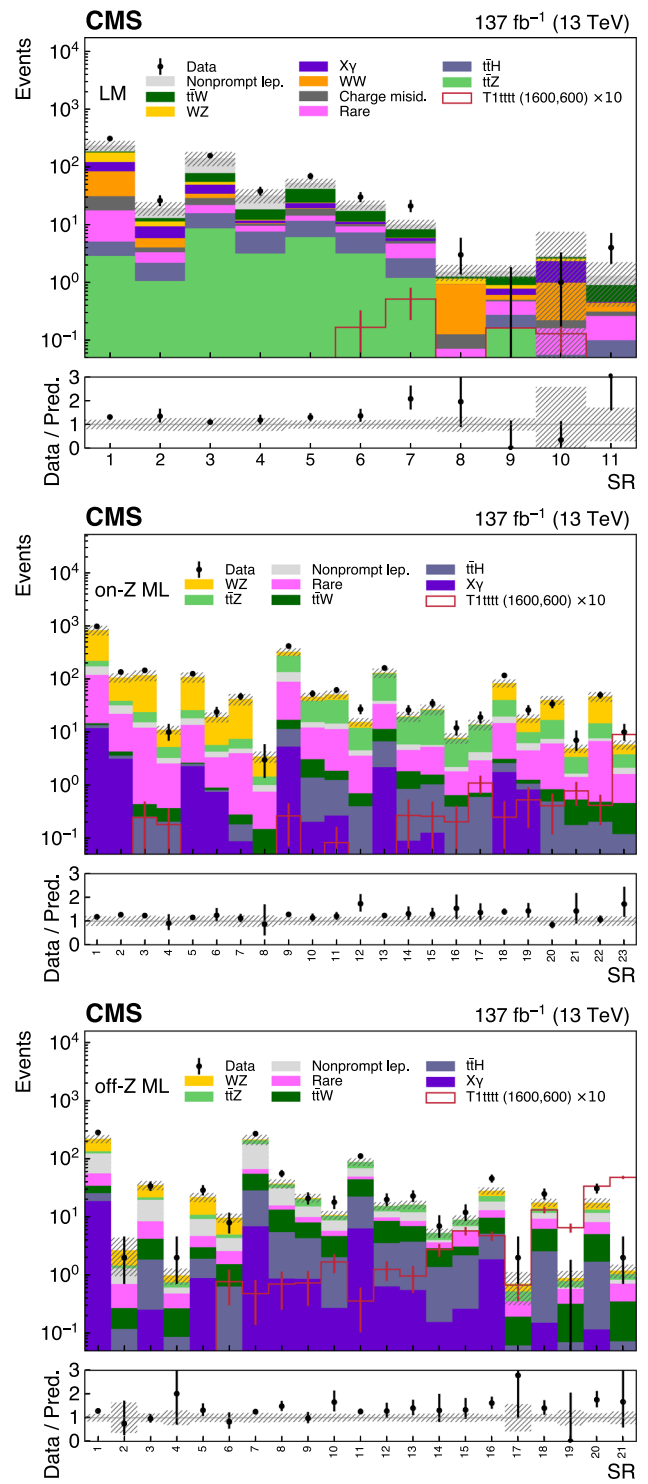
Fig. 6 Expected and observed SR yields for the LM, on-Z ML, off-Z ML signal categories. The hatched area represents the total statistical and systematic uncertainty in the background prediction

Table 9 Expected background event yields, total uncertainties, and observed event yields in the SRs used in this search

HH regions			LL regions			Off-Z ML regions		
SR	Expected SM	Obs.	SR	Expected SM	Obs.	SR	Expected SM	Obs.
1	1560 ± 300	1673	1	1390 ± 300	1593	1	235 ± 47	309
2	582 ± 93	653	2	348 ± 67	337	2	19.3 ± 5.2	26
3	100 ± 25	128	3	26.9 ± 8.8	39	3	142 ± 39	156
4	39.5 ± 8.5	54	4	35.9 ± 9.1	34	4	32.2 ± 8.8	38
5	57.7 ± 9.9	53	5	29.8 ± 6.0	34	5	53.0 ± 9.1	69
6	32.5 ± 7.1	24	6	22.2 ± 7.2	12	6	22.0 ± 4.0	30
7	5.5 ± 1.8	7	7	4.7 ± 1.4	6	7	10.1 ± 2.0	21
8	22.9 ± 5.1	33	8	1100 ± 280	1342	8	1.53 ± 0.48	3
9	19.5 ± 3.9	20	9	299 ± 71	330	9	1.58 ± 0.41	0
10	9.6 ± 1.9	11	10	9.1 ± 2.3	8	10	2.9 ± 2.9	1
11	940 ± 270	1115	11	6.4 ± 1.6	9	11	1.31 ± 0.93	4
12	340 ± 81	384	12	42.1 ± 9.2	49			

On-Z ML regions

SR	Expected SM	Obs.

HH regions			LL regions			On-Z ML regions		
13	36.3 ± 9.5	40	13	33.0 ± 8.4	39	1	840 ± 170	985
14	26.8 ± 7.4	26	14	25.8 ± 5.9	25	2	107 ± 21	136
15	42.7 ± 8.6	68	15	2.8 ± 2.0	7	3	119 ± 27	146
16	37.9 ± 8.6	41	16	2.5 ± 1.3	2	4	11.1 ± 2.1	10
17	26.5 ± 6.2	29	17	222 ± 42	260	5	109 ± 24	126
18	14.3 ± 3.6	13	18	86 ± 15	104	6	19.3 ± 4.1	24
19	10.6 ± 2.5	12	19	2.22 ± 0.90	4	7	42 ± 10	47
20	12.3 ± 2.9	14	20	3.2 ± 1.1	4	8	3.47 ± 0.84	3
21	9.2 ± 2.7	17	21	19.8 ± 3.8	28	9	327 ± 54	419
22	10.1 ± 2.1	17	22	16.1 ± 3.0	19	10	46.5 ± 8.4	53
23	272 ± 43	354	23	4.7 ± 1.3	1	11	51.3 ± 9.1	62
24	147 ± 25	177	24	4.0 ± 1.2	2	12	15.6 ± 2.8	27
25	15.3 ± 2.9	12	25	4.0 ± 1.1	5	13	131 ± 27	162
26	11.4 ± 2.4	19	26	8.5 ± 2.4	7	14	19.9 ± 4.3	26
27	33.4 ± 5.4	49	27	8.4 ± 2.5	7	15	26.9 ± 6.1	35
28	30.1 ± 4.9	38	28	8.9 ± 2.2	11	16	7.8 ± 1.8	12
29	10.4 ± 2.2	9	29	10.9 ± 3.1	11	17	14.0 ± 3.1	19
30	6.6 ± 1.3	7	30	1.25 ± 0.39	3	18	84 ± 15	117
31	6.9 ± 1.5	6	31	1.92 ± 0.37	4	19	18.2 ± 3.3	26
32	5.9 ± 1.1	14	32	2.77 ± 0.56	3	20	40.4 ± 7.6	34
33	6.1 ± 1.6	7	33	19.1 ± 4.1	23	21	4.92 ± 0.88	7
34	6.8 ± 1.3	10	34	7.5 ± 1.5	9	22	46.9 ± 9.9	50
35	8.8 ± 1.5	16	35	2.12 ± 0.49	5	23	5.8 ± 1.2	10
36	8.7 ± 2.0	11	36	0.47 ± 0.33	1			
37	9.4 ± 1.9	7	37	2.75 ± 0.77	4			
38	7.0 ± 1.3	5	38	1.68 ± 0.50	0			
39	9.6 ± 2.1	9	39	0.97 ± 0.97	0			

Off-Z ML regions

HH regions			LL regions			Off-Z ML regions		
						SR	Expected SM	Obs.
40	8.6 ± 1.7	11	40	2.83 ± 0.70	7			
41	1.10 ± 0.32	2	41	3.8 ± 3.8	0	1	222 ± 36	285
42	0.63 ± 0.49	0	42	4.9 ± 1.0	9	2	2.7 ± 1.7	2
43	0.67 ± 0.60	1	43	2.36 ± 0.72	5	3	35.5 ± 6.4	34
44	0.74 ± 0.27	1				4	0.99 ± 0.31	2
45	0.71 ± 0.53	1	**LL regions**			5	22.1 ± 4.0	29
46	47.8 ± 9.7	59	SR	Expected SM	Obs.	6	9.7 ± 1.7	8
47	17.3 ± 3.8	24	1	23.0 ± 7.2	29	7	217 ± 44	272
48	10.3 ± 2.9	11	2	5.0 ± 1.6	6	8	37.7 ± 6.8	56
49	2.06 ± 0.49	3	3	23.8 ± 6.6	27	9	21.4 ± 3.7	21
50	6.5 ± 1.1	13	4	4.7 ± 1.5	7	10	10.9 ± 1.9	18

Table 9 continued

HH regions			LL regions			Off-Z ML regions		
SR	Expected SM	Obs.	SR	Expected SM	Obs.	SR	Expected SM	Obs.
51	3.72 ± 0.79	4	5	8.0 ± 1.9	15	11	89 ± 14	112
52	1.21 ± 0.29	4	6	2.0 ± 1.1	0	12	15.6 ± 2.4	20
53	0.44 ± 0.44	2	7	1.61 ± 0.59	3	13	16.4 ± 2.7	23
54	9.8 ± 1.8	24	8	0.06 ± 0.06	0	14	5.36 ± 0.95	7
55	7.3 ± 1.4	4				15	9.0 ± 1.6	12
56	4.44 ± 0.98	6				16	28.4 ± 3.9	46
57	5.7 ± 1.1	6				17	0.72 ± 0.41	2
58	4.0 ± 1.0	6				18	17.8 ± 2.8	25
59	2.24 ± 0.53	2				19	0.89 ± 0.29	0
60	1.83 ± 0.44	5				20	17.7 ± 3.3	31
61	1.88 ± 0.40	5				21	1.20 ± 0.32	2
62	1.35 ± 0.56	0						

The final category is a subdominant background in all SRs and corresponds to events where the charge of a lepton is incorrectly measured. Charge misidentification primarily occurs when an electron undergoes bremsstrahlung in the tracker material or in the beam pipe. Similarly to the tight-to-loose method, the number of SS lepton pairs where one of the leptons has its charge misidentified can be determined using the number of OS pairs and the knowledge of the charge misidentification rate. We use simulation to parameterize this rate as a function of p_T and η for electrons and find values varying between 10^{-5} (central electrons with $p_T \approx 20\,\mathrm{GeV}$) and 5×10^{-3} (forward electrons with $p_T \approx 200\,\mathrm{GeV}$). To calibrate the charge misidentification rate, we exploit the fact that charge misidentification only has a small effect on the electron energy measurement in the calorimeter. As a result, electron pairs from Z boson decays yield a sharp peak near the Z mass even when one of the electrons has a misidentified charge. The SS dielectron invariant mass distributions in data and MC can then be used to derive a correction factor to the MC charge misidentification rate. Good agreement between data and MC is found in 2016, while the charge misidentification rate in simulation corresponding to 2017 and 2018 data needs to be scaled up by a factor of 1.4. Muon charge misidentification arises from a relatively large uncertainty in the transverse momentum at high momentum or from a poor quality track. The various criteria applied in this analysis on the quality of the muon reconstruction lead to a misidentification rate at least one order of magnitude smaller than for electrons according to simulation. The muon charge misassignment has also been studied using cosmic ray muons with p_T up to several hundred GeV, confirming the predictions from simulation [72]. It is therefore neglected. Correction factors are however applied to the simulation to account for a possible difference in the selection efficiency related to these criteria.

6 Systematic uncertainties

The predicted yields of signal and background processes are affected by several sources of uncertainty, summarized in Table 8. Depending on their source, they are treated as fully correlated or uncorrelated between the three years of data taking. Signal and background contributions estimated from simulation are affected by experimental uncertainties in the efficiency of the trigger, lepton reconstruction and identification [64,73], the efficiency of b tagging [69], the jet energy scale [67], the integrated luminosity [74–76]. An uncertainty is also assigned to the value of the inelastic cross section, which affects the pileup rate [77] and that can impact the description of the jet multiplicity or the p_T^{miss} resolution. Simulation is also affected by theoretical uncertainties, which are evaluated by varying the factorization and renormalization scales up and down by a factor of two, and by using different PDFs within the NNPDF3.0 and 3.1 PDF sets [35,36,78]. These uncertainties can affect both the overall yield (normalization) and the relative population (shape) across the SRs. Background normalization uncertainties are increased to 30%, either to account for the additional hadronic activity required (for WZ and $W^{\pm}W^{\pm}$) or to take into consideration recent measurements (for $t\bar{t}W$, $t\bar{t}Z$) [79,80]. The Rare and $X\gamma$ backgrounds, which are less well understood experimentally and theoretically, are assigned a 50% uncertainty.

To account for possible mismodeling of the flavor of additional jets, an additional 70% uncertainty is applied to $t\bar{t}W$, $t\bar{t}Z$, and $t\bar{t}H$ events produced in association with a pair of b jets, reflecting the measured ratio of $t\bar{t}b\bar{b}/t\bar{t}jj$ cross sections reported in Ref. [81].

As discussed in Sect. 5, the nonprompt lepton and charge misidentification backgrounds are estimated from CRs. The associated uncertainties include the statistical uncertainties in the CR yields, as well as the systematic uncertainties in the extrapolations from the CRs to the SRs, as described below. In the case of the nonprompt lepton background, we include
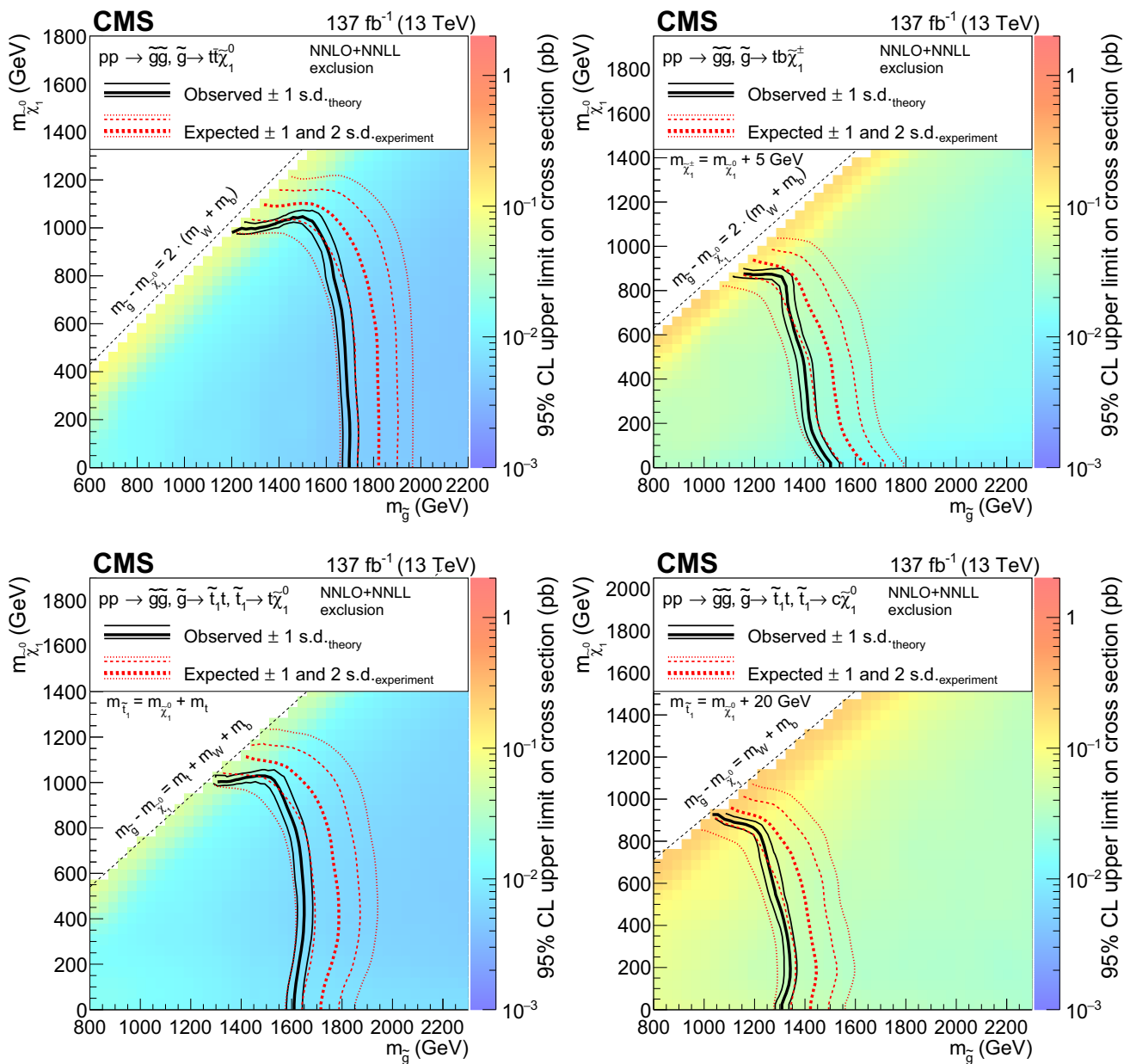
Fig. 7 Exclusion regions at 95% CL in the $m_{\tilde{\chi}_1^0}$ versus $m_{\tilde{g}}$ plane for the T1tttt (upper left) and T5ttbbWW (upper right) models, with off-shell third-generation squarks, and the T5tttt (lower left) and T5ttcc (lower right) models, with on-shell third-generation squarks. For the T5ttbbWW model, $m_{\tilde{\chi}_1^\pm} = m_{\tilde{\chi}_1^0} + 5$ GeV, for the T5tttt model, $m_{\tilde{t}} - m_{\tilde{\chi}_1^0} = m_t$, and for the T5ttcc model, $m_{\tilde{t}} - m_{\tilde{\chi}_1^0} = 20$ GeV and the decay proceeds through $\tilde{t} \rightarrow c\tilde{\chi}_1^0$. The right-hand side color scale indicates the excluded cross section values for a given point in the SUSY particle mass plane. The solid black curves represent the observed exclusion limits assuming the approximate-NNLO+NNLL cross sections [46–51,58] (thick line), or their variations of ±1 standard deviations (s.d.) (thin lines). The dashed red curves show the expected limits with the corresponding ±1 s.d. and ±2 s.d. uncertainties. Excluded regions are to the left and below the limit curves

a 30% uncertainty from studies of the closure of the method in simulation. Furthermore, the uncertainty in the measurement of the tight-to-loose ratio, because of the prompt lepton contamination, results in a 1–30% additional uncertainty in the background yields. The charge misidentification background is assigned a 20% uncertainty based on a comparison of the kinematic properties of simulated and data events in the $Z \rightarrow e^+e^-$ CR with one electron or positron having a misidentified charge.

In general, the systematic uncertainties with the largest impact on the expected limits defined below are related to the lepton identification and isolation scale factors, the cross section of the rare processes, and the WZ background normalization.
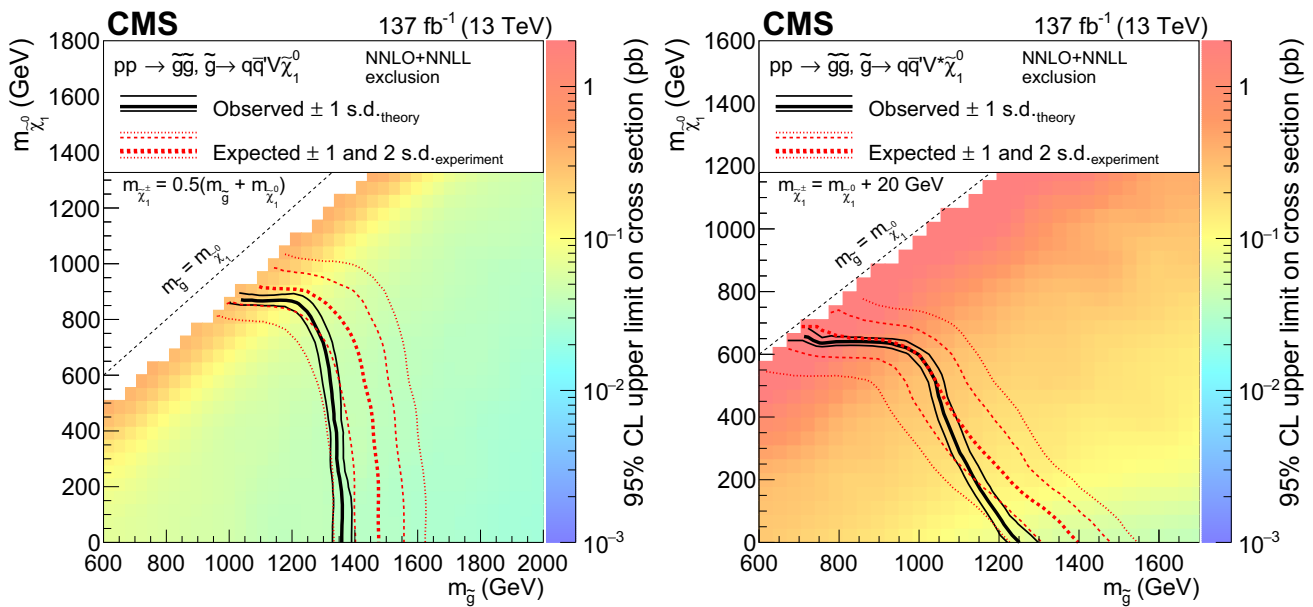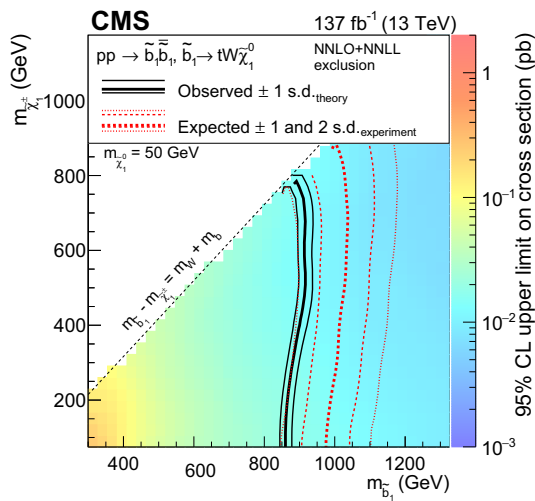
Fig. 8 Exclusion regions at 95% CL in the plane of $m_{\tilde{\chi}_1^0}$ versus $m_{\tilde{g}}$ for the T5qqqqWZ model with $m_{\tilde{\chi}_1^\pm} = 0.5(m_{\tilde{g}} + m_{\tilde{\chi}_1^0})$ (left) and with $m_{\tilde{\chi}_1^\pm} = m_{\tilde{\chi}_1^0} + 20\,\text{GeV}$ (right). The notations are as in Fig. 7
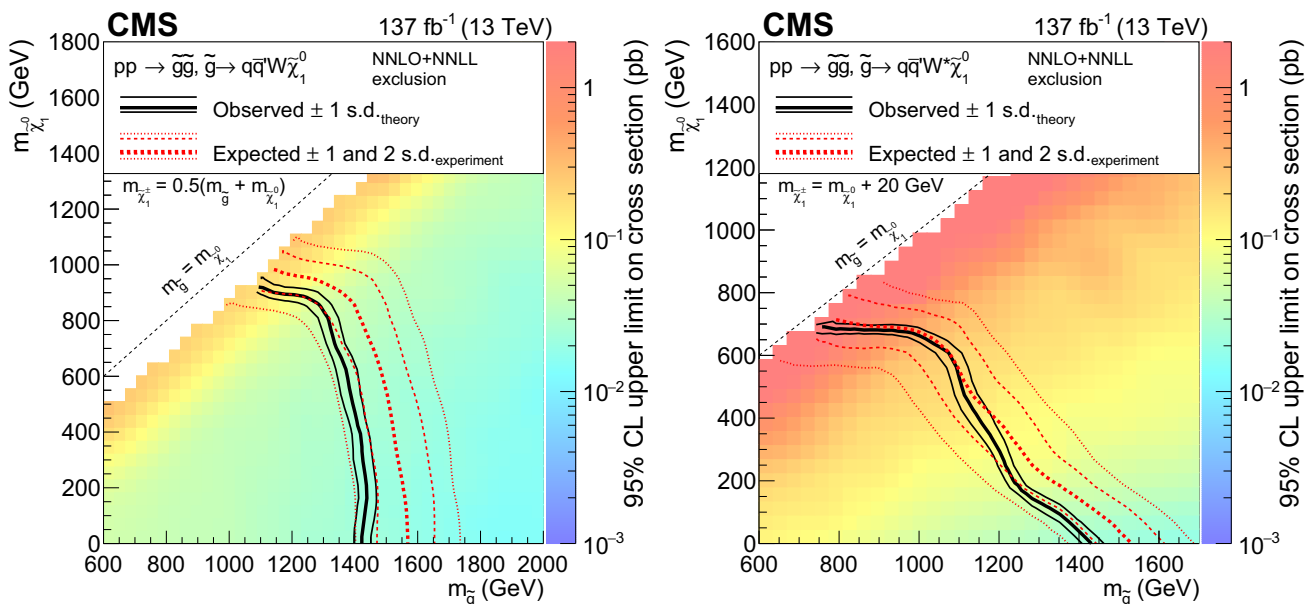
Fig. 9 Exclusion regions at 95% CL in the plane of $m_{\tilde{\chi}_1^0}$ versus $m_{\tilde{g}}$ for the T5qqqqWW model with $m_{\tilde{\chi}_1^\pm} = 0.5(m_{\tilde{g}} + m_{\tilde{\chi}_1^0})$ (left) and with $m_{\tilde{\chi}_1^\pm} = m_{\tilde{\chi}_1^0} + 20\,\text{GeV}$ (right). The notations are as in Fig. 7

7 Results and interpretation

The distributions of the variables used to define the SRs after the event selection are shown in Fig. 4. Background yields shown as stacked histograms in Figs. 4, 5, and 6 are those determined following the prescriptions detailed in Sect. 5. The overall data yields exceed expectation by an amount close to the systematic uncertainty. However, no particular

trend that is not covered by the uncertainties discussed in the previous sections, is seen in the distributions. The significance of the excess is of similar magnitude in all categories, with a maximum of around 2 standard deviations (s.d.) in the off-Z ML category.

The results of the search, broken down by SR, are presented in Figs. 5 and 6, and are summarized in Table 9. No significant deviation with respect to the SM background pre-

Fig. 10 Exclusion regions at 95% CL in the plane of $m_{\tilde{\chi}_1^\pm}$ versus $m_{\tilde{b}_1}$ for the T6ttWW model with $m_{\tilde{\chi}_1^0} = 50\,\text{GeV}$. The notations are as in Fig. 7

diction is observed. The largest excess of events found by fitting the data with the background-only hypothesis is in HH SR54, corresponding to a local significance of 2.6 s.d. Its neighboring bin, HH SR55, which is adjacent along the H_T dimension, has a deficit of events in the data corresponding to a significance of 1.8 s.d.

These results are then interpreted as experimental constraints on the cross sections for the signal models discussed in Sect. 2. For each model, event yields in all SRs are used to obtain exclusion limits on the production cross section at 95% confidence level (CL) with an asymptotic formulation of the modified frequentist CL_s criterion [82–85], where uncertainties are incorporated as nuisance parameters and profiled [84]. This procedure takes advantage of the differences in the distribution of events amongst the SR between the various SM backgrounds and the signal considered. The normalizations of the various backgrounds are in particular allowed to float within their uncertainties in the global fit, resulting in several backgrounds (nonprompt lepton, $t\bar{t}W/Z/H$ and rare processes) being pulled up by around 1 s.d. for most of the signal points considered, which are often characterized by a distinctive distribution of events across the SRs. This observation is consistent with the current measurements of $t\bar{t}W$ and $t\bar{t}Z$ processes performed by the ATLAS and CMS Collaborations [79,80]. The limits obtained are then used together with the theoretical cross section calculations to exclude regions of SUSY parameter space.

Figure 7 shows observed and expected exclusion limits for simplified models of gluino pair production with each gluino decaying to off- or on-shell third-generation squarks. These models were introduced in Sect. 2 and denoted as T1tttt, T5ttbbWW, T5tttt, and T5ttcc. Similarly, Figs. 8 and 9 show

the corresponding limits for T5qqqqWZ and T5qqqqWW, with two different assumptions on the chargino mass. Note that the T5qqqqWZ model assumes equal probabilities for the decay of the gluino into $\tilde{\chi}_1^+$, $\tilde{\chi}_1^-$, and $\tilde{\chi}_2^0$. The exclusion limits for T6ttWW and T6ttHZ are displayed in Figs. 10 and 11, respectively. In the T6ttHZ model, the heavier top squark decays into a lighter top squark and a Z or H boson. The three sets of exclusion limits shown in Fig. 11 correspond to the branching fraction $\mathcal{B}(\tilde{t}_2 \to \tilde{t}_1 Z)$ having values of 0, 50, and 100%.

Finally, Fig. 12 shows observed and expected limits on the cross section of gluino pair production as a function of the gluino masses in the two RPV models described in Sect. 2. The observed and expected exclusions on the gluino mass are similar and reach 2.1 and 1.7 TeV for the T1qqqqL and T1tbs models, respectively.

The analysis sensitivity for the various models studied in Figs. 7, 8, 9, 10 and 11 is often driven by the event yields in a few SRs (off-Z ML21, HH53 and HH52), where a slight excess of data is observed. This in particular applies to the uncompressed mass regime, resulting in an observed limit weaker than the expected one by one or two s.d. In the compressed mass regime, however, other SRs can become dominant, for example when the hadronic activity becomes limited. This happens in the T5qqqqWZ and T5qqqqWW models where the gluino and the lightest neutralino present a limited mass splitting (the region close to the diagonal in the left plots of Figs. 8, 9). In those scenarios the on-Z ML4 and HH3 SRs provide the best sensitivity, respectively. Additionally, if the intermediate chargino is nearly degenerate in mass with the lightest neutralino, both leptons become soft and LL SRs such as LL2 become relevant. Such a situation is encountered in the phase space region close to the diagonal in the right plots of Figs. 8 and 9. On-Z SRs (especially on-Z ML23) become important for models where an on-shell Z boson is produced (bottom plot in Fig. 11). The limits on the RPV models presented in Fig. 12 are mostly driven by another set of SRs (HH62 and LM11, the latter becoming more relevant for lower masses).

Compared to the previous versions of the analysis [24,25], the limits for the RPC models extend the gluino and squark mass observed and expected exclusions by up to 200 GeV because of the increase in the integrated luminosity and the corresponding re-optimization of SR definitions. These results also complement searches for gluino pair production conducted by CMS in final states with 0 or 1 lepton [86–88]. For the T1tttt scenario, the expected sensitivity of this analysis suffers from a lower branching fraction that makes it uncompetitive in the uncompressed mass regime. However, for a nearly degenerate mass spectrum, the SM background becomes of higher importance and the presence of an SS lepton pair significantly reduces it, leading to a similar sensitivity. The constraints on the two RPV models that were
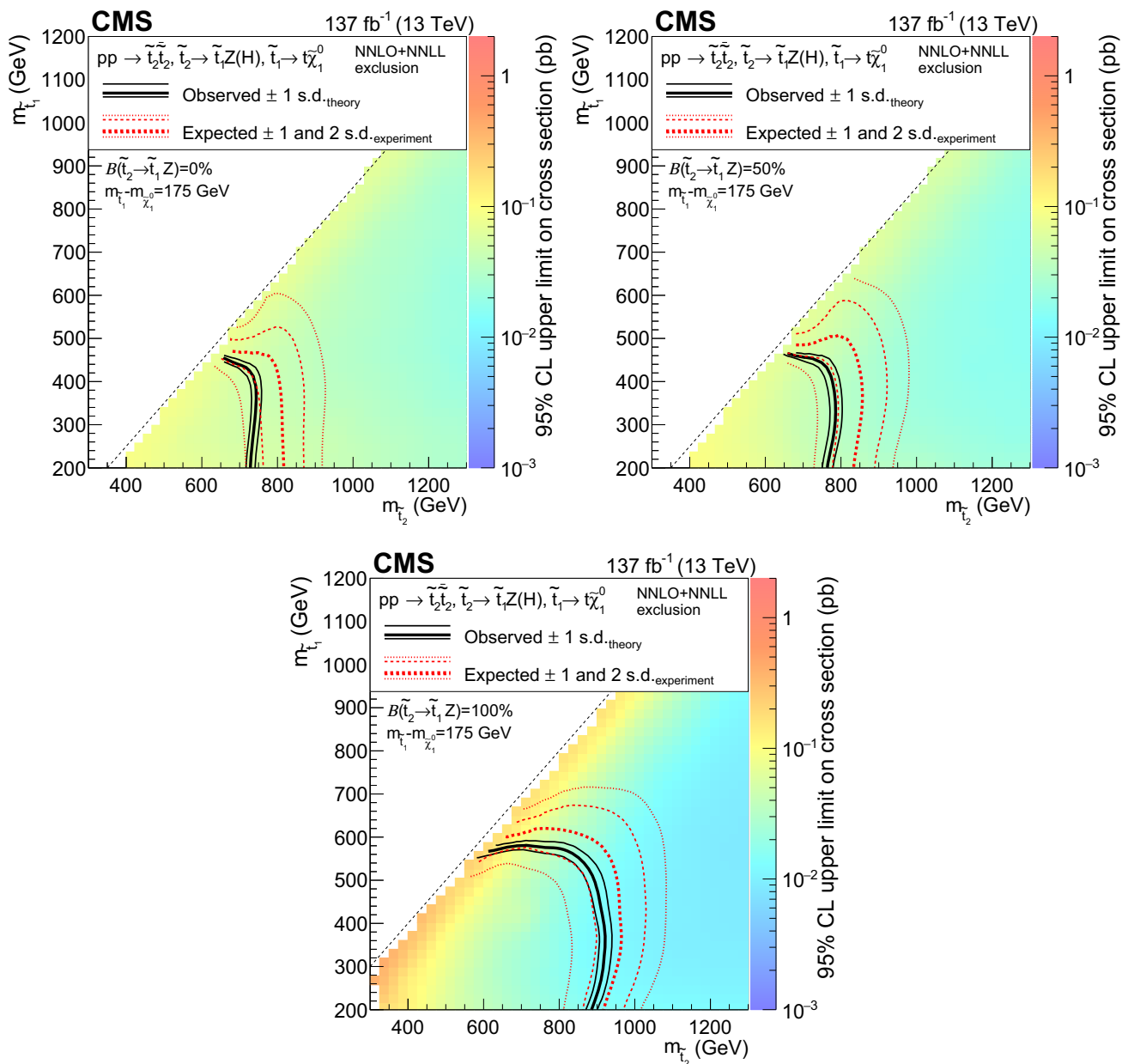
Fig. 11 Exclusion regions at 95% CL in the plane of $m(\tilde{t}_1)$ versus $m(\tilde{t}_2)$ for the T6ttHZ model with $m(\tilde{t}_1) - m(\tilde{\chi}_1^0) = 175\,\text{GeV}$. The three exclusions represent $\mathcal{B}(\tilde{t}_2 \to \tilde{t}_1 Z)$ of 0, 50, and 100%, respectively. The notations are as in Fig. 7

not previously included demonstrate the sensitivity of the analysis to RPV scenarios. The final state is particularly well suited to study the T1qqqqL model since no leptonic branching fraction penalty applies, resulting in exclusion limits on the gluino mass beyond 2.1 TeV, comparable to other results in fully hadronic final states [87,88]. The limits obtained on the T1tbs model are stronger than those previously obtained in the one-lepton channel based on the analysis of the 2016 dataset [89]. They are expected to remain competitive after an update with the full Run 2 dataset.

Model-independent limits are also set on the product of cross section, branching fraction, detector acceptance, and reconstruction efficiency, for the production of an SS lepton pair with at least two extra jets and $H_T > 300\,\text{GeV}$. For this purpose, we select events from the HH and LM categories and calculate limits as a function of minimum p_T^{miss} or H_T requirements starting at 300 and 1400 GeV, respectively. In order to remove the overlap between the two conditions, events selected for the H_T scan must also satisfy $p_T^{\text{miss}} < 300\,\text{GeV}$. The corresponding limits are presented in Fig. 13.
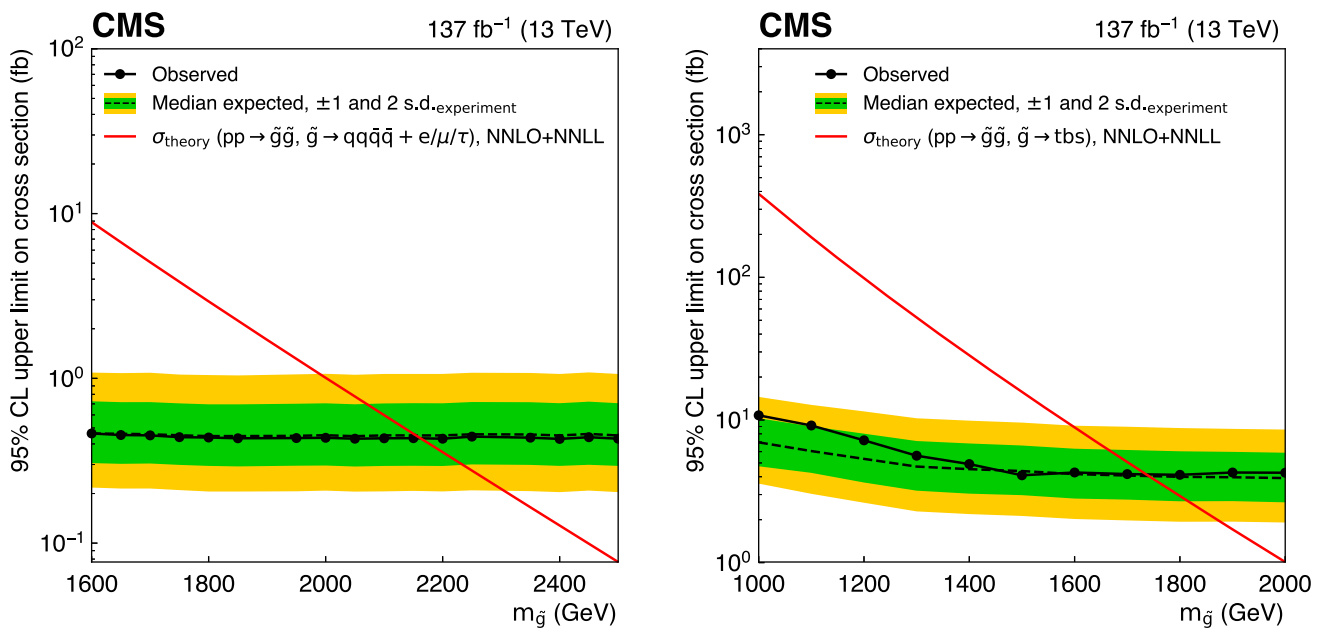
Fig. 12 Upper limits at 95% CL on the cross section for RPV gluino pair production with each gluino decaying into four quarks and one lepton (T1qqqqL, left), and each gluino decaying into a top, bottom, and strange quarks (T1tbs, right)
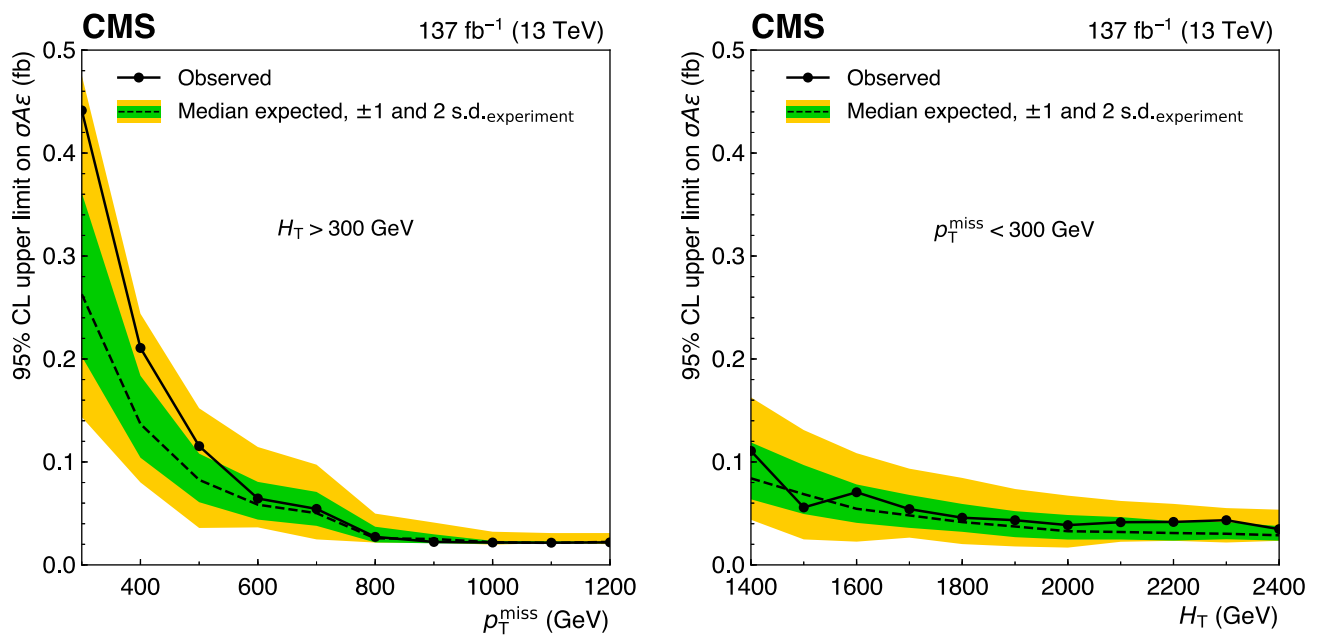
Fig. 13 Upper limits at 95% CL on the product of cross section, detector acceptance, and selection efficiency, $\sigma\mathcal{A}\epsilon$, for the production of an SS lepton pair with at least two jets, as a function of the minimum p_T^{miss} threshold, when $H_T > 300$ GeV (left), or the minimum H_T threshold, when $p_T^{miss} < 300$ GeV (right)

Finally, in order to facilitate reinterpretations of our results, we present in Table 10 the expected and observed yields for a number of inclusive SRs. This procedure focuses on events with large H_T, p_T^{miss}, N_b, and/or N_{jets}, and the SRs are defined such that they typically lead to 5 to 10 expected background events. The last column in the table indicates the upper limit at 95% CL on the number of BSM events in each SR.

8 Summary

A sample of events with two same-sign or at least three charged leptons (electrons or muons) produced in association with several jets in proton-proton collisions at 13 TeV, corresponding to an integrated luminosity of 137 fb^{-1}, has been studied to search for manifestations of physics beyond

Table 10 Inclusive SR definitions, expected background yields and uncertainties, and observed yields, as well as the observed 95% CL upper limits on the number of BSM events contributing to each region. No uncertainty in the signal acceptance is assumed in calculating these limits. A dash (–) indicates that a particular selection is not required

SR	Category	N_{jets}	N_{b}	H_{T} (GeV)	$p_{\text{T}}^{\text{miss}}$ (GeV)	$m_{\text{T}}^{\text{min}}$ (GeV)	SM expected	Obs.	$N_{\text{BSM}}^{\text{max}}$ (95% CL)
ISR1	HH	≥ 2	0	≥ 1000	≥ 250	–	12.7 ± 7.4	16	12.32
ISR2		≥ 2	≥ 2	≥ 1100	–	–	11.0 ± 3.8	14	11.33
ISR3		≥ 2	0	–	≥ 500	–	10.4 ± 9.7	13	11.26
ISR4		≥ 2	≥ 2	–	≥ 300	–	11.4 ± 3.8	17	14.22
ISR5		≥ 2	0	–	≥ 250	≥ 120	6.6 ± 5.7	10	10.77
ISR6		≥ 2	≥ 2	–	≥ 200	≥ 120	6.3 ± 1.3	8	8.22
ISR7		≥ 8	–	–	–	–	7.0 ± 2.8	12	12.17
ISR8		≥ 6	–	–	–	≥ 120	6.2 ± 1.4	10	10.45
ISR9		≥ 2	≥ 3	≥ 800	–	–	7.8 ± 3.5	8	7.53
ISR10	LL	≥ 2	–	≥ 700	–	–	10.4 ± 9.0	12	10.37
ISR11		≥ 2	–	–	≥ 200	–	12.1 ± 5.6	13	9.94
ISR12		≥ 6	–	–	–	–	7.1 ± 4.3	7	7.10
ISR13		≥ 2	≥ 3	–	–	–	1.61 ± 0.39	3	5.70
ISR14	LM	≥ 2	0	≥ 1200	< 50	–	3.6 ± 3.6	3	5.10
ISR15		≥ 2	≥ 2	≥ 1000	< 50	–	2.34 ± 0.51	4	6.41
ISR16	ML	≥ 2	0	≥ 1000	≥ 300	–	5.6 ± 1.6	7	7.78
ISR17		≥ 2	≥ 2	≥ 1000	–	–	5.7 ± 1.9	7	7.62

the standard model. The data are found to be consistent with the standard model expectations. The results are interpreted as limits on cross sections at 95% confidence level for the production of new particles in simplified supersymmetric models, considering both R parity conserving and violating scenarios. Using calculations for these cross sections as functions of particle masses, the limits are translated into lower mass limits that are as large as 2.1 TeV for gluinos and 0.9 TeV for top and bottom squarks, depending on the details of the model. The results extend the gluino and squark mass observed and expected exclusions by up to 200 GeV, compared to the previous versions of this analysis. Finally, to facilitate further interpretations of the search, model-independent limits are provided as a function of the missing transverse momentum and the scalar sum of jet transverse momenta in an event, together with the background prediction and data yields in a set of simplified signal regions.

Data Availability Statement This manuscript has no associated data or the data will not be deposited. [Authors' comment: Release and preservation of data used by the CMS Collaboration as the basis for publications is guided by the CMS policy as written in its document "CMS data preservation, re-use and open access policy" (https://cms-docdb.cern.ch/cgi-bin/PublicDocDB/RetrieveFile?docid=6032&filename=CMSDataPolicyV1.2.pdf&version=2)].

Compliance with ethical standards

Conflict of interest The authors declare that they have no conflict of interest.

Appendix A: Extended results

Tables 11, 12, 13, 14, 15 and 16, corresponding to Figs. 5 and 6, show background predictions per process within each signal region.

Table 11 Event yields in HH regions. Yields shown as "–" have a contribution smaller than 0.01, or do not contribute to a particular region

	$t\bar{t}W$	$t\bar{t}Z$	$t\bar{t}H$	WZ	WW	$X+\gamma$	Rare	Charge misid.	Nonprompt lep.	SM expected	Data
SR1	53±15	14.1±4.1	13.7±3.5	349±97	129±37	300±120	105±43	136±16	460±260	1560±300	1673
SR2	28.5±8.1	7.7±2.2	7.7±2.0	124±34	161±46	86±40	38±16	34.6±3.9	94±60	582±93	653
SR3	8.1±2.3	1.46±0.41	1.64±0.42	19.8±5.6	13.0±3.8	7.3±7.3	8.8±3.7	14.0±1.6	26±21	100±25	128
SR4	6.2±1.8	2.34±0.67	3.45±0.86	4.0±1.1	4.4±1.3	0.50±0.23	4.3±1.8	2.01±0.22	12.4±7.7	39.5±8.5	54
SR5	4.0±1.1	0.48±0.14	0.49±0.12	15.9±4.4	21.1±6.1	5.5±4.7	4.8±2.0	0.50±0.06	4.9±2.4	57.7±9.9	53
SR6	1.64±0.49	0.49±0.14	0.57±0.15	6.7±2.0	5.2±1.6	8.6±5.3	2.6±1.0	0.61±0.07	6.0±3.3	32.5±7.1	24
SR7	0.91±0.26	0.26±0.07	0.38±0.09	0.62±0.19	0.84±0.23	1.2±1.2	0.43±0.18	0.08±0.01	0.81±0.51	5.5±1.8	7
SR8	1.67±0.48	0.27±0.09	0.24±0.06	3.10±0.89	6.9±2.0	2.6±2.6	1.83±0.81	4.15±0.48	2.1±2.0	22.9±5.1	33
SR9	1.00±0.29	0.27±0.09	0.20±0.05	2.79±0.77	4.5±1.3	2.0±2.0	1.17±0.50	4.59±0.54	3.0±2.4	19.5±3.9	20
SR10	1.45±0.42	0.26±0.07	0.27±0.07	0.99±0.27	2.71±0.82	0.02±0.02	1.66±0.68	0.66±0.08	1.61±0.84	9.6±1.9	11
SR11	130±37	34.6±9.8	35.0±9.2	29.8±8.3	11.3±3.3	49±21	30±12	89±10	530±270	940±270	1115
SR12	80±22	21.2±6.0	22.3±5.7	14.2±3.9	15.8±4.7	24±11	16.3±6.7	21.7±2.5	125±76	340±81	384
SR13	12.8±3.6	1.96±0.56	1.97±0.51	1.54±0.44	0.77±0.29	1.43±0.90	1.35±0.54	3.91±0.44	10.6±8.3	36.3±9.5	40
SR14	6.5±1.8	1.93±0.56	1.96±0.51	0.54±0.19	0.31±0.13	1.05±0.57	1.03±0.42	4.15±0.47	9.4±6.9	26.8±7.4	26
SR15	13.9±3.9	4.0±1.2	6.4±1.6	0.44±0.15	0.67±0.20	0.67±0.32	3.5±1.4	1.16±0.13	12.1±7.0	42.7±8.6	68
SR16	7.8±2.2	4.0±1.2	6.2±1.6	0.35±0.11	0.35±0.10	0.86±0.41	2.7±1.1	1.18±0.13	14.4±7.9	37.9±8.6	41
SR17	9.3±2.7	1.21±0.35	1.38±0.35	1.86±0.53	1.96±0.57	3.3±3.3	1.74±0.70	0.89±0.10	4.9±3.1	26.5±6.2	29
SR18	4.1±1.2	1.05±0.31	1.30±0.33	0.72±0.21	0.54±0.16	0.76±0.39	0.94±0.39	0.95±0.11	4.0±3.1	14.3±3.6	13
SR19	2.76±0.78	0.87±0.25	1.24±0.32	0.14±0.04	0.14±0.04	1.6±1.5	0.73±0.31	0.20±0.02	2.9±1.5	10.6±2.5	12
SR20	4.9±1.4	0.76±0.22	0.60±0.15	0.54±0.17	0.66±0.19	1.7±1.7	0.72±0.31	1.17±0.13	1.2±1.2	12.3±2.9	14
SR21	2.66±0.74	0.68±0.20	0.59±0.15	0.27±0.13	0.62±0.18	0.53±0.25	0.59±0.25	1.27±0.14	1.9±1.9	9.2±2.7	17
SR22	4.5±1.3	0.75±0.22	1.00±0.25	0.16±0.06	0.30±0.09	0.42±0.19	1.30±0.55	0.49±0.05	1.2±1.2	10.1±2.1	17
SR23	77±22	20.5±5.9	22.2±6.0	1.62±0.51	0.59±0.17	22.4±9.3	8.8±3.7	56.9±6.5	61±31	272±43	354
SR24	55±16	14.8±4.2	16.8±4.4	1.16±0.35	0.85±0.25	9.4±3.6	7.8±3.2	13.6±1.6	27±15	147±25	177
SR25	7.5±2.2	1.05±0.30	1.19±0.32	0.09±0.03	–	0.60±0.35	0.79±0.33	2.18±0.25	1.9±1.7	15.3±2.9	12
SR26	4.1±1.2	0.89±0.28	1.29±0.34	0.02±0.02	0.02±0.01	0.76±0.35	0.53±0.22	2.14±0.25	1.7±1.7	11.4±2.4	19
SR27	12.2±3.6	3.7±1.1	6.0±1.6	0.15±0.06	0.05±0.03	1.01±0.49	3.9±1.6	0.96±0.11	5.4±2.8	33.4±5.4	49
SR28	7.4±2.1	3.6±1.1	6.0±1.6	0.02±0.01	0.12±0.04	0.95±0.40	3.3±1.4	1.06±0.12	7.6±3.3	30.1±4.9	38
SR29	5.4±1.5	0.61±0.18	0.79±0.21	0.16±0.06	0.04±0.03	0.16±0.09	0.65±0.27	0.39±0.04	2.2±1.5	10.4±2.2	9
SR30	2.68±0.80	0.57±0.15	0.80±0.21	0.20±0.06	0.08±0.03	0.47±0.23	0.37±0.15	0.48±0.06	0.94±0.79	6.6±1.3	7
SR31	2.74±0.84	0.56±0.17	1.16±0.30	0.06±0.02	0.07±0.03	0.15±0.06	1.10±0.46	0.18±0.02	0.92±0.92	6.9±1.5	6

Table 11 continued

	t̄W	t̄Z	t̄H	WZ	WW	X+γ	Rare	Charge misid.	Nonprompt lep.	SM expected	Data
SR32	3.41±0.96	0.60±0.18	0.47±0.12	–	0.05±0.02	0.35±0.17	0.38±0.16	0.52±0.06	0.10±0.10	5.9±1.1	14
SR33	2.09±0.60	0.59±0.18	0.58±0.15	–	0.01±0.01	0.24±0.12	0.31±0.13	0.55±0.06	1.7±1.3	6.1±1.6	7
SR34	2.97±0.90	0.67±0.20	0.81±0.21	0.02±0.00	0.08±0.03	0.24±0.10	1.12±0.46	0.33±0.04	0.58±0.58	6.8±1.3	10
SR35	3.25±0.95	0.83±0.26	1.19±0.33	–	–	0.27±0.22	0.57±0.25	0.95±0.11	1.75±0.98	8.8±1.5	16
SR36	1.83±0.55	0.80±0.24	1.22±0.34	–	–	0.48±0.28	0.49±0.21	0.97±0.11	2.9±1.8	8.7±2.0	11
SR37	3.3±1.0	0.98±0.30	1.11±0.31	–	0.02±0.01	0.40±0.17	1.03±0.42	0.55±0.06	2.0±1.3	9.4±1.9	7
SR38	1.93±0.58	0.89±0.26	1.07±0.30	0.01±0.01	–	0.38±0.27	0.97±0.40	0.56±0.07	1.17±0.80	7.0±1.3	5
SR39	2.16±0.65	0.65±0.21	1.16±0.33	0.02±0.01	–	0.22±0.09	3.4±1.4	0.20±0.02	1.7±1.1	9.6±2.1	9
SR40	1.54±0.49	0.82±0.28	1.29±0.36	–	–	0.36±0.17	3.1±1.3	0.21±0.03	1.26±0.67	8.6±1.7	11
SR41	0.46±0.14	0.14±0.04	0.16±0.05	–	–	0.07±0.04	0.13±0.05	0.14±0.02	–	1.10±0.32	2
SR42	0.24±0.09	0.08±0.05	0.08±0.03	–	–	0.02±0.02	0.17±0.07	0.04±0.01	–	0.63±0.49	0
SR43	0.21±0.09	0.04±0.04	0.07±0.02	–	–	0.12±0.12	0.14±0.06	0.04±0.01	0.04±0.04	0.67±0.60	1
SR44	0.14±0.04	0.03±0.01	0.08±0.02	–	–	0.02±0.01	0.39±0.16	0.04±0.00	0.04±0.04	0.74±0.27	1
SR45	0.16±0.08	0.04±0.04	0.07±0.03	0.03±0.03	–	0.04±0.04	0.36±0.15	0.01±0.01	–	0.71±0.53	1
SR46	9.6±2.8	0.93±0.26	0.91±0.23	8.3±2.3	14.7±4.3	6.9±6.8	3.5±1.5	0.61±0.07	2.3±2.0	47.8±9.7	59
SR47	3.5±1.0	0.84±0.28	0.92±0.23	3.04±0.84	2.92±0.88	1.9±1.9	1.51±0.62	0.66±0.07	2.0±1.4	17.3±3.8	24
SR48	1.27±0.40	0.12±0.04	0.05±0.02	1.64±0.46	4.7±1.4	1.8±1.8	0.44±0.18	0.05±0.01	0.20±0.16	10.3±2.9	11
SR49	0.37±0.11	0.13±0.04	0.08±0.02	0.62±0.23	0.41±0.13	0.02±0.01	0.34±0.17	0.04±0.00	0.03±0.03	2.06±0.49	3
SR50	2.57±0.79	0.30±0.10	0.54±0.15	0.43±0.12	0.72±0.23	0.06±0.03	1.11±0.45	0.09±0.01	0.72±0.31	6.5±1.1	13
SR51	1.16±0.38	0.35±0.14	0.57±0.15	0.20±0.07	0.15±0.06	0.02±0.01	0.79±0.34	0.08±0.01	0.40±0.38	3.72±0.79	4
SR52	0.45±0.12	0.06±0.02	0.05±0.02	0.22±0.09	0.15±0.05	0.02±0.01	0.20±0.08	–	0.05±0.05	1.21±0.29	4
SR53	0.20±0.09	0.05±0.04	0.06±0.03	–	0.03±0.03	–	0.08±0.04	0.01±0.01	–	0.44±0.44	2
SR54	1.75±0.53	0.26±0.09	0.23±0.07	0.95±0.29	4.6±1.4	0.65±0.58	0.63±0.27	0.46±0.05	0.29±0.12	9.8±1.8	24
SR55	0.99±0.28	0.15±0.05	0.12±0.04	0.78±0.23	4.0±1.1	0.03±0.03	0.58±0.24	0.35±0.04	0.33±0.33	7.3±1.4	4
SR56	0.57±0.16	0.04±0.01	0.07±0.02	0.39±0.13	2.46±0.72	0.34±0.34	0.17±0.07	0.18±0.02	0.22±0.17	4.44±0.98	6
SR57	2.04±0.59	0.48±0.13	0.53±0.16	0.29±0.10	0.47±0.15	0.04±0.02	0.71±0.29	0.22±0.03	0.89±0.73	5.7±1.1	6
SR58	1.65±0.56	0.17±0.05	0.30±0.09	0.14±0.05	0.47±0.15	–	0.70±0.31	0.13±0.02	0.48±0.48	4.0±1.0	6
SR59	0.99±0.35	0.06±0.02	0.16±0.06	0.15±0.06	0.37±0.11	–	0.27±0.12	0.13±0.01	0.11±0.11	2.24±0.53	2
SR60	0.61±0.18	0.08±0.04	0.33±0.09	–	0.01±0.01	0.03±0.02	0.67±0.29	0.04±0.00	0.06±0.06	1.83±0.44	5
SR61	0.65±0.21	0.12±0.04	0.20±0.06	0.08±0.05	0.09±0.03	–	0.50±0.20	0.03±0.00	0.19±0.14	1.88±0.40	5
SR62	0.41±0.12	0.05±0.02	0.14±0.05	0.04±0.01	0.03±0.01	0.01±0.01	0.22±0.09	0.02±0.00	0.43±0.43	1.35±0.56	0
Total	610±180	158±40	180±44	600±160	420±120	540±250	280±150	409±43	1460±740	4660±880	5376

Table 12 Event yields in HL regions. Yields shown as "—" have a contribution smaller than 0.01, or do not contribute to a particular region

	$t\bar{t}W$	$t\bar{t}Z$	$t\bar{t}H$	WZ	WW	X+γ	Rare	Charge misid.	Nonprompt lep.	SM expected	Data
SR1	17.5±4.9	6.2±1.8	6.8±1.8	168±47	49±14	145±67	51±21	33.6±3.8	910±290	1390±300	1593
SR2	7.2±2.1	2.63±0.76	3.21±0.82	38±10	46±13	41±25	11.3±4.8	6.54±0.73	192±62	348±67	337
SR3	0.97±0.28	0.20±0.07	0.34±0.09	5.0±1.4	2.24±0.68	0.04±0.04	1.88±0.79	0.24±0.03	16.0±5.3	26.9±8.8	39
SR4	1.85±0.54	0.81±0.23	1.67±0.42	1.19±0.34	1.45±0.42	0.30±0.13	1.25±0.50	0.48±0.06	26.9±9.1	35.9±9.1	34
SR5	1.15±0.33	0.20±0.06	0.23±0.06	5.5±1.5	7.8±2.3	4.2±3.7	1.12±0.46	0.10±0.01	9.4±3.0	29.8±6.0	34
SR6	0.36±0.10	0.21±0.07	0.22±0.06	2.73±0.76	1.43±0.43	8.4±6.7	0.49±0.22	0.19±0.02	8.2±2.5	22.2±7.2	12
SR7	0.22±0.07	0.10±0.05	0.19±0.05	0.29±0.10	0.25±0.09	0.07±0.04	0.32±0.14	0.02±0.00	3.2±1.4	4.7±1.4	6
SR8	46±13	16.5±4.7	18.0±4.7	14.6±4.0	3.4±1.0	36±16	13.5±5.5	25.4±2.9	920±280	1100±280	1342
SR9	22.0±6.2	8.2±2.3	9.9±2.5	4.4±1.2	4.1±1.2	8.8±3.8	4.6±1.9	4.53±0.51	232±70	299±71	330
SR10	1.65±0.48	0.27±0.08	0.35±0.09	0.16±0.05	0.16±0.05	0.64±0.29	0.22±0.11	0.23±0.03	5.5±2.1	9.1±2.3	8
SR11	0.81±0.25	0.23±0.08	0.41±0.11	0.12±0.05	0.05±0.02	0.17±0.09	0.21±0.09	0.20±0.02	4.2±1.6	6.4±1.6	9
SR12	4.2±1.2	1.26±0.38	3.23±0.82	0.08±0.03	0.25±0.10	1.58±0.86	0.85±0.34	0.29±0.03	30.3±9.0	42.1±9.2	49
SR13	1.95±0.58	1.37±0.41	3.18±0.81	0.10±0.06	0.06±0.02	1.14±0.44	0.92±0.38	0.32±0.04	24.0±8.2	33.0±8.4	39
SR14	4.3±1.3	0.88±0.25	1.16±0.30	1.14±0.33	0.90±0.26	0.51±0.23	0.59±0.25	0.45±0.05	15.9±5.5	25.8±5.9	25
SR15	0.62±0.23	0.10±0.10	0.30±0.09	—	0.04±0.04	0.03±0.03	0.15±0.08	0.03±0.01	1.6±1.6	2.8±2.0	7
SR16	0.30±0.11	0.17±0.08	0.34±0.09	0.06±0.06	0.02±0.02	—	0.14±0.07	0.03±0.01	1.4±1.2	2.5±1.3	2
SR17	28.9±8.2	10.3±3.0	11.7±3.1	0.68±0.21	0.09±0.04	15.6±6.7	3.9±1.6	17.9±2.1	133±39	222±42	260
SR18	16.8±4.8	6.2±1.8	7.9±2.1	0.53±0.15	0.24±0.08	6.4±2.6	2.40±1.00	3.34±0.38	43±13	86±15	104
SR19	0.72±0.24	0.12±0.04	0.28±0.07	—	—	0.04±0.04	0.05±0.03	0.13±0.01	0.87±0.69	2.22±0.90	4
SR20	0.58±0.17	0.11±0.04	0.26±0.07	0.05±0.03	0.03±0.02	0.12±0.05	0.09±0.04	0.13±0.01	1.8±1.1	3.2±1.1	4
SR21	4.4±1.3	1.69±0.47	3.13±0.82	—	0.11±0.03	2.5±1.9	1.23±0.50	0.25±0.03	6.5±2.2	19.8±3.8	28
SR22	2.06±0.57	1.41±0.41	3.15±0.82	—	—	1.01±0.49	0.95±0.38	0.23±0.03	7.3±2.5	16.1±3.0	19
SR23	1.96±0.56	0.21±0.08	0.42±0.11	0.05±0.02	0.09±0.04	0.21±0.09	0.16±0.07	0.12±0.01	1.5±1.0	4.7±1.3	1
SR24	0.83±0.25	0.27±0.09	0.37±0.10	0.09±0.04	0.01±0.01	0.17±0.08	0.16±0.06	0.15±0.02	1.9±1.2	4.0±1.2	2

Table 12 continued

	$t\bar{t}W$	$t\bar{t}Z$	$t\bar{t}H$	WZ	WW	$X+\gamma$	Rare	Charge misid.	Nonprompt lep.	SM expected	Data
SR25	1.11±0.34	0.26±0.08	0.57±0.15	–	–	0.21±0.09	0.31±0.13	0.05±0.01	1.52±0.98	4.0±1.1	5
SR26	1.02±0.30	0.41±0.12	0.61±0.17	–	0.01±0.00	0.49±0.20	0.21±0.09	0.27±0.03	5.4±2.3	8.5±2.4	7
SR27	0.53±0.15	0.47±0.14	0.60±0.17	–	–	0.53±0.22	0.17±0.08	0.28±0.03	5.8±2.5	8.4±2.5	7
SR28	1.36±0.41	0.60±0.20	1.14±0.31	–	–	0.21±0.09	1.02±0.42	0.18±0.02	4.4±2.0	8.9±2.2	11
SR29	0.92±0.28	0.43±0.14	1.12±0.31	–	–	0.34±0.14	0.98±0.41	0.22±0.03	6.9±3.0	10.9±3.1	11
SR30	0.36±0.13	0.15±0.05	0.20±0.06	–	–	0.02±0.01	0.30±0.12	0.03±0.00	0.18±0.18	1.25±0.39	3
SR31	0.41±0.12	0.05±0.02	0.17±0.04	0.15±0.05	0.12±0.05	0.05±0.02	0.08±0.04	0.09±0.01	0.81±0.29	1.92±0.37	4
SR32	0.73±0.24	0.06±0.02	0.19±0.05	0.18±0.07	0.31±0.11	0.06±0.03	0.33±0.14	0.07±0.01	0.83±0.38	2.77±0.56	3
SR33	2.51±0.71	0.32±0.08	0.33±0.09	2.66±0.76	5.0±1.4	0.16±0.16	1.62±0.69	0.12±0.01	6.4±1.9	19.1±4.1	23
SR34	0.99±0.27	0.24±0.07	0.30±0.08	1.19±0.34	0.70±0.21	0.08±0.05	0.72±0.32	0.11±0.01	3.2±1.2	7.5±1.5	9
SR35	0.30±0.09	0.03±0.01	0.03±0.01	0.55±0.17	0.95±0.30	0.01±0.01	0.15±0.08	–	0.09±0.09	2.12±0.49	5
SR36	0.11±0.05	0.02±0.02	–	0.10±0.10	0.06±0.06	–	0.08±0.08	–	0.09±0.09	0.47±0.33	1
SR37	0.71±0.21	0.13±0.04	0.20±0.05	0.18±0.06	0.34±0.10	0.01±0.01	0.19±0.09	0.02±0.00	0.96±0.65	2.75±0.77	4
SR38	0.19±0.06	0.11±0.04	0.21±0.06	0.02±0.02	0.06±0.02	0.01±0.01	0.18±0.08	0.02±0.00	0.88±0.45	1.68±0.50	0
SR39	0.21±0.08	0.02±0.02	0.03±0.01	–	0.07±0.06	–	0.04±0.02	–	0.59±0.59	0.97±0.97	0
SR40	0.60±0.17	0.05±0.04	0.18±0.05	0.11±0.08	1.01±0.30	–	0.30±0.13	0.05±0.01	0.54±0.43	2.83±0.70	7
SR41	0.24±0.12	0.12±0.07	0.18±0.06	0.05±0.05	0.17±0.12	2.1±2.1	0.11±0.06	0.04±0.01	0.79±0.54	3.8±3.8	0
SR42	0.92±0.29	0.12±0.04	0.15±0.05	0.27±0.08	1.59±0.46	0.03±0.01	0.21±0.09	0.06±0.01	1.57±0.81	4.9±1.0	9
SR43	0.24±0.07	0.11±0.04	0.21±0.07	0.16±0.05	0.32±0.10	0.51±0.51	0.19±0.08	0.09±0.01	0.53±0.20	2.36±0.72	5
Total	180±52	63±16	83±20	248±64	129±36	270±120	105±56	97±10	2640±590	3820±620	4402

Table 13 Event yields in LL regions. Yields shown as "–" have a contribution smaller than 0.01, or do not contribute to a particular region

	t$\bar{\text{t}}$W	t$\bar{\text{t}}$Z	t$\bar{\text{t}}$H	WZ	WW	X+γ	Rare	Charge misid.	Nonprompt lep.	SM expected	Data
SR1	0.34±0.10	0.27±0.08	0.30±0.08	1.93±0.57	2.27±0.66	0.41±0.28	0.38±0.17	0.06±0.01	17.0±7.2	23.0±7.2	29
SR2	0.10±0.04	0.05±0.03	0.07±0.02	0.93±0.31	0.86±0.25	0.03±0.01	0.37±0.16	–	2.6±1.5	5.0±1.6	6
SR3	1.00±0.27	0.90±0.26	1.03±0.26	0.19±0.06	0.14±0.04	0.14±0.14	0.33±0.14	0.09±0.01	19.9±6.5	23.8±6.6	27
SR4	0.47±0.14	0.11±0.03	0.28±0.07	0.05±0.02	0.08±0.02	0.09±0.04	0.19±0.08	0.01±0.00	3.4±1.5	4.7±1.5	7
SR5	0.92±0.26	0.68±0.20	0.96±0.25	0.01±0.00	0.02±0.02	0.16±0.14	0.28±0.12	0.09±0.01	4.8±1.8	8.0±1.9	15
SR6	0.33±0.13	0.14±0.07	0.21±0.06	–	0.04±0.04	0.03±0.03	0.05±0.02	0.02±0.01	1.2±1.1	2.0±1.1	0
SR7	0.17±0.06	0.09±0.03	0.19±0.06	–	–	0.12±0.05	0.21±0.09	0.02±0.00	0.81±0.56	1.61±0.59	3
SR8	0.02±0.02	0.01±0.01	0.01±0.01	–	–	–	–	–	–	0.06±0.06	0
Total	3.36±0.98	2.25±0.60	3.04±0.80	3.09±0.82	3.42±0.96	0.79±0.42	1.84±0.97	0.30±0.03	50±13	68±13	87

Table 14 Event yields in on-Z ML regions. Yields shown as "–" have a contribution smaller than 0.01, or do not contribute to a particular region

	t$\bar{\text{t}}$W	t$\bar{\text{t}}$Z	t$\bar{\text{t}}$H	WZ	X+γ	Rare	Nonprompt lep.	SM expected	Data
SR1	1.12±0.30	46±13	1.67±0.43	620±170	11.9±5.7	105±42	54±18	840±170	985
SR2	0.71±0.21	6.8±1.9	0.46±0.12	68±19	3.1±2.6	17.8±7.3	9.9±4.6	107±21	136
SR3	0.18±0.05	8.5±2.4	0.23±0.06	95±26	0.02±0.01	11.7±4.8	3.2±1.8	119±27	146
SR4	0.17±0.06	1.99±0.54	0.17±0.04	5.8±1.6	0.03±0.01	2.19±0.87	0.68±0.46	11.1±2.1	10
SR5	0.13±0.04	7.7±2.2	0.25±0.06	83±23	2.3±1.2	11.0±4.5	4.5±2.1	109±24	126
SR6	0.09±0.03	1.42±0.39	0.06±0.02	13.6±3.8	0.74±0.61	2.5±1.0	0.93±0.69	19.3±4.1	24
SR7	0.10±0.03	2.55±0.73	0.09±0.02	35±10	0.09±0.04	3.7±1.6	0.89±0.53	42±10	47
SR8	0.11±0.03	0.45±0.15	0.04±0.01	2.02±0.67	–	0.61±0.25	0.25±0.18	3.47±0.84	3
SR9	5.6±1.6	140±39	6.1±1.6	52±14	5.3±2.4	72±29	46±17	327±54	419
SR10	1.70±0.48	23.4±6.7	1.18±0.31	7.6±2.1	0.20±0.09	9.1±3.8	3.2±2.0	46.5±8.4	53
SR11	0.61±0.17	25.9±7.5	0.98±0.25	11.0±3.0	0.27±0.16	9.5±3.9	3.1±1.3	51.3±9.1	62
SR12	0.30±0.08	7.5±2.1	0.36±0.09	3.48±0.99	0.04±0.02	2.9±1.2	0.95±0.67	15.6±2.8	27
SR13	4.8±1.4	89±25	4.5±1.2	3.7±1.0	2.17±0.90	22.4±9.0	4.9±1.9	131±27	162
SR14	0.98±0.29	13.4±3.9	0.76±0.20	0.62±0.19	0.09±0.03	2.8±1.1	1.24±0.83	19.9±4.3	26
SR15	0.54±0.16	20.3±5.8	0.91±0.24	0.96±0.29	0.13±0.06	3.7±1.5	0.42±0.31	26.9±6.1	35
SR16	0.25±0.08	5.2±1.6	0.34±0.09	0.38±0.12	0.05±0.02	1.17±0.48	0.38±0.38	7.8±1.8	12
SR17	0.12±0.04	9.5±2.8	0.56±0.16	0.24±0.07	0.04±0.02	2.22±0.90	1.25±0.98	14.0±3.1	19
SR18	0.52±0.16	20.5±5.9	0.84±0.22	44±12	1.8±1.1	11.7±4.8	4.8±1.6	84±15	117
SR19	0.20±0.06	3.8±1.1	0.24±0.06	8.2±2.3	0.83±0.61	3.3±1.3	1.66±0.84	18.2±3.3	26
SR20	0.34±0.11	9.5±2.7	0.48±0.12	23.5±6.5	0.01±0.01	5.3±2.2	1.34±0.66	40.4±7.6	34
SR21	0.36±0.10	1.75±0.51	0.17±0.05	1.52±0.48	0.01±0.01	0.89±0.36	0.23±0.10	4.92±0.88	7
SR22	0.28±0.09	7.0±2.0	0.20±0.05	32.3±9.1	–	6.3±2.6	0.87±0.34	46.9±9.9	50
SR23	0.34±0.10	1.68±0.48	0.12±0.03	2.02±0.59	–	1.16±0.46	0.50±0.50	5.8±1.2	10
Total	19.5±5.6	450±110	20.8±5.0	1110±280	29±12	310±160	145±41	2090±360	2536

Table 15 Event yields in off-Z ML regions. Yields shown as "–" have a contribution smaller than 0.01, or do not contribute to a particular region

	t̄tW	t̄tZ	t̄tH	WZ	X+γ	Rare	Nonprompt lep.	SM expected	Data
SR1	8.8±2.5	11.2±3.2	7.0±1.8	87±24	18.8±9.5	22.0±9.0	68±25	222±36	285
SR2	0.15±0.07	0.15±0.08	0.10±0.03	1.23±0.50	0.02±0.02	0.43±0.22	0.61±0.61	2.7±1.7	2
SR3	2.38±0.69	2.07±0.59	1.60±0.42	13.6±3.8	0.26±0.11	4.2±1.7	11.3±4.9	35.5±6.4	34
SR4	0.18±0.06	0.14±0.04	0.08±0.02	0.24±0.11	–	0.22±0.12	0.13±0.13	0.99±0.31	2
SR5	1.11±0.31	1.64±0.47	1.02±0.26	11.2±3.1	0.89±0.84	1.68±0.68	4.6±2.0	22.1±4.0	29
SR6	0.91±0.25	0.64±0.19	0.59±0.15	4.7±1.4	0.05±0.02	1.05±0.44	1.76±0.80	9.7±1.7	8
SR7	26.8±7.5	29.7±8.5	21.9±5.7	7.0±2.0	6.9±3.3	11.3±4.7	113±41	217±44	272
SR8	7.9±2.3	5.0±1.5	4.6±1.2	1.14±0.36	0.87±0.37	2.43±0.99	15.7±5.6	37.7±6.8	56
SR9	3.8±1.1	5.3±1.5	3.47±0.89	0.82±0.26	0.86±0.40	1.91±0.78	5.2±2.5	21.4±3.7	21
SR10	2.69±0.78	1.78±0.52	1.76±0.45	0.35±0.12	0.27±0.11	1.07±0.45	2.9±1.4	10.9±1.9	18
SR11	22.1±6.4	19.5±5.7	16.1±4.3	0.44±0.13	6.4±2.6	5.1±2.1	19.4±6.6	89±14	112
SR12	5.0±1.5	2.99±0.86	2.93±0.79	0.09±0.03	0.64±0.27	1.28±0.53	2.67±0.94	15.6±2.4	20
SR13	3.22±0.96	4.2±1.2	3.21±0.84	0.12±0.05	0.56±0.24	1.56±0.64	3.5±1.7	16.4±2.7	23
SR14	1.53±0.45	1.31±0.38	1.23±0.32	–	0.16±0.07	0.77±0.32	0.36±0.36	5.36±0.95	7
SR15	0.91±0.28	2.00±0.60	1.94±0.54	0.03±0.01	0.26±0.11	2.6±1.1	1.27±0.83	9.0±1.6	12
SR16	4.6±1.4	4.6±1.3	3.30±0.87	5.4±1.5	1.9±1.1	3.4±1.4	5.3±1.7	28.4±3.9	46
SR17	0.13±0.06	0.18±0.07	0.05±0.02	0.19±0.19	–	0.16±0.11	–	0.72±0.41	2
SR18	3.7±1.1	2.24±0.67	2.42±0.66	3.8±1.1	0.15±0.07	3.1±1.3	2.4±1.1	17.8±2.8	25
SR19	0.25±0.09	0.18±0.05	0.07±0.02	0.10±0.03	–	0.26±0.12	0.04±0.04	0.89±0.29	0
SR20	3.4±1.0	1.71±0.50	1.59±0.42	4.2±1.2	0.12±0.05	3.1±1.3	3.6±2.0	17.7±3.3	31
SR21	0.28±0.09	0.21±0.06	0.07±0.02	0.16±0.07	–	0.36±0.15	0.12±0.12	1.20±0.32	2
Total	100±29	97±24	75±19	141±36	38±18	68±36	262±73	780±100	1007

Table 16 Event yields in LM regions. Yields shown as "–" have a contribution smaller than 0.01, or do not contribute to a particular region

	t̄tW	t̄tZ	t̄tH	WZ	WW	X+γ	Rare	Charge misid.	Nonprompt lep.	SM expected	Data
SR1	7.7±2.1	2.86±0.84	2.22±0.57	56±15	53±15	38±19	12.5±5.3	13.4±1.5	51±36	235±47	309
SR2	1.69±0.50	1.06±0.30	1.12±0.28	1.99±0.56	1.80±0.53	3.5±2.3	1.14±0.53	0.70±0.08	6.3±4.3	19.3±5.2	26
SR3	23.0±6.4	8.6±2.5	7.1±1.9	5.9±1.7	5.5±1.6	14.8±7.7	6.1±2.6	6.97±0.79	64±37	142±39	156
SR4	6.3±1.8	3.15±0.89	4.4±1.1	0.34±0.09	0.25±0.10	1.22±0.57	1.96±0.81	0.77±0.09	13.8±8.2	32.2±8.8	38
SR5	17.6±5.0	6.1±1.7	5.6±1.5	0.48±0.14	0.37±0.12	4.2±2.1	2.6±1.1	4.71±0.54	11.4±5.8	53.0±9.1	69
SR6	6.0±1.7	3.17±0.91	4.2±1.1	0.10±0.04	0.12±0.04	1.05±0.45	2.00±0.83	0.68±0.08	4.8±3.0	22.0±4.0	30
SR7	2.37±0.71	1.19±0.36	1.42±0.40	0.08±0.03	–	0.61±0.36	2.08±0.86	0.53±0.06	1.8±1.4	10.1±2.0	21
SR8	0.09±0.05	0.01±0.01	0.02±0.01	0.23±0.10	0.80±0.22	–	0.04±0.02	0.06±0.01	0.27±0.27	1.53±0.48	3
SR9	0.36±0.11	0.17±0.06	0.11±0.03	0.12±0.04	0.11±0.04	0.17±0.10	0.19±0.08	0.03±0.00	0.32±0.30	1.58±0.41	0
SR10	0.16±0.08	0.04±0.03	0.01±0.01	0.25±0.17	0.77±0.27	1.3±1.3	0.10±0.10	0.06±0.02	0.16±0.16	2.9±2.9	1
SR11	0.44±0.18	0.02±0.02	0.08±0.03	–	0.13±0.08	0.01±0.01	0.16±0.07	0.05±0.02	0.41±0.41	1.31±0.93	4
Total	66±19	26.3±6.6	26.2±6.5	65±17	62±18	65±32	29±16	27.9±3.0	154±89	520±110	657

Appendix B: Top five SRs for several representative models

Table 17 presents the top five SRs for several representative models, ranked based on the largest values of $N_{\text{sig.}}/\sqrt{N_{\text{bkg.}} + N_{\text{sig.}}}$, where $N_{\text{sig.}}$ and $N_{\text{bkg.}}$ are the signal and total background yields in each SR, respectively.

Table 17 Top five SRs for several representative models, ranked based on the largest values of $N_{\text{sig.}}/\sqrt{N_{\text{bkg.}} + N_{\text{sig.}}}$, where $N_{\text{sig.}}$ and $N_{\text{bkg.}}$ are the signal and total background yields in each SR, respectively

Model	Mass point	Top SRs
T1tttt	$m_{\tilde{g}} = 1400, m_{\tilde{\chi}_1^0} = 400$	off-Z ML21, HH53, HH52, HH51, HH50
T1tttt	$m_{\tilde{g}} = 2000, m_{\tilde{\chi}_1^0} = 100$	HH53, HH52, off-Z ML21, HL39, HH49
T1tttt	$m_{\tilde{g}} = 1800, m_{\tilde{\chi}_1^0} = 100$	HH53, off-Z ML21, HH52, HL39, HH51
T1tttt	$m_{\tilde{g}} = 1800, m_{\tilde{\chi}_1^0} = 1000$	off-Z ML21, HH53, HH52, HH51, HH50
T1tttt	$m_{\tilde{g}} = 1800, m_{\tilde{\chi}_1^0} = 1550$	HH53, HL39, off-Z ML21, HH49, HH52
T6ttWW	$m_{\tilde{b}_1} = 1000, m_{\tilde{\chi}_1^\pm} = 600$	off-Z ML21, HH53, HH51, HH50, HH52
T6ttWW	$m_{\tilde{b}_1} = 900, m_{\tilde{\chi}_1^\pm} = 400$	off-Z ML21, HH51, HH50, HH53, off-Z ML20
T6ttWW	$m_{\tilde{b}_1} = 800, m_{\tilde{\chi}_1^\pm} = 400$	off-Z ML21, HH51, HH50, HH34, off-Z ML20
T5qqqqWZ	$m_{\tilde{g}} = 1400, m_{\tilde{\chi}_1^0} = 1$	on-Z ML23, HH53, HH52, HH51, HH49
T5qqqqWZ	$m_{\tilde{g}} = 900, m_{\tilde{\chi}_1^0} = 600$	on-Z ML4, HH3, HH10, on-Z ML23, HH4
T5qqqqWW	$m_{\tilde{g}} = 1400, m_{\tilde{\chi}_1^0} = 1$	HH53, HH52, HH49, HH51, HH50
T5qqqqWW	$m_{\tilde{g}} = 900, m_{\tilde{\chi}_1^0} = 600$	HH3, HH10, HH4, HH7, HH50
T5qqqqWZ ($m_{\tilde{\chi}_1^\pm} = m_{\tilde{\chi}_1^0} + 20\,\text{GeV}$)	$m_{\tilde{g}} = 1400, m_{\tilde{\chi}_1^0} = 1$	HH59, HH53, HH52, HH62, HH51
T5qqqqWZ ($m_{\tilde{\chi}_1^\pm} = m_{\tilde{\chi}_1^0} + 20\,\text{GeV}$)	$m_{\tilde{g}} = 900, m_{\tilde{\chi}_1^0} = 600$	LL2, LL1, LL4, HL39, HL37
T5qqqqWW ($m_{\tilde{\chi}_1^\pm} = m_{\tilde{\chi}_1^0} + 20\,\text{GeV}$)	$m_{\tilde{g}} = 1400, m_{\tilde{\chi}_1^0} = 1$	HH59, HH53, HH52, HH51, HH62
T5qqqqWW ($m_{\tilde{\chi}_1^\pm} = m_{\tilde{\chi}_1^0} + 20\,\text{GeV}$)	$m_{\tilde{g}} = 900, m_{\tilde{\chi}_1^0} = 600$	LL2, LL4, HL39, LL1, HL37
T6ttHZ ($\mathcal{B}(\tilde{t}_2 \to \tilde{t}_1 Z)=1$)	$m_{\tilde{t}_2} = 850, m_{\tilde{t}_1} = 625$	on-Z ML23, on-Z ML21, on-Z ML16, on-Z ML14, on-Z ML17
T6ttHZ ($\mathcal{B}(\tilde{t}_2 \to \tilde{t}_1 Z)=0.5$)	$m_{\tilde{t}_2} = 850, m_{\tilde{t}_1} = 625$	on-Z ML17, on-Z ML23, on-Z ML21, on-Z ML14, on-Z ML16
T6ttHZ ($\mathcal{B}(\tilde{t}_2 \to \tilde{t}_1 Z)=0$)	$m_{\tilde{t}_2} = 850, m_{\tilde{t}_1} = 625$	off-Z ML15, HH40, HH39, HH45, HH44
T1qqqqL	$m_{\tilde{g}} = 1600$	HH62, LM11, HH59, HH61, HH51
T1qqqqL	$m_{\tilde{g}} = 2400$	HH62, LM11, HH59, HH53, HH52
T1tbs	$m_{\tilde{g}} = 1200$	HH62, HH50, HH59, HH61, HH58
T1tbs	$m_{\tilde{g}} = 1700$	HH62, HH59, HH50, HH52, LM11

References

1. R.M. Barnett, J.F. Gunion, H.E. Haber, Discovering supersymmetry with like-sign dileptons. Phys. Lett. B **315**, 349 (1993). https://doi.org/10.1016/0370-2693(93)91623-U. arXiv:hep-ph/9306204

2. M. Guchait, D.P. Roy, Like-sign dilepton signature for gluino production at CERN LHC including top quark and Higgs boson effects. Phys. Rev. D **52**, 133 (1995). https://doi.org/10.1103/PhysRevD.52.133. arXiv:hep-ph/9412329

3. Y. Bai, Z. Han, Top-antitop and top-top resonances in the dilepton channel at the CERN LHC. JHEP **04**, 056 (2009). https://doi.org/10.1088/1126-6708/2009/04/056. arXiv:0809.4487

4. E.L. Berger et al., Top quark forward-backward asymmetry and same-sign top quark pairs. Phys. Rev. Lett. **106**, 201801 (2011). https://doi.org/10.1103/PhysRevLett.106.201801. arXiv:1101.5625

5. T. Plehn, T.M.P. Tait, Seeking sgluons. J. Phys. G **36**, 075001 (2009). https://doi.org/10.1088/0954-3899/36/7/075001. arXiv:0810.3919

6. S. Calvet, B. Fuks, P. Gris, L. Valery, Searching for sgluons in multitop events at a center-of-mass energy of 8 TeV. JHEP **04**, 043 (2013). https://doi.org/10.1007/JHEP04(2013)043. arXiv:1212.3360

7. K.J.F. Gaemers, F. Hoogeveen, Higgs production and decay into heavy flavors with the gluon fusion mechanism. Phys. Lett. B **146**, 347 (1984). https://doi.org/10.1016/0370-2693(84)91711-8

8. G.C. Branco et al., Theory and phenomenology of two-Higgs-doublet models. Phys. Rep. **516**, 1 (2012). https://doi.org/10.1016/j.physrep.2012.02.002. arXiv:1106.0034

9. F.M.L. Almeida Jr. et al., Same-sign dileptons as a signature for heavy Majorana neutrinos in hadron-hadron collisions. Phys. Lett. B **400**, 331 (1997). https://doi.org/10.1016/S0370-2693(97)00143-3. arXiv:hep-ph/9703441

10. R. Contino, G. Servant, Discovering the top partners at the LHC using same-sign dilepton final states. JHEP **06**, 026 (2008). https://doi.org/10.1088/1126-6708/2008/06/026. arXiv:0801.1679

11. P. Ramond, Dual theory for free fermions. Phys. Rev. D **3**, 2415 (1971). https://doi.org/10.1103/PhysRevD.3.2415

12. Y.A. Gol'fand, E.P. Likhtman, Extension of the algebra of Poincaré group generators and violation of P invariance. JETP Lett. **13**, 323 (1971). http://www.jetpletters.ac.ru/ps/1584/article_24309.pdf

13. A. Neveu, J.H. Schwarz, Factorizable dual model of pions. Nucl. Phys. B **31**, 86 (1971). https://doi.org/10.1016/0550-3213(71)90448-2

14. D.V. Volkov, V.P. Akulov, Possible universal neutrino interaction. JETP Lett. **16**, 438 (1972). http://www.jetpletters.ac.ru/ps/1766/article_26864.pdf

15. J. Wess, B. Zumino, A Lagrangian model invariant under supergauge transformations. Phys. Lett. B **49**, 52 (1974). https://doi.org/10.1016/0370-2693(74)90578-4

16. J. Wess, B. Zumino, Supergauge transformations in four-dimensions. Nucl. Phys. B **70**, 39 (1974). https://doi.org/10.1016/0550-3213(74)90355-1

17. P. Fayet, Supergauge invariant extension of the Higgs mechanism and a model for the electron and its neutrino. Nucl. Phys. B **90**, 104 (1975). https://doi.org/10.1016/0550-3213(75)90636-7

18. H.P. Nilles, Supersymmetry, supergravity and particle physics. Phys. Rep. **110**, 1 (1984). https://doi.org/10.1016/0370-1573(84)90008-5

19. S.P. Martin, A supersymmetry primer, in *Perspectives on Supersymmetry II. Adv. Ser. Direct. High Energy Phys.*, vol. 21, ed. by G.L. Kane (World Scientific, Singapore, 2010), p. 1. https://doi.org/10.1142/9789814307505_0001

20. G.R. Farrar, P. Fayet, Phenomenology of the production, decay, and detection of new hadronic states associated with supersymmetry. Phys. Lett. B **76**, 575 (1978). https://doi.org/10.1016/0370-2693(78)90858-4

21. E. Nikolidakis, C. Smith, Minimal flavor violation, seesaw mechanism, and *R*-parity. Phys. Rev. D **77**, 015021 (2008). https://doi.org/10.1103/PhysRevD.77.015021. arXiv:0710.3129

22. C. Csáki, Y. Grossman, B. Heidenreich, Minimal flavor violation supersymmetry: a natural theory for *R*-parity violation. Phys. Rev. D **85**, 095009 (2012). https://doi.org/10.1103/PhysRevD.85.095009. arXiv:1111.1239

23. ATLAS Collaboration, Search for supersymmetry in final states with two same-sign or three leptons and jets using 36 fb^{-1} of $\sqrt{s}$ = 13 TeV *pp* collision data with the ATLAS detector. JHEP **09**, 084 (2017). https://doi.org/10.1007/JHEP09(2017)084. arXiv:1706.03731

24. CMS Collaboration, Search for physics beyond the standard model in events with two leptons of same sign, missing transverse momentum, and jets in proton-proton collisions at $\sqrt{s}$ = 13 TeV. Eur. Phys. J. C **77**, 578 (2017). https://doi.org/10.1140/epjc/s10052-017-5079-z. arXiv:1704.07323

25. CMS Collaboration, Search for supersymmetry in events with at least three electrons or muons, jets, and missing transverse momentum in proton-proton collisions at $\sqrt{s}$ = 13 TeV. JHEP **02**, 067 (2018). https://doi.org/10.1007/JHEP02(2018)067. arXiv:1710.09154

26. ATLAS Collaboration, Search for squarks and gluinos in final states with same-sign leptons and jets using 139 fb^{-1} of data collected with the ATLAS detector. JHEP 06, 046 (2020). https://doi.org/10.1007/JHEP06(2020)046

27. J. Alwall et al., The automated computation of tree-level and next-to-leading order differential cross sections, and their matching to parton shower simulations. JHEP **07**, 079 (2014). https://doi.org/10.1007/JHEP07(2014)079. arXiv:1405.0301

28. J. Alwall et al., Comparative study of various algorithms for the merging of parton showers and matrix elements in hadronic collisions. Eur. Phys. J. C **53**, 473 (2008). https://doi.org/10.1140/epjc/s10052-007-0490-5. arXiv:0706.2569

29. R. Frederix, S. Frixione, Merging meets matching in MC@NLO. JHEP **12**, 061 (2012). https://doi.org/10.1007/JHEP12(2012)061. arXiv:1209.6215

30. P. Nason, A new method for combining NLO QCD with shower Monte Carlo algorithms. JHEP **11**, 040 (2004). https://doi.org/10.1088/1126-6708/2004/11/040. arXiv:hep-ph/0409146

31. S. Frixione, P. Nason, C. Oleari, Matching NLO QCD computations with parton shower simulations: the POWHEG method. JHEP **11**, 070 (2007). https://doi.org/10.1088/1126-6708/2007/11/070. arXiv:0709.2092

32. S. Alioli, P. Nason, C. Oleari, E. Re, A general framework for implementing NLO calculations in shower Monte Carlo programs: the POWHEG BOX. JHEP **06**, 043 (2010). https://doi.org/10.1007/JHEP06(2010)043. arXiv:1002.2581

33. T. Melia, P. Nason, R. Röntsch, G. Zanderighi, W^+W^-, WZ and ZZ production in the POWHEG BOX. JHEP **11**, 078 (2011). https://doi.org/10.1007/JHEP11(2011)078. arXiv:1107.5051

34. P. Nason, G. Zanderighi, W^+W^-, WZ and ZZ production in the POWHEG BOX V2. Eur. Phys. J. C **74**, 2702 (2014). https://doi.org/10.1140/epjc/s10052-013-2702-5. arXiv:1311.1365

35. NNPDF Collaboration, Parton distributions for the LHC Run II. JHEP **04**, 040 (2015). https://doi.org/10.1007/JHEP04(2015)040. arXiv:1410.8849

36. NNPDF Collaboration, Parton distributions from high-precision collider data. Eur. Phys. J. C **77**, 663 (2017). https://doi.org/10.1140/epjc/s10052-017-5199-5. arXiv:1706.00428

37. T. Sjöstrand et al., An introduction to PYTHIA 8.2. Comput. Phys. Commun. **191**, 159 (2015). https://doi.org/10.1016/j.cpc.2015.01.024. arXiv:1410.3012

38. P. Skands, S. Carrazza, J. Rojo, Tuning PYTHIA 8.1: the Monash, tune. Eur. Phys. J. C **74**(2014), 3024 (2013). https://doi.org/10.1140/epjc/s10052-014-3024-y. arXiv:1404.5630

39. CMS Collaboration, Event generator tunes obtained from underlying event and multiparton scattering measurements. Eur. Phys. J. C **76**, 155 (2016). https://doi.org/10.1140/epjc/s10052-016-3988-x. arXiv:1512.00815

40. CMS Collaboration, Extraction and validation of a new set of CMS PYTHIA8 tunes from underlying-event measurements. Eur. Phys. J. C **80**, 4 (2020). https://doi.org/10.1140/epjc/s10052-019-7499-4. arXiv:1903.12179

41. GEANT4 Collaboration, GEANT4—a simulation toolkit. Nucl. Instrum. Methods A **506**, 250 (2003). https://doi.org/10.1016/S0168-9002(03)01368-8

42. S. Abdullin et al., The fast simulation of the CMS detector at LHC. J. Phys. Conf. Ser. **331**, 032049 (2011). https://doi.org/10.1088/1742-6596/331/3/032049

43. A. Giammanco, The fast simulation of the CMS experiment. J. Phys. Conf. Ser. **513**, 022012 (2014). https://doi.org/10.1088/1742-6596/513/2/022012

44. D. Alves et al., Simplified models for LHC new physics searches. J. Phys. G **39**, 105005 (2012). https://doi.org/10.1088/0954-3899/39/10/105005. arXiv:1105.2838

45. CMS Collaboration, Interpretation of searches for supersymmetry with simplified models. Phys. Rev. D **88**, 052017 (2013). https://doi.org/10.1103/PhysRevD.88.052017. arXiv:1301.2175

46. W. Beenakker et al., NNLL-fast: predictions for coloured supersymmetric particle production at the LHC with threshold and Coulomb resummation. JHEP **12**, 133 (2016). https://doi.org/10.1007/JHEP12(2016)133. arXiv:1607.07741

47. W. Beenakker, R. Höpker, M. Spira, P.M. Zerwas, Squark and gluino production at hadron colliders. Nucl. Phys. B **492**, 51 (1997). https://doi.org/10.1016/S0550-3213(97)80027-2. arXiv:hep-ph/9610490

48. A. Kulesza, L. Motyka, Threshold resummation for squark-antisquark and gluino-pair production at the LHC. Phys. Rev. Lett. **102**, 111802 (2009). https://doi.org/10.1103/PhysRevLett.102.111802. arXiv:0807.2405

49. A. Kulesza, L. Motyka, Soft gluon resummation for the production of gluino-gluino and squark-antisquark pairs at the LHC. Phys. Rev. D **80**, 095004 (2009). https://doi.org/10.1103/PhysRevD.80.095004. arXiv:0905.4749

50. W. Beenakker et al., Soft-gluon resummation for squark and gluino hadroproduction. JHEP **12**, 041 (2009). https://doi.org/10.1088/1126-6708/2009/12/041. arXiv:0909.4418

51. W. Beenakker et al., Squark and gluino hadroproduction. Int. J. Mod. Phys. A **26**, 2637 (2011). https://doi.org/10.1142/S0217751X11053560. arXiv:1105.1110

52. W. Beenakker et al., NNLL resummation for squark-antisquark pair production at the LHC. JHEP **01**, 076 (2012). https://doi.org/10.1007/JHEP01(2012)076. arXiv:1110.2446

53. W. Beenakker et al., Towards NNLL resummation: hard matching coefficients for squark and gluino hadroproduction. JHEP **10**, 120 (2013). https://doi.org/10.1007/JHEP10(2013)120. arXiv:1304.6354

54. W. Beenakker et al., NNLL resummation for squark and gluino production at the LHC. JHEP **12**, 023 (2014). https://doi.org/10.1007/JHEP12(2014)023. arXiv:1404.3134

55. W. Beenakker et al., Stop production at hadron colliders. Nucl. Phys. B **515**, 3 (1998). https://doi.org/10.1016/S0550-3213(98)00014-5. arXiv:hep-ph/9710451

56. W. Beenakker et al., Supersymmetric top and bottom squark production at hadron colliders. JHEP **08**, 098 (2010). https://doi.org/10.1007/JHEP08(2010)098. arXiv:1006.4771

57. W. Beenakker et al., NNLL resummation for stop pair-production at the LHC. JHEP **05**, 153 (2016). https://doi.org/10.1007/JHEP05(2016)153. arXiv:1601.02954

58. C. Borschensky et al., Squark and gluino production cross sections in pp collisions at $\sqrt{s} = 13$, 14, 33 and 100 TeV. Eur. Phys. J. C **74**, 3174 (2014). https://doi.org/10.1140/epjc/s10052-014-3174-y. arXiv:1407.5066

59. CMS Collaboration, The CMS experiment at the CERN LHC. JINST **3**, S08004 (2008). https://doi.org/10.1088/1748-0221/3/08/S08004

60. CMS Collaboration, The CMS trigger system. JINST **12**, P01020 (2017). https://doi.org/10.1088/1748-0221/12/01/P01020. arXiv:1609.02366

61. M. Cacciari, G.P. Salam, G. Soyez, The anti-k_T jet clustering algorithm. JHEP **04**, 063 (2008). https://doi.org/10.1088/1126-6708/2008/04/063. arXiv:0802.1189

62. M. Cacciari, G.P. Salam, G. Soyez, FastJet user manual. Eur. Phys. J. C **72**, 1896 (2012). https://doi.org/10.1140/epjc/s10052-012-1896-2. arXiv:1111.6097

63. CMS Collaboration, Particle-flow reconstruction and global event description with the CMS detector. JINST **12**, P10003 (2017). https://doi.org/10.1088/1748-0221/12/10/P10003. arXiv:1706.04965

64. CMS Collaboration, Performance of electron reconstruction and selection with the CMS detector in proton-proton collisions at $\sqrt{s} = 8$ TeV. JINST **10**, P06005 (2015). https://doi.org/10.1088/1748-0221/10/06/P06005. arXiv:1502.02701

65. CMS Collaboration, Performance of the CMS muon detector and muon reconstruction with proton-proton collisions at $\sqrt{s} = 13$ TeV. JINST **13**, P06015 (2018). https://doi.org/10.1088/1748-0221/13/06/P06015. arXiv:1804.04528

66. M. Cacciari, G.P. Salam, Pileup subtraction using jet areas. Phys. Lett. B **659**, 119 (2008). https://doi.org/10.1016/j.physletb.2007.09.077. arXiv:0707.1378

67. CMS Collaboration, Jet energy scale and resolution in the CMS experiment in pp collisions at 8 TeV. JINST **12**, P02014 (2016). https://doi.org/10.1088/1748-0221/12/02/P02014. arXiv:1607.03663

68. CMS Collaboration, Jet algorithms performance in 13 TeV data. CMS Physics Analysis Summary CMS-PAS-JME-16-003 (2017). https://cds.cern.ch/record/2256875

69. CMS Collaboration, Identification of heavy-flavour jets with the CMS detector in pp collisions at 13 TeV. JINST **13**, P05011 (2018). https://doi.org/10.1088/1748-0221/13/05/P05011. arXiv:1712.07158

70. CMS Collaboration, Performance of missing transverse momentum reconstruction in proton-proton collisions at $\sqrt{s} = 13$ TeV using the CMS detector. JINST **14**, P07004 (2019). https://doi.org/10.1088/1748-0221/14/07/P07004. arXiv:1903.06078

71. CMS Collaboration, Search for new physics in same-sign dilepton events in proton-proton collisions at $\sqrt{s} = 13$ TeV. Eur. Phys. J. C **76**, 439 (2016). https://doi.org/10.1140/epjc/s10052-016-4261-z. arXiv:1605.03171

72. CMS Collaboration, Performance of the reconstruction and identification of high-momentum muons in proton-proton collisions at $\sqrt{s} = 13$ TeV. JINST **15**, P02027 (2020). https://doi.org/10.1088/1748-0221/15/02/P02027. arXiv:1912.03516

73. CMS Collaboration, Performance of CMS muon reconstruction in pp collision events at $\sqrt{s} = 7$ TeV. JINST **7**, P10002 (2012). https://doi.org/10.1088/1748-0221/7/10/P10002. arXiv:1206.4071

74. CMS Collaboration, CMS luminosity measurements for the 2016 data-taking period. CMS Physics Analysis Summary CMS-PAS-LUM-17-001 (2017). http://cds.cern.ch/record/2257069

75. CMS Collaboration, CMS luminosity measurement for the 2017 data-taking period at $\sqrt{s} = 13$ TeV. CMS Physics Analysis Summary CMS-PAS-LUM-17-004 (2018). https://cds.cern.ch/record/2621960

76. CMS Collaboration, CMS luminosity measurement for the 2018 data-taking period at $\sqrt{s} = 13$ TeV. CMS Physics Analysis Summary CMS-PAS-LUM-18-002 (2019). https://cds.cern.ch/record/2676164

77. CMS Collaboration, Measurement of the inelastic proton-proton cross section at $\sqrt{s} = 13$ TeV. JHEP **07**, 161 (2018). https://doi.org/10.1007/JHEP07(2018)161. arXiv:1802.02613

78. A. Kalogeropoulos, J. Alwall, The SysCalc code: a tool to derive theoretical systematic uncertainties (2018). arXiv:1801.08401

79. ATLAS Collaboration, Measurement of the t$\bar{\text{t}}$Z and t$\bar{\text{t}}$W cross sections in proton-proton collisions at $\sqrt{s} = 13$ TeV with the ATLAS detector. Phys. Rev. D **99**, 072009 (2019). https://doi.org/10.1103/PhysRevD.99.072009. arXiv:1901.03584

80. CMS Collaboration, Measurement of the cross section for top quark pair production in association with a W or Z boson in proton-proton collisions at $\sqrt{s} = 13$ TeV. JHEP **08**, 011 (2018). https://doi.org/10.1007/JHEP08(2018)011. arXiv:1711.02547

81. CMS Collaboration, Measurements of t$\bar{\text{t}}$ cross sections in association with b jets and inclusive jets and their ratio using dilepton final states in pp collisions at $\sqrt{s} = 13$ TeV. Phys. Lett. B **776**, 355 (2018). https://doi.org/10.1016/j.physletb.2017.11.043. arXiv:1705.10141

82. T. Junk, Confidence level computation for combining searches with small statistics. Nucl. Instrum. Methods A **434**, 435 (1999). https://doi.org/10.1016/S0168-9002(99)00498-2. arXiv:hep-ex/9902006

83. A.L. Read, Presentation of search results: the CL$_s$ technique. J. Phys. G **28**, 2693 (2002). https://doi.org/10.1088/0954-3899/28/10/313. (**Durham IPPP Workshop: Advanced Statistical Techniques in Particle Physics**)

84. ATLAS and CMS Collaborations, Procedure for the LHC Higgs boson search combination in summer 2011. ATL-PHYS-PUB-2011-011, CMS NOTE-2011/005 (2011). https://cdsweb.cern.ch/record/1379837

85. G. Cowan, K. Cranmer, E. Gross, O. Vitells, Asymptotic formulae for likelihood-based tests of new physics. Eur. Phys. J. C **71**, 1554 (2011). https://doi.org/10.1140/epjc/s10052-011-1554-0. arXiv:1007.1727. [Erratum: https://doi.org/10.1140/epjc/s10052-013-2501-z]

86. CMS Collaboration, Search for supersymmetry in pp collisions at $\sqrt{s} = 13$ TeV with 137 fb^{-1} in final states with a single lepton using the sum of masses of large-radius jets. Phys. Rev. D **101**(5), 052010 (2020). https://doi.org/10.1103/PhysRevD.101.052010. arXiv:1911.07558

87. CMS Collaboration, Search for supersymmetry in proton-proton collisions at 13 TeV in final states with jets and missing transverse momentum. JHEP **10**, 244 (2019). https://doi.org/10.1007/JHEP10(2019)244. arXiv:1908.04722

88. CMS Collaboration, Searches for physics beyond the standard model with the M_{T2} variable in hadronic final states with and without disappearing tracks in proton-proton collisions at $\sqrt{s} = 13$ TeV. Eur. Phys. J. C **80**(1), 3 (2020). https://doi.org/10.1140/epjc/s10052-019-7493-x. arXiv:1909.03460

89. CMS Collaboration, Search for R-parity violating supersymmetry in pp collisions at $\sqrt{s} = 13$ TeV using b jets in a final state with a single lepton, many jets, and high sum of large-radius jet masses. Phys. Lett. B **783**, 114 (2018). https://doi.org/10.1016/j.physletb.2018.06.028. arXiv:1712.08920

CMS Collaboration

Yerevan Physics Institute, Yerevan, Armenia
A. M. Sirunyan[†], A. Tumasyan

Institut für Hochenergiephysik, Wien, Austria
W. Adam, F. Ambrogi, T. Bergauer, M. Dragicevic, J. Erö, A. Escalante Del Valle, M. Flechl, R. Frühwirth[1], M. Jeitler[1], N. Krammer, I. Krätschmer, D. Liko, T. Madlener, I. Mikulec, N. Rad, J. Schieck[1], R. Schöfbeck, M. Spanring, W. Waltenberger, C.-E. Wulz[1], M. Zarucki

Institute for Nuclear Problems, Minsk, Belarus
V. Drugakov, V. Mossolov, J. Suarez Gonzalez

Universiteit Antwerpen, Antwerpen, Belgium
M. R. Darwish, E. A. De Wolf, D. Di Croce, X. Janssen, A. Lelek, M. Pieters, H. Rejeb Sfar, H. Van Haevermaet, P. Van Mechelen, S. Van Putte, N. Van Remortel

Vrije Universiteit Brussel, Brussels, Belgium
F. Blekman, E. S. Bols, S. S. Chhibra, J. D'Hondt, J. De Clercq, D. Lontkovskyi, S. Lowette, I. Marchesini, S. Moortgat, Q. Python, S. Tavernier, W. Van Doninck, P. Van Mulders

Université Libre de Bruxelles, Brussels, Belgium
D. Beghin, B. Bilin, B. Clerbaux, G. De Lentdecker, H. Delannoy, B. Dorney, L. Favart, A. Grebenyuk, A. K. Kalsi, L. Moureaux, A. Popov, N. Postiau, E. Starling, L. Thomas, C. Vander Velde, P. Vanlaer, D. Vannerom

Ghent University, Ghent, Belgium
T. Cornelis, D. Dobur, I. Khvastunov[2], M. Niedziela, C. Roskas, K. Skovpen, M. Tytgat, W. Verbeke, B. Vermassen, M. Vit

Université Catholique de Louvain, Louvain-la-Neuve, Belgium

O. Bondu, G. Bruno, C. Caputo, P. David, C. Delaere, M. Delcourt, A. Giammanco, V. Lemaitre, J. Prisciandaro, A. Saggio, M. Vidal Marono, P. Vischia, J. Zobec

Centro Brasileiro de Pesquisas Fisicas, Rio de Janeiro, Brazil

G. A. Alves, G. Correia Silva, C. Hensel, A. Moraes

Universidade do Estado do Rio de Janeiro, Rio de Janeiro, Brazil

E. Belchior Batista Das Chagas, W. Carvalho, J. Chinellato[3], E. Coelho, E. M. Da Costa, G. G. Da Silveira[4], D. De Jesus Damiao, C. De Oliveira Martins, S. Fonseca De Souza, L. M. Huertas Guativa, H. Malbouisson, J. Martins[5], D. Matos Figueiredo, M. Medina Jaime[6], M. Melo De Almeida, C. Mora Herrera, L. Mundim, H. Nogima, W. L. Prado Da Silva, P. Rebello Teles, L. J. Sanchez Rosas, A. Santoro, A. Sznajder, M. Thiel, E. J. Tonelli Manganote[3], F. Torres Da Silva De Araujo, A. Vilela Pereira

Universidade Estadual Paulista[a], Universidade Federal do ABC[b], São Paulo, Brazil

C. A. Bernardes[a], L. Calligaris[a], T. R. Fernandez Perez Tomei[a], E. M. Gregores[b], D. S. Lemos, P. G. Mercadante[b], S. F. Novaes[a], S. S. Padula[a]

Institute for Nuclear Research and Nuclear Energy, Bulgarian Academy of Sciences, Sofia, Bulgaria

A. Aleksandrov, G. Antchev, R. Hadjiiska, P. Iaydjiev, M. Misheva, M. Rodozov, M. Shopova, G. Sultanov

University of Sofia, Sofia, Bulgaria

M. Bonchev, A. Dimitrov, T. Ivanov, L. Litov, B. Pavlov, P. Petkov, A. Petrov

Beihang University, Beijing, China

W. Fang[7], X. Gao[7], L. Yuan

Department of Physics, Tsinghua University, Beijing, China

M. Ahmad, Z. Hu, Y. Wang

Institute of High Energy Physics, Beijing, China

G. M. Chen[8], H. S. Chen[8], M. Chen, C. H. Jiang, D. Leggat, H. Liao, Z. Liu, A. Spiezia, J. Tao, E. Yazgan, H. Zhang, S. Zhang[8], J. Zhao

State Key Laboratory of Nuclear Physics and Technology, Peking University, Beijing, China

A. Agapitos, Y. Ban, G. Chen, A. Levin, J. Li, L. Li, Q. Li, Y. Mao, S. J. Qian, D. Wang, Q. Wang

Zhejiang University, Hangzhou, China

M. Xiao

Universidad de Los Andes, Bogotá, Colombia

C. Avila, A. Cabrera, C. Florez, C. F. González Hernández, M. A. Segura Delgado

Universidad de Antioquia, Medellin, Colombia

J. Mejia Guisao, J. D. Ruiz Alvarez, C. A. Salazar González, N. Vanegas Arbelaez

University of Split, Faculty of Electrical Engineering, Mechanical Engineering and Naval Architecture, Split, Croatia

D. Giljanović, N. Godinovic, D. Lelas, I. Puljak, T. Sculac

University of Split, Faculty of Science, Split, Croatia

Z. Antunovic, M. Kovac

Institute Rudjer Boskovic, Zagreb, Croatia

V. Brigljevic, D. Ferencek, K. Kadija, B. Mesic, M. Roguljic, A. Starodumov[9], T. Susa

University of Cyprus, Nicosia, Cyprus

M. W. Ather, A. Attikis, E. Erodotou, A. Ioannou, M. Kolosova, S. Konstantinou, G. Mavromanolakis, J. Mousa, C. Nicolaou, F. Ptochos, P. A. Razis, H. Rykaczewski, H. Saka, D. Tsiakkouri

Charles University, Prague, Czech Republic

M. Finger[10], M. Finger Jr.[10], A. Kveton, J. Tomsa

Escuela Politecnica Nacional, Quito, Ecuador
E. Ayala

Universidad San Francisco de Quito, Quito, Ecuador
E. Carrera Jarrin

Academy of Scientific Research and Technology of the Arab Republic of Egypt, Egyptian Network of High Energy Physics, Cairo, Egypt
H. Abdalla[11], S. Khalil[12]

National Institute of Chemical Physics and Biophysics, Tallinn, Estonia
S. Bhowmik, A. Carvalho Antunes De Oliveira, R. K. Dewanjee, K. Ehataht, M. Kadastik, M. Raidal, C. Veelken

Department of Physics, University of Helsinki, Helsinki, Finland
P. Eerola, L. Forthomme, H. Kirschenmann, K. Osterberg, M. Voutilainen

Helsinki Institute of Physics, Helsinki, Finland
F. Garcia, J. Havukainen, J. K. Heikkilä, V. Karimäki, M. S. Kim, R. Kinnunen, T. Lampén, K. Lassila-Perini, S. Laurila, S. Lehti, T. Lindén, H. Siikonen, E. Tuominen, J. Tuominiemi

Lappeenranta University of Technology, Lappeenranta, Finland
P. Luukka, T. Tuuva

IRFU, CEA, Université Paris-Saclay, Gif-sur-Yvette, France
M. Besancon, F. Couderc, M. Dejardin, D. Denegri, B. Fabbro, J. L. Faure, F. Ferri, S. Ganjour, A. Givernaud, P. Gras, G. Hamel de Monchenault, P. Jarry, C. Leloup, B. Lenzi, E. Locci, J. Malcles, J. Rander, A. Rosowsky, M. Ö. Sahin, A. Savoy-Navarro[13], M. Titov, G. B. Yu

Laboratoire Leprince-Ringuet, CNRS/IN2P3, Ecole Polytechnique, Institut Polytechnique de Paris, Paris, France
S. Ahuja, C. Amendola, F. Beaudette, P. Busson, C. Charlot, B. Diab, G. Falmagne, R. Granier de Cassagnac, I. Kucher, A. Lobanov, C. Martin Perez, M. Nguyen, C. Ochando, P. Paganini, J. Rembser, R. Salerno, J. B. Sauvan, Y. Sirois, A. Zabi, A. Zghiche

Université de Strasbourg, CNRS, IPHC UMR 7178, Strasbourg, France
J.-L. Agram[14], J. Andrea, D. Bloch, G. Bourgatte, J.-M. Brom, E. C. Chabert, C. Collard, E. Conte[14], J.-C. Fontaine[14], D. Gelé, U. Goerlach, M. Jansová, A.-C. Le Bihan, N. Tonon, P. Van Hove

Centre de Calcul de l'Institut National de Physique Nucleaire et de Physique des Particules, CNRS/IN2P3, Villeurbanne, France
S. Gadrat

CNRS-IN2P3, Institut de Physique Nucléaire de Lyon, Université de Lyon, Université Claude Bernard Lyon 1, Villeurbanne, France
S. Beauceron, C. Bernet, G. Boudoul, C. Camen, A. Carle, N. Chanon, R. Chierici, D. Contardo, P. Depasse, H. El Mamouni, J. Fay, S. Gascon, M. Gouzevitch, B. Ille, Sa. Jain, I. B. Laktineh, H. Lattaud, A. Lesauvage, M. Lethuillier, L. Mirabito, S. Perries, V. Sordini, L. Torterotot, G. Touquet, M. Vander Donckt, S. Viret

Georgian Technical University, Tbilisi, Georgia
A. Khvedelidze[10]

Tbilisi State University, Tbilisi, Georgia
Z. Tsamalaidze[10]

RWTH Aachen University, I. Physikalisches Institut, Aachen, Germany
C. Autermann, L. Feld, K. Klein, M. Lipinski, D. Meuser, A. Pauls, M. Preuten, M. P. Rauch, J. Schulz, M. Teroerde

RWTH Aachen University, III. Physikalisches Institut A, Aachen, Germany
M. Erdmann, B. Fischer, S. Ghosh, T. Hebbeker, K. Hoepfner, H. Keller, L. Mastrolorenzo, M. Merschmeyer, A. Meyer, P. Millet, G. Mocellin, S. Mondal, S. Mukherjee, D. Noll, A. Novak, T. Pook, A. Pozdnyakov, T. Quast, M. Radziej, Y. Rath, H. Reithler, J. Roemer, A. Schmidt, S. C. Schuler, A. Sharma, S. Wiedenbeck, S. Zaleski

RWTH Aachen University, III. Physikalisches Institut B, Aachen, Germany
G. Flügge, W. Haj Ahmad[15], O. Hlushchenko, T. Kress, T. Müller, A. Nowack, C. Pistone, O. Pooth, D. Roy, H. Sert, A. Stahl[16]

Deutsches Elektronen-Synchrotron, Hamburg, Germany
M. Aldaya Martin, P. Asmuss, I. Babounikau, H. Bakhshiansohi, K. Beernaert, O. Behnke, A. Bermúdez Martínez, A. A. Bin Anuar, K. Borras[17], V. Botta, A. Campbell, A. Cardini, P. Connor, S. Consuegra Rodríguez, C. Contreras-Campana, V. Danilov, A. De Wit, M. M. Defranchis, C. Diez Pardos, D. Domínguez Damiani, G. Eckerlin, D. Eckstein, T. Eichhorn, A. Elwood, E. Eren, E. Gallo[18], A. Geiser, A. Grohsjean, M. Guthoff, M. Haranko, A. Harb, A. Jafari[19], N. Z. Jomhari, H. Jung, A. Kasem[17], M. Kasemann, H. Kaveh, J. Keaveney, C. Kleinwort, J. Knolle, D. Krücker, W. Lange, T. Lenz, J. Lidrych, K. Lipka, W. Lohmann[20], R. Mankel, I.-A. Melzer-Pellmann, A. B. Meyer, M. Meyer, M. Missiroli, J. Mnich, A. Mussgiller, V. Myronenko, D. Pérez Adán, S. K. Pflitsch, D. Pitzl, A. Raspereza, A. Saibel, M. Savitskyi, V. Scheurer, P. Schütze, C. Schwanenberger, R. Shevchenko, A. Singh, R. E. Sosa Ricardo, H. Tholen, O. Turkot, A. Vagnerini, M. Van De Klundert, R. Walsh, Y. Wen, K. Wichmann, C. Wissing, O. Zenaiev, R. Zlebcik

University of Hamburg, Hamburg, Germany
R. Aggleton, S. Bein, L. Benato, A. Benecke, T. Dreyer, A. Ebrahimi, F. Feindt, A. Fröhlich, C. Garbers, E. Garutti, D. Gonzalez, P. Gunnellini, J. Haller, A. Hinzmann, A. Karavdina, G. Kasieczka, R. Klanner, R. Kogler, N. Kovalchuk, S. Kurz, V. Kutzner, J. Lange, T. Lange, A. Malara, J. Multhaup, C. E. N. Niemeyer, A. Reimers, O. Rieger, P. Schleper, S. Schumann, J. Schwandt, J. Sonneveld, H. Stadie, G. Steinbrück, B. Vormwald, I. Zoi

Karlsruher Institut fuer Technologie, Karlsruhe, Germany
M. Akbiyik, M. Baselga, S. Baur, T. Berger, E. Butz, R. Caspart, T. Chwalek, W. De Boer, A. Dierlamm, K. El Morabit, N. Faltermann, M. Giffels, A. Gottmann, M. A. Harrendorf, F. Hartmann[16], C. Heidecker, U. Husemann, S. Kudella, S. Maier, S. Mitra, M. U. Mozer, D. Müller, Th. Müller, M. Musich, A. Nürnberg, G. Quast, K. Rabbertz, D. Schäfer, M. Schröder, I. Shvetsov, H. J. Simonis, R. Ulrich, M. Wassmer, M. Weber, C. Wöhrmann, R. Wolf, S. Wozniewski

Institute of Nuclear and Particle Physics (INPP), NCSR Demokritos, Aghia Paraskevi, Greece
G. Anagnostou, P. Asenov, G. Daskalakis, T. Geralis, A. Kyriakis, D. Loukas, G. Paspalaki

National and Kapodistrian University of Athens, Athens, Greece
M. Diamantopoulou, G. Karathanasis, P. Kontaxakis, A. Manousakis-katsikakis, A. Panagiotou, I. Papavergou, N. Saoulidou, A. Stakia, K. Theofilatos, K. Vellidis, E. Vourliotis

National Technical University of Athens, Athens, Greece
G. Bakas, K. Kousouris, I. Papakrivopoulos, G. Tsipolitis

University of Ioánnina, Ioánnina, Greece
I. Evangelou, C. Foudas, P. Gianneios, P. Katsoulis, P. Kokkas, S. Mallios, K. Manitara, N. Manthos, I. Papadopoulos, J. Strologas, F. A. Triantis, D. Tsitsonis

MTA-ELTE Lendület CMS Particle and Nuclear Physics Group, Eötvös Loránd University, Budapest, Hungary
M. Bartók[21], R. Chudasama, M. Csanad, P. Major, K. Mandal, A. Mehta, G. Pasztor, O. Surányi, G. I. Veres

Wigner Research Centre for Physics, Budapest, Hungary
G. Bencze, C. Hajdu, D. Horvath[22], F. Sikler, V. Veszpremi, G. Vesztergombi[†]

Institute of Nuclear Research ATOMKI, Debrecen, Hungary
N. Beni, S. Czellar, J. Karancsi[21], J. Molnar, Z. Szillasi

Institute of Physics, University of Debrecen, Debrecen, Hungary
P. Raics, D. Teyssier, Z. L. Trocsanyi, B. Ujvari

Eszterhazy Karoly University, Karoly Robert Campus, Gyongyos, Hungary
T. Csorgo, W. J. Metzger, F. Nemes, T. Novak

Indian Institute of Science (IISc), Bangalore, India
S. Choudhury, J. R. Komaragiri, P. C. Tiwari

National Institute of Science Education and Research, HBNI, Bhubaneswar, India

S. Bahinipati[24], C. Kar, G. Kole, P. Mal, V. K. Muraleedharan Nair Bindhu, A. Nayak[25], D. K. Sahoo[24], S. K. Swain

Panjab University, Chandigarh, India

S. Bansal, S. B. Beri, V. Bhatnagar, S. Chauhan, N. Dhingra[26], R. Gupta, A. Kaur, M. Kaur, S. Kaur, P. Kumari, M. Lohan, M. Meena, K. Sandeep, S. Sharma, J. B. Singh, A. K. Virdi, G. Walia

University of Delhi, Delhi, India

A. Bhardwaj, B. C. Choudhary, R. B. Garg, M. Gola, S. Keshri, A. Kumar, M. Naimuddin, P. Priyanka, K. Ranjan, A. Shah, R. Sharma

Saha Institute of Nuclear Physics, HBNI, Kolkata, India

R. Bhardwaj[27], M. Bharti[27], R. Bhattacharya, S. Bhattacharya, U. Bhawandeep[27], D. Bhowmik, S. Dutta, S. Ghosh, B. Gomber[28], M. Maity[29], K. Mondal, S. Nandan, A. Purohit, P. K. Rout, G. Saha, S. Sarkar, T. Sarkar[29], M. Sharan, B. Singh[27], S. Thakur[27]

Indian Institute of Technology Madras, Chennai, India

P. K. Behera, P. Kalbhor, A. Muhammad, P. R. Pujahari, A. Sharma, A. K. Sikdar

Bhabha Atomic Research Centre, Mumbai, India

D. Dutta, V. Jha, D. K. Mishra, P. K. Netrakanti, L. M. Pant, P. Shukla

Tata Institute of Fundamental Research-A, Mumbai, India

T. Aziz, M. A. Bhat, S. Dugad, G. B. Mohanty, N. Sur, R. K. Verma

Tata Institute of Fundamental Research-B, Mumbai, India

S. Banerjee, S. Bhattacharya, S. Chatterjee, P. Das, M. Guchait, S. Karmakar, S. Kumar, G. Majumder, K. Mazumdar, N. Sahoo, S. Sawant

Indian Institute of Science Education and Research (IISER), Pune, India

S. Dube, B. Kansal, A. Kapoor, K. Kothekar, S. Pandey, A. Rane, A. Rastogi, S. Sharma

Institute for Research in Fundamental Sciences (IPM), Tehran, Iran

S. Chenarani, S. M. Etesami, M. Khakzad, M. Mohammadi Najafabadi, M. Naseri, F. Rezaei Hosseinabadi

University College Dublin, Dublin, Ireland

M. Felcini, M. Grunewald

INFN Sezione di Bari^a, Università di Bari^b, Politecnico di Bari^c, Bari, Italy

M. Abbrescia^{a,b}, R. Aly^{a,b,30}, C. Calabria^{a,b}, A. Colaleo^a, D. Creanza^{a,c}, L. Cristella^{a,b}, N. De Filippis^{a,c}, M. De Palma^{a,b}, A. Di Florio^{a,b}, W. Elmetenawee^{a,b}, L. Fiore^a, A. Gelmi^{a,b}, G. Iaselli^{a,c}, M. Ince^{a,b}, S. Lezki^{a,b}, G. Maggi^{a,c}, M. Maggi^a, J. A. Merlin^a, G. Miniello^{a,b}, S. My^{a,b}, S. Nuzzo^{a,b}, A. Pompili^{a,b}, G. Pugliese^{a,c}, R. Radogna^a, A. Ranieri^a, G. Selvaggi^{a,b}, L. Silvestris^a, F. M. Simone^{a,b}, R. Venditti^a, P. Verwilligen^a

INFN Sezione di Bologna^a, Università di Bologna^b, Bologna, Italy

G. Abbiendi^a, C. Battilana^{a,b}, D. Bonacorsi^{a,b}, L. Borgonovi^{a,b}, S. Braibant-Giacomelli^{a,b}, R. Campanini^{a,b}, P. Capiluppi^{a,b}, A. Castro^{a,b}, F. R. Cavallo^a, C. Ciocca^a, G. Codispoti^{a,b}, M. Cuffiani^{a,b}, G. M. Dallavalle^a, F. Fabbri^a, A. Fanfani^{a,b}, E. Fontanesi^{a,b}, P. Giacomelli^a, C. Grandi^a, L. Guiducci^{a,b}, F. Iemmi^{a,b}, S. Lo Meo^{a,31}, S. Marcellini^a, G. Masetti^a, F. L. Navarria^{a,b}, A. Perrotta^a, F. Primavera^{a,b}, A. M. Rossi^{a,b}, T. Rovelli^{a,b}, G. P. Siroli^{a,b}, N. Tosi^a

INFN Sezione di Catania^a, Università di Catania^b, Catania, Italy

S. Albergo^{a,b,32}, S. Costa^{a,b}, A. Di Mattia^a, R. Potenza^{a,b}, A. Tricomi^{a,b,32}, C. Tuve^{a,b}

INFN Sezione di Firenze^a, Università di Firenze^b, Firenze, Italy

G. Barbagli^a, A. Cassese, R. Ceccarelli, V. Ciulli^{a,b}, C. Civinini^a, R. D'Alessandro^{a,b}, F. Fiori^{a,c}, E. Focardi^{a,b}, G. Latino^{a,b}, P. Lenzi^{a,b}, M. Meschini^a, S. Paoletti^a, G. Sguazzoni^a, L. Viliani^a

INFN Laboratori Nazionali di Frascati, Frascati, Italy

L. Benussi, S. Bianco, D. Piccolo

INFN Sezione di Genova[a], Università di Genova[b], Genoa, Italy

M. Bozzo[a,b], F. Ferro[a], R. Mulargia[a,b], E. Robutti[a], S. Tosi[a,b]

INFN Sezione di Milano-Bicocca[a], Università di Milano-Bicocca[b], Milan, Italy

A. Benaglia[a], A. Beschi[a,b], F. Brivio[a,b], V. Ciriolo[a,b,16], M. E. Dinardo[a,b], P. Dini[a], S. Gennai[a], A. Ghezzi[a,b],
P. Govoni[a,b], L. Guzzi[a,b], M. Malberti[a], S. Malvezzi[a], D. Menasce[a], F. Monti[a,b], L. Moroni[a], M. Paganoni[a,b], D. Pedrini[a],
S. Ragazzi[a,b], T. Tabarelli de Fatis[a,b], D. Valsecchi[a,b], D. Zuolo[a,b]

INFN Sezione di Napoli[a], Università di Napoli 'Federico II'[b], Napoli, Italy, Università della Basilicata[c], Potenza, Italy, Università G. Marconi[d], Rome, Italy

S. Buontempo[a], N. Cavallo[a,c], A. De Iorio[a,b], A. Di Crescenzo[a,b], F. Fabozzi[a,c], F. Fienga[a], G. Galati[a], A. O. M. Iorio[a,b],
L. Layer[a,b], L. Lista[a,b], S. Meola[a,d,16], P. Paolucci[a,16], B. Rossi[a], C. Sciacca[a,b], E. Voevodina[a,b]

INFN Sezione di Padova[a], Università di Padova[b], Padova, Italy, Università di Trento[c], Trento, Italy

P. Azzi[a], N. Bacchetta[a], D. Bisello[a,b], A. Boletti[a,b], A. Bragagnolo[a,b], R. Carlin[a,b], P. Checchia[a], P. De Castro Manzano[a],
T. Dorigo[a], U. Dosselli[a], F. Gasparini[a,b], U. Gasparini[a,b], A. Gozzelino[a], S. Y. Hoh[a,b], M. Margoni[a,b],
A. T. Meneguzzo[a,b], J. Pazzini[a,b], M. Presilla[b], P. Ronchese[a,b], R. Rossin[a,b], F. Simonetto[a,b], A. Tiko[a], M. Tosi[a,b],
M. Zanetti[a,b], P. Zotto[a,b], G. Zumerle[a,b]

INFN Sezione di Pavia[a], Università di Pavia[b], Pavia, Italy

A. Braghieri[a], D. Fiorina[a,b], P. Montagna[a,b], S. P. Ratti[a,b], V. Re[a], M. Ressegotti[a,b], C. Riccardi[a,b], P. Salvini[a], I. Vai[a],
P. Vitulo[a,b]

INFN Sezione di Perugia[a], Università di Perugia[b], Perugia, Italy

M. Biasini[a,b], G. M. Bilei[a], D. Ciangottini[a,b], L. Fanò[a,b], P. Lariccia[a,b], R. Leonardi[a,b], E. Manoni[a], G. Mantovani[a,b],
V. Mariani[a,b], M. Menichelli[a], A. Rossi[a,b], A. Santocchia[a,b], D. Spiga[a]

INFN Sezione di Pisa[a], Università di Pisa[b], Scuola Normale Superiore di Pisa[c], Pisa, Italy

K. Androsov[a], P. Azzurri[a], G. Bagliesi[a], V. Bertacchi[a,c], L. Bianchini[a], T. Boccali[a], R. Castaldi[a], M. A. Ciocci[a,b],
R. Dell'Orso[a], S. Donato[a], L. Giannini[a,c], A. Giassi[a], M. T. Grippo[a], F. Ligabue[a,c], E. Manca[a,c], G. Mandorli[a,c],
A. Messineo[a,b], F. Palla[a], A. Rizzi[a,b], G. Rolandi[33], S. Roy Chowdhury, A. Scribano[a], P. Spagnolo[a], R. Tenchini[a],
G. Tonelli[a,b], N. Turini, A. Venturi[a], P. G. Verdini[a]

INFN Sezione di Roma[a], Sapienza Università di Roma[b], Rome, Italy

F. Cavallari[a], M. Cipriani[a,b], D. Del Re[a,b], E. Di Marco[a], M. Diemoz[a], E. Longo[a,b], P. Meridiani[a], G. Organtini[a,b],
F. Pandolfi[a], R. Paramatti[a,b], C. Quaranta[a,b], S. Rahatlou[a,b], C. Rovelli[a], F. Santanastasio[a,b], L. Soffi[a,b]

INFN Sezione di Torino[a], Università di Torino[b], Torino, Italy, Università del Piemonte Orientale[c], Novara, Italy

N. Amapane[a,b], R. Arcidiacono[a,c], S. Argiro[a,b], M. Arneodo[a,c], N. Bartosik[a], R. Bellan[a,b], A. Bellora, C. Biino[a],
A. Cappati[a,b], N. Cartiglia[a], S. Cometti[a], M. Costa[a,b], R. Covarelli[a,b], N. Demaria[a], B. Kiani[a,b], F. Legger, C. Mariotti[a],
S. Maselli[a], E. Migliore[a,b], V. Monaco[a,b], E. Monteil[a,b], M. Monteno[a], M. M. Obertino[a,b], G. Ortona[a,b], L. Pacher[a,b],
N. Pastrone[a], M. Pelliccioni[a], G. L. Pinna Angioni[a,b], A. Romero[a,b], M. Ruspa[a,c], R. Salvatico[a,b], V. Sola[a], A. Solano[a,b],
D. Soldi[a,b], A. Staiano[a], D. Trocino[a,b]

INFN Sezione di Trieste [a], Università di Trieste [b], Trieste, Italy

S. Belforte[a], V. Candelise[a,b], M. Casarsa[a], F. Cossutti[a], A. Da Rold[a,b], G. Della Ricca[a,b], F. Vazzoler[a,b], A. Zanetti[a]

Kyungpook National University, Daegu, Korea

B. Kim, D. H. Kim, G. N. Kim, J. Lee, S. W. Lee, C. S. Moon, Y. D. Oh, S. I. Pak, S. Sekmen, D. C. Son, Y. C. Yang

Chonnam National University, Institute for Universe and Elementary Particles, Kwangju, Korea

H. Kim, D. H. Moon, G. Oh

Hanyang University, Seoul, Korea

B. Francois, T. J. Kim, J. Park

Korea University, Seoul, Korea

S. Cho, S. Choi, Y. Go, S. Ha, B. Hong, K. Lee, K. S. Lee, J. Lim, J. Park, S. K. Park, Y. Roh, J. Yoo

Department of Physics, Kyung Hee University, Seoul, Korea
J. Goh

Sejong University, Seoul, Korea
H. S. Kim

Seoul National University, Seoul, Korea
J. Almond, J. H. Bhyun, J. Choi, S. Jeon, J. Kim, J. S. Kim, H. Lee, K. Lee, S. Lee, K. Nam, M. Oh, S. B. Oh,
B. C. Radburn-Smith, U. K. Yang, H. D. Yoo, I. Yoon

University of Seoul, Seoul, Korea
D. Jeon, J. H. Kim, J. S. H. Lee, I. C. Park, I. J. Watson

Sungkyunkwan University, Suwon, Korea
Y. Choi, C. Hwang, Y. Jeong, J. Lee, Y. Lee, I. Yu

Riga Technical University, Riga, Latvia
V. Veckalns[34]

Vilnius University, Vilnius, Lithuania
V. Dudenas, A. Juodagalvis, A. Rinkevicius, G. Tamulaitis, J. Vaitkus

National Centre for Particle Physics, Universiti Malaya, Kuala Lumpur, Malaysia
Z. A. Ibrahim, F. Mohamad Idris[35], W. A. T. Wan Abdullah, M. N. Yusli, Z. Zolkapli

Universidad de Sonora (UNISON), Hermosillo, Mexico
J. F. Benitez, A. Castaneda Hernandez, J. A. Murillo Quijada, L. Valencia Palomo

Centro de Investigacion y de Estudios Avanzados del IPN, Mexico City, Mexico
H. Castilla-Valdez, E. De La Cruz-Burelo, I. Heredia-De La Cruz[36], R. Lopez-Fernandez, A. Sanchez-Hernandez

Universidad Iberoamericana, Mexico City, Mexico
S. Carrillo Moreno, C. Oropeza Barrera, M. Ramirez-Garcia, F. Vazquez Valencia

Benemerita Universidad Autonoma de Puebla, Puebla, Mexico
J. Eysermans, I. Pedraza, H. A. Salazar Ibarguen, C. Uribe Estrada

Universidad Autónoma de San Luis Potosí, San Luis Potosí, Mexico
A. Morelos Pineda

University of Montenegro, Podgorica, Montenegro
J. Mijuskovic[2], N. Raicevic

University of Auckland, Auckland, New Zealand
D. Krofcheck

University of Canterbury, Christchurch, New Zealand
S. Bheesette, P. H. Butler, P. Lujan

National Centre for Physics, Quaid-I-Azam University, Islamabad, Pakistan
A. Ahmad, M. Ahmad, M. I. M. Awan, Q. Hassan, H. R. Hoorani, W. A. Khan, M. A. Shah, M. Shoaib, M. Waqas

AGH University of Science and Technology Faculty of Computer Science, Electronics and Telecommunications, Kraków, Poland
V. Avati, L. Grzanka, M. Malawski

National Centre for Nuclear Research, Swierk, Poland
H. Bialkowska, M. Bluj, B. Boimska, M. Górski, M. Kazana, M. Szleper, P. Zalewski

Institute of Experimental Physics, Faculty of Physics, University of Warsaw, Warsaw, Poland
K. Bunkowski, A. Byszuk[37], K. Doroba, A. Kalinowski, M. Konecki, J. Krolikowski, M. Olszewski, M. Walczak

Laboratório de Instrumentação e Física Experimental de Partículas, Lisbon, Portugal
M. Araujo, P. Bargassa, D. Bastos, A. Di Francesco, P. Faccioli, B. Galinhas, M. Gallinaro, J. Hollar, N. Leonardo,
T. Niknejad, J. Seixas, K. Shchelina, G. Strong, O. Toldaiev, J. Varela

Joint Institute for Nuclear Research, Dubna, Russia
S. Afanasiev, P. Bunin, M. Gavrilenko, I. Golutvin, I. Gorbunov, A. Kamenev, V. Karjavine, A. Lanev, A. Malakhov,
V. Matveev[38, 39], P. Moisenz, V. Palichik, V. Perelygin, M. Savina, S. Shmatov, S. Shulha, N. Skatchkov, V. Smirnov,
N. Voytishin, A. Zarubin

Petersburg Nuclear Physics Institute, Gatchina (St. Petersburg), Russia
L. Chtchipounov, V. Golovtcov, Y. Ivanov, V. Kim[40], E. Kuznetsova[41], P. Levchenko, V. Murzin, V. Oreshkin, I. Smirnov,
D. Sosnov, V. Sulimov, L. Uvarov, A. Vorobyev

Institute for Nuclear Research, Moscow, Russia
Yu. Andreev, A. Dermenev, S. Gninenko, N. Golubev, A. Karneyeu, M. Kirsanov, N. Krasnikov, A. Pashenkov, D. Tlisov,
A. Toropin

Institute for Theoretical and Experimental Physics named by A.I. Alikhanov of NRC 'Kurchatov Institute', Moscow, Russia
V. Epshteyn, V. Gavrilov, N. Lychkovskaya, A. Nikitenko[42], V. Popov, I. Pozdnyakov, G. Safronov, A. Spiridonov,
A. Stepennov, M. Toms, E. Vlasov, A. Zhokin

Moscow Institute of Physics and Technology, Moscow, Russia
T. Aushev

National Research Nuclear University 'Moscow Engineering Physics Institute' (MEPhI), Moscow, Russia
R. Chistov[43], M. Danilov[43], P. Parygin, S. Polikarpov[43], E. Tarkovskii

P.N. Lebedev Physical Institute, Moscow, Russia
V. Andreev, M. Azarkin, I. Dremin, M. Kirakosyan, A. Terkulov

Skobeltsyn Institute of Nuclear Physics, Lomonosov Moscow State University, Moscow, Russia
A. Belyaev, E. Boos, M. Dubinin[44], L. Dudko, A. Ershov, A. Gribushin, V. Klyukhin, O. Kodolova, I. Lokhtin,
S. Obraztsov, S. Petrushanko, V. Savrin, A. Snigirev

Novosibirsk State University (NSU), Novosibirsk, Russia
A. Barnyakov[45], V. Blinov[45], T. Dimova[45], L. Kardapoltsev[45], Y. Skovpen[45]

Institute for High Energy Physics of National Research Centre 'Kurchatov Institute', Protvino, Russia
I. Azhgirey, I. Bayshev, S. Bitioukov, V. Kachanov, D. Konstantinov, P. Mandrik, V. Petrov, R. Ryutin, S. Slabospitskii,
A. Sobol, S. Troshin, N. Tyurin, A. Uzunian, A. Volkov

National Research Tomsk Polytechnic University, Tomsk, Russia
A. Babaev, A. Iuzhakov, V. Okhotnikov

Tomsk State University, Tomsk, Russia
V. Borchsh, V. Ivanchenko, E. Tcherniaev

Faculty of Physics and VINCA Institute of Nuclear Sciences, University of Belgrade, Belgrade, Serbia
P. Adzic[46], P. Cirkovic, M. Dordevic, P. Milenovic, J. Milosevic, M. Stojanovic

Centro de Investigaciones Energéticas Medioambientales y Tecnológicas (CIEMAT), Madrid, Spain
M. Aguilar-Benitez, J. Alcaraz Maestre, A. Álvarez Fernández, I. Bachiller, M. Barrio Luna, C. F. Bedoya,
J. A. Brochero Cifuentes, C. A. Carrillo Montoya, M. Cepeda, M. Cerrada, N. Colino, B. De La Cruz, A. Delgado Peris,
J. P. Fernández Ramos, J. Flix, M. C. Fouz, O. Gonzalez Lopez, S. Goy Lopez, J. M. Hernandez, M. I. Josa, D. Moran,
Á. Navarro Tobar, A. Pérez-Calero Yzquierdo, J. Puerta Pelayo, I. Redondo, L. Romero, S. Sánchez Navas, M. S. Soares,
A. Triossi, C. Willmott

Universidad Autónoma de Madrid, Madrid, Spain
C. Albajar, J. F. de Trocóniz, R. Reyes-Almanza

Instituto Universitario de Ciencias y Tecnologías Espaciales de Asturias (ICTEA), Universidad de Oviedo, Oviedo, Spain

B. Alvarez Gonzalez, J. Cuevas, C. Erice, J. Fernandez Menendez, S. Folgueras, I. Gonzalez Caballero, J. R. González Fernández, E. Palencia Cortezon, V. Rodríguez Bouza, S. Sanchez Cruz

Instituto de Física de Cantabria (IFCA), CSIC-Universidad de Cantabria, Santander, Spain

I. J. Cabrillo, A. Calderon, B. Chazin Quero, J. Duarte Campderros, M. Fernandez, P. J. Fernández Manteca, A. García Alonso, G. Gomez, C. Martinez Rivero, P. Martinez Ruiz del Arbol, F. Matorras, J. Piedra Gomez, C. Prieels, T. Rodrigo, A. Ruiz-Jimeno, L. Russo[47], L. Scodellaro, I. Vila, J. M. Vizan Garcia

University of Colombo, Colombo, Sri Lanka

D. U. J. Sonnadara

Department of Physics, University of Ruhuna, Matara, Sri Lanka

W. G. D. Dharmaratna, N. Wickramage

CERN, European Organization for Nuclear Research, Geneva, Switzerland

D. Abbaneo, B. Akgun, E. Auffray, G. Auzinger, J. Baechler, P. Baillon, A. H. Ball, D. Barney, J. Bendavid, M. Bianco, A. Bocci, P. Bortignon, E. Bossini, E. Brondolin, T. Camporesi, A. Caratelli, G. Cerminara, E. Chapon, G. Cucciati, D. d'Enterria, A. Dabrowski, N. Daci, V. Daponte, A. David, O. Davignon, A. De Roeck, M. Deile, R. Di Maria, M. Dobson, M. Dünser, N. Dupont, A. Elliott-Peisert, N. Emriskova, F. Fallavollita[48], D. Fasanella, S. Fiorendi, G. Franzoni, J. Fulcher, W. Funk, S. Giani, D. Gigi, K. Gill, F. Glege, L. Gouskos, M. Gruchala, M. Guilbaud, D. Gulhan, J. Hegeman, C. Heidegger, Y. Iiyama, V. Innocente, T. James, P. Janot, O. Karacheban[20], J. Kaspar, J. Kieseler, M. Krammer[1], N. Kratochwil, C. Lange, P. Lecoq, C. Lourenço, L. Malgeri, M. Mannelli, A. Massironi, F. Meijers, S. Mersi, E. Meschi, F. Moortgat, M. Mulders, J. Ngadiuba, J. Niedziela, S. Nourbakhsh, S. Orfanelli, L. Orsini, F. Pantaleo[16], L. Pape, E. Perez, M. Peruzzi, A. Petrilli, G. Petrucciani, A. Pfeiffer, M. Pierini, F. M. Pitters, D. Rabady, A. Racz, M. Rieger, M. Rovere, H. Sakulin, J. Salfeld-Nebgen, S. Scarfi, C. Schäfer, C. Schwick, M. Selvaggi, A. Sharma, P. Silva, W. Snoeys, P. Sphicas[49], J. Steggemann, S. Summers, V. R. Tavolaro, D. Treille, A. Tsirou, G. P. Van Onsem, A. Vartak, M. Verzetti, W. D. Zeuner

Paul Scherrer Institut, Villigen, Switzerland

L. Caminada[50], K. Deiters, W. Erdmann, R. Horisberger, Q. Ingram, H. C. Kaestli, D. Kotlinski, U. Langenegger, T. Rohe

ETH Zurich-Institute for Particle Physics and Astrophysics (IPA), Zurich, Switzerland

M. Backhaus, P. Berger, N. Chernyavskaya, G. Dissertori, M. Dittmar, M. Donegà, C. Dorfer, T. A. Gómez Espinosa, C. Grab, D. Hits, W. Lustermann, R. A. Manzoni, M. T. Meinhard, F. Micheli, P. Musella, F. Nessi-Tedaldi, F. Pauss, G. Perrin, L. Perrozzi, S. Pigazzini, M. G. Ratti, M. Reichmann, C. Reissel, T. Reitenspiess, B. Ristic, D. Ruini, D. A. Sanz Becerra, M. Schönenberger, L. Shchutska, M. L. Vesterbacka Olsson, R. Wallny, D. H. Zhu

Universität Zürich, Zurich, Switzerland

T. K. Aarrestad, C. Amsler[51], C. Botta, D. Brzhechko, M. F. Canelli, A. De Cosa, R. Del Burgo, B. Kilminster, S. Leontsinis, V. M. Mikuni, I. Neutelings, G. Rauco, P. Robmann, K. Schweiger, C. Seitz, Y. Takahashi, S. Wertz, A. Zucchetta

National Central University, Chung-Li, Taiwan

C. M. Kuo, W. Lin, A. Roy, S. S. Yu

National Taiwan University (NTU), Taipei, Taiwan

P. Chang, Y. Chao, K. F. Chen, P. H. Chen, W.-S. Hou, Y.y. Li, R.-S. Lu, E. Paganis, A. Psallidas, A. Steen

Department of Physics, Faculty of Science, Chulalongkorn University, Bangkok, Thailand

B. Asavapibhop, C. Asawatangtrakuldee, N. Srimanobhas, N. Suwonjandee

Physics Department, Science and Art Faculty, Çukurova University, Adana, Turkey

A. Bat, F. Boran, A. Celik[52], S. Damarseckin[53], Z. S. Demiroglu, F. Dolek, C. Dozen[54], I. Dumanoglu, G. Gokbulut, E. G. Guler[55], Y. Guler, I. Hos[56], C. Isik, E. E. Kangal[57], O. Kara, A. Kayis Topaksu, U. Kiminsu, G. Onengut, K. Ozdemir[58], S. Ozturk[59], A. E. Simsek, U. G. Tok, S. Turkcapar, I. S. Zorbakir, C. Zorbilmez

Physics Department, Middle East Technical University, Ankara, Turkey
B. Isildak[60], G. Karapinar[61], M. Yalvac

Bogazici University, Istanbul, Turkey
I. O. Atakisi, E. Gülmez, M. Kaya[62], O. Kaya[63], Ö. Özçelik, S. Tekten, E. A. Yetkin[64]

Istanbul Technical University, Istanbul, Turkey
A. Cakir, K. Cankocak[65], Y. Komurcu, S. Sen[66]

Istanbul University, Istanbul, Turkey
S. Cerci[67], B. Kaynak, S. Ozkorucuklu, D. Sunar Cerci[67]

Institute for Scintillation Materials of National Academy of Science of Ukraine, Kharkov, Ukraine
B. Grynyov

National Scientific Center, Kharkov Institute of Physics and Technology, Kharkov, Ukraine
L. Levchuk

University of Bristol, Bristol, UK
E. Bhal, S. Bologna, J. J. Brooke, D. Burns[68], E. Clement, D. Cussans, H. Flacher, J. Goldstein, G. P. Heath, H. F. Heath,
L. Kreczko, B. Krikler, S. Paramesvaran, T. Sakuma, S. Seif El Nasr-Storey, V. J. Smith, J. Taylor, A. Titterton

Rutherford Appleton Laboratory, Didcot, UK
K. W. Bell, A. Belyaev[69], C. Brew, R. M. Brown, D. J. A. Cockerill, J. A. Coughlan, K. Harder, S. Harper, J. Linacre,
K. Manolopoulos, D. M. Newbold, E. Olaiya, D. Petyt, T. Reis, T. Schuh, C. H. Shepherd-Themistocleous, A. Thea,
I. R. Tomalin, T. Williams

Imperial College, London, UK
R. Bainbridge, P. Bloch, J. Borg, S. Breeze, O. Buchmuller, A. Bundock, G. S. Chahal[70], D. Colling, P. Dauncey, G. Davies,
M. Della Negra, P. Everaerts, G. Hall, G. Iles, M. Komm, L. Lyons, A.-M. Magnan, S. Malik, A. Martelli, V. Milosevic,
A. Morton, J. Nash[71], V. Palladino, M. Pesaresi, D. M. Raymond, A. Richards, A. Rose, E. Scott, C. Seez, A. Shtipliyski,
M. Stoye, T. Strebler, A. Tapper, K. Uchida, T. Virdee[16], N. Wardle, D. Winterbottom, A. G. Zecchinelli, S. C. Zenz

Brunel University, Uxbridge, UK
J. E. Cole, P. R. Hobson, A. Khan, P. Kyberd, C. K. Mackay, I. D. Reid, L. Teodorescu, S. Zahid

Baylor University, Waco, USA
A. Brinkerhoff, K. Call, B. Caraway, J. Dittmann, K. Hatakeyama, C. Madrid, B. McMaster, N. Pastika, C. Smith

Catholic University of America, Washington, DC, USA
R. Bartek, A. Dominguez, R. Uniyal, A. M. Vargas Hernandez

The University of Alabama, Tuscaloosa, USA
A. Buccilli, S. I. Cooper, S. V. Gleyzer, C. Hen derson, P. Rumerio, C. West

Boston University, Boston, USA
A. Albert, D. Arcaro, Z. Demiragli, D. Gastler, C. Richardson, J. Rohlf, D. Sperka, D. Spitzbart, I. Suarez, L. Sulak, D. Zou

Brown University, Providence, USA
G. Benelli, B. Burkle, X. Coubez[17], D. Cutts, Y.t. Duh, M. Hadley, U. Heintz, J. M. Hogan[72], K. H. M. Kwok, E. Laird,
G. Landsberg, K. T. Lau, J. Lee, M. Narain, S. Sagir[73], R. Syarif, E. Usai, W. Y. Wong, D. Yu, W. Zhang

University of California, Davis, Davis, USA
R. Band, C. Brainerd, R. Breedon, M. Calderon De La Barca Sanchez, M. Chertok, J. Conway, R. Conway, P. T. Cox,
R. Erbacher, C. Flores, G. Funk, F. Jensen, W. Ko[†], O. Kukral, R. Lander, M. Mulhearn, D. Pellett, J. Pilot, M. Shi,
D. Taylor, K. Tos, M. Tripathi, Z. Wang, F. Zhang

University of California, Los Angeles, USA
M. Bachtis, C. Bravo, R. Cousins, A. Dasgupta, A. Florent, J. Hauser, M. Ignatenko, N. Mccoll, W. A. Nash, S. Regnard,
D. Saltzberg, C. Schnaible, B. Stone, V. Valuev

University of California, Riverside, Riverside, USA
K. Burt, Y. Chen, R. Clare, J. W. Gary, S. M. A. Ghiasi Shirazi, G. Hanson, G. Karapostoli, O. R. Long,
M. Olmedo Negrete, M. I. Paneva, W. Si, L. Wang, S. Wimpenny, B. R. Yates, Y. Zhang

University of California, San Diego, La Jolla, USA
J. G. Branson, P. Chang, S. Cittolin, S. Cooperstein, N. Deelen, M. Derdzinski, J. Duarte, R. Gerosa, D. Gilbert,
B. Hashemi, D. Klein, V. Krutelyov, J. Letts, M. Masciovecchio, S. May, S. Padhi, M. Pieri, V. Sharma, M. Tadel,
F. Würthwein, A. Yagil, G. Zevi Della Porta

Department of Physics, University of California, Santa Barbara, Santa Barbara, USA
N. Amin, R. Bhandari, C. Campagnari, M. Citron, V. Dutta, M. Franco Sevilla, J. Incandela, J. Ling, B. Marsh, H. Mei,
A. Ovcharova, H. Qu, J. Richman, U. Sarica, D. Stuart, S. Wang

California Institute of Technology, Pasadena, USA
D. Anderson, A. Bornheim, O. Cerri, I. Dutta, J. M. Lawhorn, N. Lu, J. Mao, H. B. Newman, T. Q. Nguyen, J. Pata,
M. Spiropulu, J. R. Vlimant, S. Xie, Z. Zhang, R. Y. Zhu

Carnegie Mellon University, Pittsburgh, USA
M. B. Andrews, T. Ferguson, T. Mudholkar, M. Paulini, M. Sun, I. Vorobiev, M. Weinberg

University of Colorado Boulder, Boulder, USA
J. P. Cumalat, W. T. Ford, E. MacDonald, T. Mulholland, R. Patel, A. Perloff, K. Stenson, K. A. Ulmer, S. R. Wagner

Cornell University, Ithaca, USA
J. Alexander, Y. Cheng, J. Chu, A. Datta, A. Frankenthal, K. Mcdermott, J. R. Patterson, D. Quach, A. Ryd, S. M. Tan,
Z. Tao, J. Thom, P. Wittich, M. Zientek

Fermi National Accelerator Laboratory, Batavia, USA
S. Abdullin, M. Albrow, M. Alyari, G. Apollinari, A. Apresyan, A. Apyan, S. Banerjee, L. A. T. Bauerdick, A. Beretvas,
D. Berry, J. Berryhill, P. C. Bhat, K. Burkett, J. N. Butler, A. Canepa, G. B. Cerati, H. W. K. Cheung, F. Chlebana,
M. Cremonesi, V. D. Elvira, J. Freeman, Z. Gecse, E. Gottschalk, L. Gray, D. Green, S. Grünendahl, O. Gutsche,
J. Hanlon, R. M. Harris, S. Hasegawa, R. Heller, J. Hirschauer, B. Jayatilaka, S. Jindariani, M. Johnson, U. Joshi,
T. Klijnsma, B. Klima, M. J. Kortelainen, B. Kreis, S. Lammel, J. Lewis, D. Lincoln, R. Lipton, M. Liu, T. Liu, J. Lykken,
K. Maeshima, J. M. Marraffino, D. Mason, P. McBride, P. Merkel, S. Mrenna, S. Nahn, V. O'Dell, V. Papadimitriou,
K. Pedro, C. Pena, F. Ravera, A. Reinsvold Hall, L. Ristori, B. Schneider, E. Sexton-Kennedy, N. Smith, A. Soha,
W. J. Spalding, L. Spiegel, S. Stoynev, J. Strait, L. Taylor, S. Tkaczyk, N. V. Tran, L. Uplegger, E. W. Vaandering,
C. Vernieri, R. Vidal, M. Wang, H. A. Weber, A. Woodard

University of Florida, Gainesville, USA
D. Acosta, P. Avery, D. Bourilkov, L. Cadamuro, V. Cherepanov, F. Errico, R. D. Field, D. Guerrero, B. M. Joshi, M. Kim,
J. Konigsberg, A. Korytov, K. H. Lo, K. Matchev, N. Menendez, G. Mitselmakher, D. Rosenzweig, K. Shi, J. Wang,
S. Wang, X. Zuo

Florida International University, Miami, USA
Y. R. Joshi

Florida State University, Tallahassee, USA
T. Adams, A. Askew, S. Hagopian, V. Hagopian, K. F. Johnson, R. Khurana, T. Kolberg, G. Martinez, T. Perry, H. Prosper,
C. Schiber, R. Yohay, J. Zhang

Florida Institute of Technology, Melbourne, USA
M. M. Baarmand, M. Hohlmann, D. Noonan, M. Rahmani, M. Saunders, F. Yumiceva

University of Illinois at Chicago (UIC), Chicago, USA
M. R. Adams, L. Apanasevich, R. R. Betts, R. Cavanaugh, X. Chen, S. Dittmer, O. Evdokimov, C. E. Gerber, D. A. Hangal,
D. J. Hofman, V. Kumar, C. Mills, T. Roy, M. B. Tonjes, N. Varelas, J. Viinikainen, H. Wang, X. Wang, Z. Wu

The University of Iowa, Iowa City, USA
M. Alhusseini, B. Bilki[55], K. Dilsiz[74], S. Durgut, R. P. Gandrajula, M. Haytmyradov, V. Khristenko, O. K. Köseyan,

J.-P. Merlo, A. Mestvirishvili[75], A. Moeller, J. Nachtman, H. Ogul[76], Y. Onel, F. Ozok[77], A. Penzo, C. Snyder, E. Tiras, J. Wetzel

Johns Hopkins University, Baltimore, USA
B. Blumenfeld, A. Cocoros, N. Eminizer, A. V. Gritsan, W. T. Hung, S. Kyriacou, P. Maksimovic, J. Roskes, M. Swartz, T.Á. Vámi

The University of Kansas, Lawrence, USA
C. Baldenegro Barrera, P. Baringer, A. Bean, S. Boren, A. Bylinkin, T. Isidori, S. Khalil, J. King, G. Krintiras, A. Kropivnitskaya, C. Lindsey, D. Majumder, W. Mcbrayer, N. Minafra, M. Murray, C. Rogan, C. Royon, S. Sanders, E. Schmitz, J. D. Tapia Takaki, Q. Wang, J. Williams, G. Wilson

Kansas State University, Manhattan, USA
S. Duric, A. Ivanov, K. Kaadze, D. Kim, Y. Maravin, D. R. Mendis, T. Mitchell, A. Modak, A. Mohammadi

Lawrence Livermore National Laboratory, Livermore, USA
F. Rebassoo, D. Wright

University of Maryland, College Park, USA
A. Baden, O. Baron, A. Belloni, S. C. Eno, Y. Feng, N. J. Hadley, S. Jabeen, G. Y. Jeng, R. G. Kellogg, A. C. Mignerey, S. Nabili, F. Ricci-Tam, M. Seidel, Y. H. Shin, A. Skuja, S. C. Tonwar, K. Wong

Massachusetts Institute of Technology, Cambridge, USA
D. Abercrombie, B. Allen, R. Bi, S. Brandt, W. Busza, I. A. Cali, M. D'Alfonso, G. Gomez Ceballos, M. Goncharov, P. Harris, D. Hsu, M. Hu, M. Klute, D. Kovalskyi, Y.-J. Lee, P. D. Luckey, B. Maier, A. C. Marini, C. Mcginn, C. Mironov, S. Narayanan, X. Niu, C. Paus, D. Rankin, C. Roland, G. Roland, Z. Shi, G. S. F. Stephans, K. Sumorok, K. Tatar, D. Velicanu, J. Wang, T. W. Wang, B. Wyslouch

University of Minnesota, Minneapolis, USA
R. M. Chatterjee, A. Evans, S. Guts[†], P. Hansen, J. Hiltbrand, Sh. Jain, Y. Kubota, Z. Lesko, J. Mans, M. Revering, R. Rusack, R. Saradhy, N. Schroeder, N. Strobbe, M. A. Wadud

University of Mississippi, Oxford, USA
J. G. Acosta, S. Oliveros

University of Nebraska-Lincoln, Lincoln, USA
K. Bloom, S. Chauhan, D. R. Claes, C. Fangmeier, L. Finco, F. Golf, R. Kamalieddin, I. Kravchenko, J. E. Siado, G. R. Snow[†], B. Stieger, W. Tabb

State University of New York at Buffalo, Buffalo, USA
G. Agarwal, C. Harrington, I. Iashvili, A. Kharchilava, C. McLean, D. Nguyen, A. Parker, J. Pekkanen, S. Rappoccio, B. Roozbahani

Northeastern University, Boston, USA
G. Alverson, E. Barberis, C. Freer, Y. Haddad, A. Hortiangtham, G. Madigan, B. Marzocchi, D. M. Morse, T. Orimoto, L. Skinnari, A. Tishelman-Charny, T. Wamorkar, B. Wang, A. Wisecarver, D. Wood

Northwestern University, Evanston, USA
S. Bhattacharya, J. Bueghly, G. Fedi, A. Gilbert, T. Gunter, K. A. Hahn, N. Odell, M. H. Schmitt, K. Sung, M. Velasco

University of Notre Dame, Notre Dame, USA
R. Bucci, N. Dev, R. Goldouzian, M. Hildreth, K. Hurtado Anampa, C. Jessop, D. J. Karmgard, K. Lannon, W. Li, N. Loukas, N. Marinelli, I. Mcalister, F. Meng, Y. Musienko[38], R. Ruchti, P. Siddireddy, G. Smith, S. Taroni, M. Wayne, A. Wightman, M. Wolf

The Ohio State University, Columbus, USA
J. Alimena, B. Bylsma, L. S. Durkin, B. Francis, C. Hill, W. Ji, A. Lefeld, T. Y. Ling, B. L. Winer

Princeton University, Princeton, USA
G. Dezoort, P. Elmer, J. Hardenbrook, N. Haubrich, S. Higginbotham, A. Kalogeropoulos, S. Kwan, D. Lange, M. T. Lucchini, J. Luo, D. Marlow, K. Mei, I. Ojalvo, J. Olsen, C. Palmer, P. Piroué, D. Stickland, C. Tully

University of Puerto Rico, Mayaguez, USA
S. Malik, S. Norberg

Purdue University, West Lafayette, USA
A. Barker, V. E. Barnes, R. Chawla, S. Das, L. Gutay, M. Jones, A. W. Jung, B. Mahakud, D. H. Miller, G. Negro, N. Neumeister, C. C. Peng, S. Piperov, H. Qiu, J. F. Schulte, N. Trevisani, F. Wang, R. Xiao, W. Xie

Purdue University Northwest, Hammond, USA
T. Cheng, J. Dolen, N. Parashar

Rice University, Houston, USA
A. Baty, U. Behrens, S. Dildick, K. M. Ecklund, S. Freed, F. J. M. Geurts, M. Kilpatrick, A. Kumar, W. Li, B. P. Padley, R. Redjimi, J. Roberts, J. Rorie, W. Shi, A. G. Stahl Leiton, Z. Tu, A. Zhang

University of Rochester, Rochester, USA
A. Bodek, P. de Barbaro, R. Demina, J. L. Dulemba, C. Fallon, T. Ferbel, M. Galanti, A. Garcia-Bellido, O. Hindrichs, A. Khukhunaishvili, E. Ranken, R. Taus

Rutgers, The State University of New Jersey, Piscataway, USA
B. Chiarito, J. P. Chou, A. Gandrakota, Y. Gershtein, E. Halkiadakis, A. Hart, M. Heindl, E. Hughes, S. Kaplan, I. Laflotte, A. Lath, R. Montalvo, K. Nash, M. Osherson, S. Salur, S. Schnetzer, S. Somalwar, R. Stone, S. Thomas

University of Tennessee, Knoxville, USA
H. Acharya, A. G. Delannoy, S. Spanier

Texas A&M University, College Station, USA
O. Bouhali[78], M. Dalchenko, M. De Mattia, A. Delgado, R. Eusebi, J. Gilmore, T. Huang, T. Kamon[79], H. Kim, S. Luo, S. Malhotra, D. Marley, R. Mueller, D. Overton, L. Perniè, D. Rathjens, A. Safonov

Texas Tech University, Lubbock, USA
N. Akchurin, J. Damgov, F. De Guio, V. Hegde, S. Kunori, K. Lamichhane, S. W. Lee, T. Mengke, S. Muthumuni, T. Peltola, S. Undleeb, I. Volobouev, Z. Wang, A. Whitbeck

Vanderbilt University, Nashville, USA
S. Greene, A. Gurrola, R. Janjam, W. Johns, C. Maguire, A. Melo, H. Ni, K. Padeken, F. Romeo, P. Sheldon, S. Tuo, J. Velkovska, M. Verweij

University of Virginia, Charlottesville, USA
M. W. Arenton, P. Barria, B. Cox, G. Cummings, J. Hakala, R. Hirosky, M. Joyce, A. Ledovskoy, C. Neu, B. Tannenwald, Y. Wang, E. Wolfe, F. Xia

Wayne State University, Detroit, USA
R. Harr, P. E. Karchin, N. Poudyal, J. Sturdy, P. Thapa

University of Wisconsin-Madison, Madison, WI, USA
K. Black, T. Bose, J. Buchanan, C. Caillol, D. Carlsmith, S. Dasu, I. De Bruyn, L. Dodd, C. Galloni, H. He, M. Herndon, A. Hervé, U. Hussain, A. Lanaro, A. Loeliger, K. Long, R. Loveless, J. Madhusudanan Sreekala, A. Mallampalli, D. Pinna, T. Ruggles, A. Savin, V. Sharma, W. H. Smith, D. Teague, S. Trembath-reichert

† **Deceased**

 1: Also at Vienna University of Technology, Vienna, Austria
 2: Also at IRFU, CEA, Université Paris-Saclay, Gif-sur-Yvette, France
 3: Also at Universidade Estadual de Campinas, Campinas, Brazil
 4: Also at Federal University of Rio Grande do Sul, Porto Alegre, Brazil
 5: Also at UFMS, Nova Andradina, Brazil

6: Also at Universidade Federal de Pelotas, Pelotas, Brazil

7: Also at Université Libre de Bruxelles, Bruxelles, Belgium

8: Also at University of Chinese Academy of Sciences, Beijing, China

9: Also at Institute for Theoretical and Experimental Physics named by A.I. Alikhanov of NRC 'Kurchatov Institute', Moscow, Russia

10: Also at Joint Institute for Nuclear Research, Dubna, Russia

11: Also at Cairo University, Cairo, Egypt

12: Also at Zewail City of Science and Technology, Zewail, Egypt

13: Also at Purdue University, West Lafayette, USA

14: Also at Université de Haute Alsace, Mulhouse, France

15: Also at Erzincan Binali Yildirim University, Erzincan, Turkey

16: Also at CERN, European Organization for Nuclear Research, Geneva, Switzerland

17: Also at RWTH Aachen University, III. Physikalisches Institut A, Aachen, Germany

18: Also at University of Hamburg, Hamburg, Germany

19: Also at Isfahan University of Technology, Isfahan, Iran

20: Also at Brandenburg University of Technology, Cottbus, Germany

21: Also at Institute of Physics, University of Debrecen, Debrecen, Hungary, Debrecen, Hungary

22: Also at Institute of Nuclear Research ATOMKI, Debrecen, Hungary

23: Also at MTA-ELTE Lendület CMS Particle and Nuclear Physics Group, Eötvös Loránd University, Budapest, Hungary, Budapest, Hungary

24: Also at IIT Bhubaneswar, Bhubaneswar, India, Bhubaneswar, India

25: Also at Institute of Physics, Bhubaneswar, India

26: Also at G.H.G. Khalsa College, Punjab, India

27: Also at Shoolini University, Solan, India

28: Also at University of Hyderabad, Hyderabad, India

29: Also at University of Visva-Bharati, Santiniketan, India

30: Now at INFN Sezione di Bari^a, Università di Bari^b, Politecnico di Bari^c, Bari, Italy

31: Also at Italian National Agency for New Technologies, Energy and Sustainable Economic Development, Bologna, Italy

32: Also at Centro Siciliano di Fisica Nucleare e di Struttura Della Materia, Catania, Italy

33: Also at Scuola Normale e Sezione dell'INFN, Pisa, Italy

34: Also at Riga Technical University, Riga, Latvia, Riga, Latvia

35: Also at Malaysian Nuclear Agency, MOSTI, Kajang, Malaysia

36: Also at Consejo Nacional de Ciencia y Tecnología, Mexico City, Mexico

37: Also at Warsaw University of Technology, Institute of Electronic Systems, Warsaw, Poland

38: Also at Institute for Nuclear Research, Moscow, Russia

39: Now at National Research Nuclear University 'Moscow Engineering Physics Institute' (MEPhI), Moscow, Russia

40: Also at St. Petersburg State Polytechnical University, St. Petersburg, Russia

41: Also at University of Florida, Gainesville, USA

42: Also at Imperial College, London, United Kingdom

43: Also at P.N. Lebedev Physical Institute, Moscow, Russia

44: Also at California Institute of Technology, Pasadena, USA

45: Also at Budker Institute of Nuclear Physics, Novosibirsk, Russia

46: Also at Faculty of Physics, University of Belgrade, Belgrade, Serbia

47: Also at Università degli Studi di Siena, Siena, Italy

48: Also at INFN Sezione di Pavia^a, Università di Pavia^b, Pavia, Italy, Pavia, Italy

49: Also at National and Kapodistrian University of Athens, Athens, Greece

50: Also at Universität Zürich, Zurich, Switzerland

51: Also at Stefan Meyer Institute for Subatomic Physics, Vienna, Austria, Vienna, Austria

52: Also at Burdur Mehmet Akif Ersoy University, BURDUR, Turkey

53: Also at Şırnak University, Sirnak, Turkey

54: Also at Department of Physics, Tsinghua University, Beijing, China, Beijing, China

55: Also at Beykent University, Istanbul, Turkey, Istanbul, Turkey

56: Also at Istanbul Aydin University, Application and Research Center for Advanced Studies (App. & Res. Cent. for Advanced Studies), Istanbul, Turkey

57: Also at Mersin University, Mersin, Turkey

58: Also at Piri Reis University, Istanbul, Turkey

59: Also at Gaziosmanpasa University, Tokat, Turkey

60: Also at Ozyegin University, Istanbul, Turkey

61: Also at Izmir Institute of Technology, Izmir, Turkey

62: Also at Marmara University, Istanbul, Turkey

63: Also at Kafkas University, Kars, Turkey

64: Also at Istanbul Bilgi University, Istanbul, Turkey

65: Also at Near East University, Research Center of Experimental Health Science, Nicosia, Turkey

66: Also at Hacettepe University, Ankara, Turkey

67: Also at Adiyaman University, Adiyaman, Turkey

68: Also at Vrije Universiteit Brussel, Brussel, Belgium

69: Also at School of Physics and Astronomy, University of Southampton, Southampton, United Kingdom

70: Also at IPPP Durham University, Durham, United Kingdom

71: Also at Monash University, Faculty of Science, Clayton, Australia

72: Also at Bethel University, St. Paul, Minneapolis, USA, St. Paul, USA

73: Also at Karamanoğlu Mehmetbey University, Karaman, Turkey

74: Also at Bingol University, Bingol, Turkey

75: Also at Georgian Technical University, Tbilisi, Georgia

76: Also at Sinop University, Sinop, Turkey

77: Also at Mimar Sinan University, Istanbul, Istanbul, Turkey

78: Also at Texas A&M University at Qatar, Doha, Qatar

79: Also at Kyungpook National University, Daegu, Korea, Daegu, Korea